Copyright Warning & Restrictions

The copyright law of the United States (Title 17, United States Code) governs the making of photocopies or other reproductions of copyrighted material.

Under certain conditions specified in the law, libraries and archives are authorized to furnish a photocopy or other reproduction. One of these specified conditions is that the photocopy or reproduction is not to be "used for any purpose other than private study, scholarship, or research." If a, user makes a request for, or later uses, a photocopy or reproduction for purposes in excess of "fair use" that user may be liable for copyright infringement,

This institution reserves the right to refuse to accept a copying order if, in its judgment, fulfillment of the order would involve violation of copyright law.

Please Note: The author retains the copyright while the New Jersey Institute of Technology reserves the right to distribute this thesis or dissertation

Printing note: If you do not wish to print this page, then select "Pages from: first page # to: last page #" on the print dialog screen

ABSTRACT

IDENTIFICATION OF NEUROBIOLOGICAL MECHANISMS ASSOCIATED WITH ATTENTION DEFICITS IN ADULTS POST TRAUMATIC BRAIN INJURY

by
Ziyan Wu

Traumatic Brain Injury (TBI) is one of the major public health concerns with approximately 70 million new cases occurring worldwide per year. It is often caused by a forceful bump, blow, or jolt to the head, resulting in brain tissue damage and normal brain functions disruption. All grades of TBI, ranging from mild to severe, can cause wide-ranging and long-term effects on affected individuals, resulting in physical impairments, and neurocognitive consequences that permanently affect their abilities to perform daily activities. Attention deficits are the most common persisting neurocognitive consequences following TBI, which significantly contribute to poor academic and social functioning, and life-long learning difficulties of affected individuals. However, attention deficits have been evaluated and treated based on symptom endorsements from subjective observations, with few therapeutic interventions successfully translated to the clinic. The consensus regarding appropriate evaluation and treatment of TBI induced attention deficits in this cohort is rather limited due to the lack of investigations of the neurobiological substrates associated with this syndrome.

The overall aim of this dissertation research is to systematically investigate the neurobiological mechanisms associated with attention deficits in adults post TBI by utilizing multiple powerful neuroimaging techniques including the functional near-infrared spectroscopy (fNIRS) and multimodal magnetic resonance imaging (MRI), with an ultimate goal of translating hypothesis-driven neurobiological correlates into the

quantitatively measurable biomarkers for diagnosis of TBI-induced attention deficits and development of more refined long-term treatment and intervention strategies.

This dissertation research is conducted through three specific projects. Project 1 focuses on the investigation of brain functional patterns including the regional cortical brain activation and between-regional pairwise functional connectivity responding to visual sustained attention processing in individuals with and without TBI, by utilizing the fNIRS technique. Project 2 continues the examination of brain functional patterns by assessing the whole brain network topological properties responding to visual sustained attention processing in a larger sample of individuals with and without TBI, by utilizing the functional MRI technique and a graph theoretic approach. Project 3, on the other hand, investigates the brain structural characteristics based on the same sample involved in Project 2, by utilizing the structural MRI and diffusion tensor imaging techniques. For all these three projects, the differences of these brain imaging measures are compared between the groups of TBI and control. Correlation analyses are further conducted between those brain imaging measures which shows significant between-group differences and attention-related behaviors. In addition, Project 3 additionally investigates gender-specific patterns of the altered brain structural properties in TBI patients, relative to controls.

The outcome of this novel and valuable dissertation research may shed light on the neural mechanisms of attention deficits in adults post TBI, and may suggest the neurobiological targets for treatment of this severe and common condition. It may also provide important neural foundation for future research to develop effective rehabilitation strategies to improve attention processing in adults post TBI.

IDENTIFICATION OF NEUROBIOLOGICAL MECHANISMS ASSOCIATED WITH ATTENTION DEFICITS IN ADULTS POST TRAUMATIC BRAIN INJURY

by
Ziyan Wu

A Dissertation
Submitted to the Faculty of
New Jersey Institute of Technology
in Partial Fulfillment of the Requirements for the Degree of
Doctor of Philosophy in Electrical Engineering

Helen and John C. Hartmann Department of
Electrical and Computer Engineering

May 2020

APPROVAL PAGE

IDENTIFICATION OF NEUROBIOLOGICAL MECHANISMS ASSOCIATED WITH ATTENTION DEFICITS IN ADULTS POST TRAUMATIC BRAIN INJURY

Ziyan Wu

Dr. Xiaobo Li, Dissertation Advisor — Date
Associate Professor of Biomedical Engineering, NJIT

Dr. Durgamadhab Misra, Committee Member — Date
Professor of Electrical and Computer Engineering, NJIT

Dr. Abdallah Khreishah, Committee Member — Date
Associate Professor of Electrical and Computer Engineering, NJIT

Dr. Xuan Liu, Committee Member — Date
Assistant Professor of Electrical and Computer Engineering, NJIT

Dr. Tara L. Alvarez, Committee Member — Date
Professor of Biomedical Engineering, NJIT

Dr. Yun-Qing Shi, Committee Member — Date
Professor Emeritus of Electrical and Computer Engineering, NJIT

BIOGRAPHICAL SKETCH

Author: Ziyan Wu

Degree: Doctor of Philosophy

Date: May 2020

Undergraduate and Graduate Education:

- Doctor of Philosophy in Electrical Engineering,
  New Jersey Institute of Technology, Newark, NJ, 2020

- Master of Science in Electrical Engineering,
  New Jersey Institute of Technology, Newark, NJ, 2015

- Bachelor of Science in Electrical Engineering,
  Wuchang University of Technology, Wuhan, China, 2013

Major: Electrical Engineering

Journal Publications:

Wu, Z., Mazzola, C.A., Goodman, A., Gao, Y., Alvarez, T., Li, X. (2020). Structural brain alterations and their associations with inattentive and hyperactive behaviors show differentiated patterns in females and males with traumatic brain injury. *J. Neurotrauma*, Submitted.

Wu, Z., Mazzola, C.A., Goodman, A., Gao, Y., Li, X. (2020). Atypical topological properties of visual sustained attention processing network and their associations with inattentive and hyperactive behaviors in adults with traumatic brain injury. In preparation for journal submission.

Wu, Z., Luo, Y., Gao, Y., Han, Y., Wu, K., Li, X. (2019). The Role of prefrontal and occipital cortices in visual sustained attention processing in young adults with attention-deficit/hyperactivity disorder: a functional near-infrared spectroscopy study. *Neurosci Bull*, In press.

Huang, Y., Wu, T., Gao, Y., Luo, Y., Wu, Z., Fagan, S., Leung, S., Li, X. (2019). The Impact of callous-unemotional traits and externalizing tendencies on neural responsivity to reward and punishment in healthy adolescents. *Front. Neurosci.* 13, 1319.

Koenig, S., Wu, Z., Gao, Y., Li, X. (2019). Abnormal cortical activation in visual attention processing in sub-clinical psychopathy and traumatic brain injury: evidence from an fNIRS study. *J. Psychopathol. Behav. Assess,* In press.

Wu, Z., Mazzola, C.A., Catania, L., Owoeye, O., Yaramothu, C., Gao, Y., Li, X. (2018). Altered cortical activation and connectivity patterns for visual attention processing in young adults post traumatic brain injury: a functional near infrared spectroscopy study. *CNS Neurosci Ther.*, 24, 539-548.

Li, X., Thermenos, H.W., Wu, Z., Nomura, Y., Wu, K., Keshavan, M., Seidman, L., DeLisi, L.E. (2016). Abnormal interactions of verbal- and spatial-memory networks in young people at familial high-risk for schizophrenia. *Schizophrenia Research*, 176, 100-105.

Conference Proceedings and Abstracts:

Wu, Z., Wang, R., Li, X. (2019). Reduced occipital hemodynamic response during visual attention processing in young adults with attention-deficit hyperactivity disorder – a functional near-infrared spectroscopy study. *Biomedical Engineering Society (BMES) Annual Meeting*, Philadelphia, Pennsylvania, USA.

Wu, Z., Li, X. (2018). Parietal-thalamic dysconnectivity during sustained attention processing in young adults with traumatic brain injury. *The 44th Northeast Bioengineering Conference (NEBEC)*, Philadelphia, Pennsylvania, USA.

Gao, Y., Wu, Z. and Li, X. (2018). Attention deficits in college students with psychopathic traits. *The 2018 International Conference on Education, Psychology, and Learning (ICEPL-SUMMER 2018)*, Tokyo, Japan.

Wu, Z., Luo, Y., Baskar, A., Li, X. (2017). Testing cortical activation responding to visual attention in young adults with traumatic brain injury – a functional near-infrared spectroscopy pilot study. *The 43rd Northeast Bioengineering Conference (NEBEC)*, Newark, New Jersey, USA.

路漫漫其修远兮， 吾将上下而求索

— 屈原 《离骚》

To my lovely parents, Wen Wu and Xiaoqing Sun and my grandparents for their endless love and support.

To my dear advisor, Dr. Xiaobo Li for her constant encouragement.

To my beloved fiancé, Shaocong Shi for his companionship, tolerance and understanding.

To all my friends for their great kindness.

To myself for never, ever giving up.

ACKNOWLEDGMENT

I would like to express my deepest gratitude to my dissertation advisor, Dr. Xiaobo Li, for her tremendous guidance throughout my Ph.D. study. From the beginning to the end, she has provided me with insightful information and invaluable suggestions. I want to thank her for inspiring and motivating me to take on every challenge. My pursuing of Ph.D. will not be possible without her frequent encouragement, immense patience, and constant support.

I would also like to express my appreciation to the distinguished members of the dissertation committee: Drs. Durgamadhab Misra, Abdallah Khreishah, Xuan Liu, Tara L. Alvarez, and Yun-Qing Shi for their time, active participation, and invaluable comments.

I want to acknowledge the support from the New Jersey Commission on Brain Injury Research (CBIR17PIL012), the National Institutes of Mental Health (R03MH109791, R15MH117368, and R01MH060698), and New Jersey Institute of Technology Start-up Award to Dr. Xiaobo Li, for allowing the successful execution of this dissertation research.

My sincere thanks to my friends, Yuyang Luo, Jincheng Li, Meng Cao, and Shaocong Shi for their kindly assistance during my graduate study life.

Finally, I would like to thank my parents, Wen Wu and Xiaoqing Sun, for their immeasurable love and encouragement throughout my entire life.

TABLE OF CONTENTS

TABLE OF CONTENTS
(Continued)

Chapter **Page**

TABLE OF CONTENTS
(Continued)

Chapter **Page**

TABLE OF CONTENTS
(Continued)

LIST OF TABLES

LIST OF FIGURES

LIST OF FIGURES
(Continued)

Figure **Page**

CHAPTER 1

INTRODUCTION

1.1 General Introduction to Traumatic Brain Injury

Traumatic Brain Injury (TBI) is one of the major public health concerns with approximately 70 million new cases occurring worldwide per year (Dewan et al., 2018). There are two broad types of head injuries, including penetrating and non-penetrating. Penetrating TBI, also known as open TBI, occurs when the skull is pierced by an object (e.g., a bullet, shrapnel, or by a weapon such as baseball bat), while non-penetrating TBI, also known as closed head injury or blunt TBI, is caused by an external force (e.g., falls, motor vehicle crashes, sports injuries) that produces movement of the brain within the skull. According to data from the Centers for Disease Control and Prevention, leading causes of TBI include falls and unintentional blunt trauma such as motor vehicle accidents and sports-related injuries. Additionally, TBIs caused by blast trauma is a common injury to service members in military conflicts.

The most common type of effct following TBI is the damage to the brain's white matter (WM). WM is composed of bundles of axons (projections of nerve cells that carry electrical impulses for biochemical information transmission). Shearing and rotational forces or sudden deceleration caused by TBI can stretch or tear the axon bundles, which disrupts the neural circuits and breakdown of overall communication among nerve cells in the brain. TBI can lead to both physical impairments such as seizures, muscle spasticity, fatigue, headaches and balance problems and neurocognitive consequences such as depression, mood swings, anxiety, impulsivity, agitation, memory loss, slowed ability to

process information, trouble concentrating, organizational problems, poor judgement and difficulty initiating activities. Acute symptoms such as headache, dizziness, confusion, and fatigue following TBI may have quick and full recoveries. However, at least 15-30% of TBI subjects develop prolonged cognitive and behavioral impairments which can cause profound effects to individuals abilities for performing daily activities (Langlois et al., 2006; Daneshvar et al., 2011; McKee and Daneshvar, 2015), resulting in a conservative estimate of direct and indirect costs of $50-$100 billion for their treatment and rehabilitation annually in the U.S. (Anderson et al., 2005; Max et al., 2005b; Ford et al., 2013; Hampshire et al., 2013; Hart et al., 2013).

1.2 Review of Existing Studies of Traumatic Brain Injury

1.2.1 Review of Observational Studies of Traumatic Brain Injury

In order to provide recommendations for the appropriate and effective interventions and treatments of the chronic cognitive and behavioral impairments following TBI, large numbers of observational studies have been conducted by implementing corresponding neuropsychological evaluations. In particular, large numbers of existing studies have reported TBI-induced attention deficits in multiple specific components, including impairments in the sustained attention (Chan, 2000), supervisory attentional control (Spikman et al., 1996; Rios et al., 2004), divided attention (Park et al., 1999; Leclercq et al., 2000; Lengenfelder et al., 2002), oriented attention (Cremona-Meteyard et al., 1992), as well as focused/selective attention (Vakil et al., 1991; Chan, 2000; 2002; Mangels et al., 2002). Meanwhile, memory is suggested as another most frequently disrupted domain after TBI (Kinsella et al., 1996; Shum et al., 1999; Carlesimo et al., 2004; Kliegel et al., 2004;

Schmitter-Edgecombe and Wright, 2004; Knight et al., 2005; Mathias and Mansfield, 2005; Knight et al., 2006; Henry et al., 2007; Tay et al., 2010). Evidences have also shown that deficits of executive functioning occur with high frequency following TBI (Mangeot et al., 2002; McDonald et al., 2002; Nadebaum et al., 2007; Shah et al., 2017). Besides, reduction in speed of information processing following TBI has been consistently found (Brouwer et al., 1989; Ponsford and Kinsella, 1992; Brouwer et al., 2002; Felmingham et al., 2004; Johansson et al., 2009; Dymowski et al., 2015). Moreover, disrupted skills in other aspects such as intellectual functioning, academic achievement, and language are also observed in individuals affected by TBI (Wood and Rutterford, 2006; Vas et al., 2015; Konigs et al., 2016; Treble-Barna et al., 2017).

It has been shown that neurocognitive consequences primarily in the domains of attention, memory, executive functioning and information processing, which are the most reported health issues following TBI, can cause profound effects on injured individuals and their families. However, such TBI-induced long-term neurocognitive impairments have been evaluated and treated based on symptom endorsements from subjective observations (i.e., data derived from self/parental interviews and questionnaire, and school records), with divergent results regarding effectiveness reported in clinical studies (Echemendia et al., 2015; Kennedy et al., 2017; Paterno et al., 2017). So far, there are few therapeutic interventions successfully translated to the clinic (Bramlett and Dietrich, 2015).

1.2.2 Review of Structural Neuroimaging Studies of Traumatic Brain Injury

Advances in modern neuroimaging techniques enable the assessments of objectively measurable brain structural and functional properties, allowing the investigations of not only the altered brain patterns due to TBI, but also the role which these brain abnormalities

play in neurocognitive consequences following TBI. Over the past two decades, increasing attention has been given to the examination of brain alterations in both gray matter (GM) and WM structures, in order to address the neurobiological mechanisms of TBI in the anatomical aspect. The structural magnetic resonance imaging (MRI) and diffusion tensor imaging (DTI) have become the most popular techniques in this research field.

Structural MRI examines the anatomy of the brain by quantifying GM morphological measures, including the thickness, surface area and volume. In the literature, abnormalities of the GM volume are largely reported in TBI patients, relative to controls, including reductions in cortical areas such as the frontal lobe (Fujiwara et al., 2008; Strangman et al., 2010; Yurgelun-Todd et al., 2011), parietal lobe (Warner et al., 2010b), occipital lobe (Warner et al., 2010b), temporal lobe (Bergeson et al., 2004; Gale et al., 2005; Levine et al., 2008), cingulate gyrus (Yount et al., 2002; Gale et al., 2005; Levine et al., 2008; Strangman et al., 2010), as well as subcortical regions such as hippocampus (Bigler et al., 1997; Tate and Bigler, 2000; Himanen et al., 2005; Strangman et al., 2010), amygdala (Warner et al., 2010a; Warner et al., 2010b), thalamus (Yount et al., 2002; Strangman et al., 2010), and putamen (Warner et al., 2010b). In addition, volume reductions in overall GM are also observed in those with TBI, when compared with controls (Gale et al., 1995; MacKenzie et al., 2002; Yount et al., 2002; Gale et al., 2005; Cohen et al., 2007; Trivedi et al., 2007; Ding et al., 2008; Fujiwara et al., 2008; Levine et al., 2008; Schonberger et al., 2009).

Meanwhile, evidences have also suggested significant associations between these altered anatomical patterns and cognitive/behavioral impairments following TBI. In particular, frontal and temporal lobes atrophies have been linked with deficits in memory

and executive function (Bergeson et al., 2004). Reduced GM concentration in frontal and temporal cortices, cingulate gyrus, subcortical regions and in the cerebellum have been correlated with lower scores on tests of attention and lower Glasgow Coma Score (GCS) (a neurological scale which aims to give a reliable and objective way of recording the state of a person's consciousness for initial as well as subsequent assessment) (Gale et al., 2005). Cerebral peduncle and corpus callosum (CC) volume alterations have been linked with motor function (Gale et al., 1995). Reduced hippocampal volume and temporal horn enlargement have been correlated with intellectual functioning and verbal memory function (Bigler et al., 1997). Hippocampal volume abnormality have also been correlated with degree of brain injury severity (Tate and Bigler, 2000). Increased lateral ventricular volumes have been correlated with impaired memory function, and executive functions (Himanen et al., 2005). Bilateral thalamic volumes have been linked with the ability of processing speed (Warner et al., 2010b). Furthermore, alterations in terms of cortical thickness and surface area in the middle frontal gyrus (MFG), dorsal superior frontal gyrus, inferior and superior temporal regions, middle temporal gyrus, superior parietal lobes, postcentral gyrus, as well as their relationship with neurocognitive outcomes have also been observed in patients with TBI (Tate et al., 2014; Wang et al., 2015; Dall'Acqua et al., 2016; Govindarajan et al., 2016).

DTI technique quantifies the diffusion of water molecules, commonly using the value of fractional anisotropy (FA) for the description. Numerous existing studies have demonstrated altered FA of various WM regions as well as their associations with cognitive and behavioral performances following TBI. Specifically, relative to controls, patients with TBI have significantly reduced FA in the CC, internal capsule (Adams et al., 1989;

Blumbergs et al., 1994; Arfanakis et al., 2002; Bigler, 2004) (Lipton et al., 2008), centrum semiovale (Inglese et al., 2005), sagittal stratum, superior longitudinal fasciculus (SLF) (Kraus et al., 2007), uncinate fasciculus, inferior fronto-occipital fasciculus (FOF) (Smits et al., 2011), dorsolateral prefrontal cortex (DLPFC) (Lipton et al., 2009), anterior corona radiata, inferior longitudinal fasciculus, and cingulum bundle (Niogi et al., 2008a).

In terms of associations between WM disruptions and cognitive/behavior outcomes, lower FA in the uncinate fasciculus and inferior FOF have been correlated with severity of post-concussive symptom (Smits et al., 2011). Reduced FA in DLPFC has been linked with worse executive functioning (Lipton et al., 2009). Decreased FA in the anterior corona radiata, uncinate fasciculus, genu of the CC, inferior longitudinal fasciculus, and cingulum bundle have been linked with attention processing (Niogi et al., 2008a). Decreased FA in the SLF, sagittal stratum, and uncinate fasciculus have been correlated with poor performance on verbal memory processing (Geary et al., 2010). In addition, reduced FA in anterior corona radiata, the genu of CC, and the left superior cerebellar peduncle have been correlated with spatial processing involved in attention (Maruta et al., 2010). In contrast, increased FA in the CC, uncinate fasciculus, internal capsule, and corona radiata (Lo et al., 2009; Mayer et al., 2010; Henry et al., 2011) in TBI patients or no differences of FA values between injured and non-injured individuals (Lange et al., 2012) have also been reported.

1.2.3 Review of Functional Neuroimaging Studies of Traumatic Brain Injury

As known, TBI not only affects brain tissue structures, but also alters blood-oxygen level dependent responses (Astafiev et al., 2015; Dona et al., 2017; Amyot et al., 2018). Functional neuroimaging techniques offer great promise for elucidating the underlying neuropathology associated with neurocognitive consequences following TBI in this

specific aspect. Functional MRI is a powerful technique which enables such assessment both under the resting-state (when a subject is awake but not performing a specific cognitive task or responding to sensory stimuli) and during the processing of various cognitive tasks (McDonald et al., 2012).

Since the earliest work using functional MRI to examine cognitive changes in individuals with TBI (McAllister et al., 1999), an increasing but limited numbers of studies have examined the cognitive and behavioral sequelae in this cohort. Specifically, brain functional alterations in widespread regions have been reported in TBI patients when performing attentional processing, including the significantly increased brain activations in the bilateral inferior frontal gyri, bilateral DLPFC, precentral gyrus, postcentral gyrus and superior parietal regions (Witt et al., 2010), and significant hypoactivation in bilatral frontal eye fields, ventrolateral prefrontal cortex, posterior parietal cortex, pre-supplementary motor area, thalamus, striatum, midbrain nuclei, and cerebellum (Mayer et al., 2009; Keightley et al., 2014). During the performance of working memory tasks, TBI patients show significantly reduced brain activations in the frontal and parietal regions, temporal lobes, putamen, caudate nucleus, and thalamus (McAllister et al., 2001; Stulemeijer et al., 2010; Gosselin et al., 2011). In addition, significantly increased activations in dorsolateral and anterior MFG, DLPFC, and ventrolateral PFC have also been observed in TBI patients in other task-based functional MRI studies (Scheibel et al., 2007; Turner and Levine, 2008; Kohl et al., 2009; Zhang et al., 2010). In terms of resting-state functional MRI studies in TBI, significantly greater resting functional connectivities between thalamus and widespread cortical regions including the cingulate gyrus, frontal and temporal lobes (Tang et al., 2011), and decreased connectivity in frontal and parietal

regions (Borich et al., 2015) have been observed in those with TBI, relative to controls. Moreover, altered functional brain patterns have been linked with various types of cognitive/behavioral outcomes. In particular, the hypoactivations in brain regions involved in attentional networks are associated with memory performances (Hammeke et al., 2013), hypoactivation of the temporal lobe are correlated with injury severities (Stulemeijer et al., 2010), and increased brain activation in the posterior cerebellum are linked to additional demand for inhibitory control (Krivitzky et al., 2011).

Besides that, other functional neuromodalities such as the magnetic resonance spectroscopy, positron emission tomography, magnetoencephalography, electroencephalography, and functional near-infrared spectroscopy (fNIRS) have also been implemented in the research field of TBI and provide valuable insights into the understanding of the its underlying neurobiological basis (Hibino et al., 2013; Byrnes et al., 2014; Kontos et al., 2014; Rodriguez Merzagora et al., 2014; Vakorin et al., 2016; Brown et al., 2018; Lewine et al., 2019).

1.3 Attention Deficits Following Traumatic Brain Injury

Attention deficits, as one of the most common persisting neurocognitive consequences following TBI, can significantly contribute to poor academic and social functioning and life-long learning difficulties of affected individuals (Stuss et al., 1989; Mirsky et al., 1991; Ponsford and Kinsella, 1992; Kaufmann et al., 1993; Emanuelson and v Wendt, 1997; Eker et al., 2000; Novack et al., 2001; Max et al., 2005a; b; Yeates et al., 2005; Langlois et al., 2006; Kramer et al., 2008; McKinlay et al., 2008; Ginstfeldt and Emanuelson, 2010; Miotto et al., 2010; Catroppa et al., 2011; Daneshvar et al., 2011; Sinopoli et al., 2011; Petersen

and Posner, 2012; Bramlett and Dietrich, 2015; de Freitas Cardoso et al., 2019). The conventional thinking regarding the relatively high prevalence rate of this sequalae is that certain brain regions (i.e., brainstem, fronto-temporal and fronto-parietal regions) which subserve attentional processing function are particularly vulnerable to TBI (Mirsky et al., 1991; Anderson et al., 2005; Petersen and Posner, 2012). In fact, deficits of attention can be more problematic, as disruption of this basic cognitive function may even cause or exacerbate additional disturbances in executive function, communication, and other relatively more complex cognitive functions. However, to date, only small numbers of neuroimaging studies have investigated this severe health condition in the TBI field (Witt et al., 2010) (Keightley et al., 2014) (Mayer et al., 2009). The consensus regarding appropriate evaluation and treatment of TBI induced attention deficits in this cohort is rather limited due to the lack of investigations of the neurobiological substrates associated with this syndrome.

1.4 Objective, Specific Projects and Significance of this Dissertation Research

With this perspective, the overall aim of this dissertation research is to systematically investigate the neurobiological mechanisms associated with attention deficits in adults post TBI, with an ultimate goal of translating hypothesis-driven neurobiological correlates into the quantitatively measurable biomarkers for diagnosis of TBI-induced attention deficits. In order to achieve the overall goal, in this dissertation research, three projects are conducted in different levels and aspects. Details of each project are introduced below.

Project 1 focuses on assessing and comparing differences of brain functional properties, including the regional cortical brain activities and between-regional functional

connectivities, responding to visual attention processing in subjects with and without TBI, by utilizing a novel optical neuroimaging modality, called fNIRS. Associations between altered brain functional properties and attention-related behavioral measures following TBI are further analyzed. Based on the findings of previous studies in TBI (Soeda et al., 2005; Scheibel et al., 2007; Turner and Levine, 2008; Kohl et al., 2009; Mayer et al., 2009; Zhang et al., 2010; Krivitzky et al., 2011; Sozda et al., 2011; Hibino et al., 2013; Kontos et al., 2014; Rodriguez Merzagora et al., 2014; Borich et al., 2015; Saluja et al., 2015; Zhou, 2017; Li et al., 2019), we hypothesize that functional brain alterations specifically in frontal and occipital brain regions would be observed in the TBI group. We further expect that these brain abnormalities would significantly contribute to TBI induced inattention and/or hyperactivity in the affected individuals. Specific experimental procedures, data analysis approaches, results and discussion of Project 1 are introduced in Chapter 3.

Project 2 examines and compares the whole brain network topological properties responding to visual sustained attention processing in individuals with and without TBI, by implementing the functional MRI technique, with a graph theoretic approach for data analysis. Specifically, both nodal-level and global-level functional network properties regarding efficiency, degree, betweenness centrality (BC), and network hub are assessed for both groups. Again, associations between significantly differentiated brain functional network properties and attention-related behaviors following TBI are further analyzed. Based on the findings of existing TBI studies conducted by our research teams and others (Soeda et al., 2005; Scheibel et al., 2007; Turner and Levine, 2008; Kohl et al., 2009; Mayer et al., 2009; Nakamura et al., 2009; Zhang et al., 2010; Krivitzky et al., 2011; Sozda et al., 2011; Caeyenberghs et al., 2012; Hibino et al., 2013; Messe et al., 2013; Pandit et al., 2013;

Kontos et al., 2014; Rodriguez Merzagora et al., 2014; Borich et al., 2015; Saluja et al., 2015; Yan et al., 2017; Zhou, 2017; Li et al., 2019), we hypothesize that altered topological characteristics of the functional brain network for visual attention processing would be observed in adults with TBI, relative to matched controls. We further expect that these functional abnormalities would significantly correlate with inattentive and/or hyperactive behaviors post TBI. Specific experimental procedures, data analysis approaches, results and discussion of Project 2 are introduced in Chapter 4.

Projects 1 and 2 specifically focus on assessing the group-differentiated brain properties in the functional aspect. In Project 3, we investigate the neurobiological substrates associated with attention deficits post TBI in another equally important aspect, which is the structural pattern. The study sample which involved in Project 3 completely overlap with those involved in Project 2. Specifically, brain structural characteristics of both GM and WM tissues are acquired, by utilizing the structural MRI and DTI techniques. Brain imaging measures and then compared between individuals with and without TBI. Correlation analyses are conducted between the brain imaging measures which shows significant between-group differences and attention-related behaviors. Besides that, Project 3 additionally investigate gender-specific patterns of the altered brain structural properties as well as their impacts to behavioral measures. Based on findings of previous studies conducted by our team and other researchers (Gale et al., 2005; Mayer et al., 2009; McGlade et al., 2015; Wu et al., 2018b), we hypothesize that injury induced structural alterations associated with frontal, parietal and occipital cortices, regions well-recognized to play important roles in attentional and inhibitory deployment, would significantly contribute to inattentive and hyperactive behaviors in affected individuals. We further

expect that these anatomical abnormalities would differ between genders. Specific experimental procedures, data analysis approaches, results and discussion of Project 3 are introduced in Chapter 5.

In addition, general methodologies implemented in these three projects are introduced in Chapter 2. Study conclusions and future directions of this dissertation research work are provided in Chapter 6.

Significances of this dissertation research is summarized in the following aspects. First, understanding the neurobiological basis of the most significant long-term neurocognitive consequence in individuals post TBI is urgently needed and vitally important for public health that can inform and ultimately guide effective rehabilitation strategies for treatment and interventions of this syndrome.; Second, compared to most of the existing exploratory and data-driven neuroimaging studies in adults post TBI, this dissertation research is hypothesis-driven, based on the solid understanding of the neurobiology of attention deficits in human brain; Third, relative to existing studies in the imaging setting which utilize isolated neuroimaging techniques, our systematical investigation of the neural basis through full-scale, multi-perspective imaging and analytic approaches have the potential for identifying reliable neurobiological signatures for helping prognosis, diagnosis, treatment, and rehabilitation of neurocognitive consequences following TBI; Fourth, the outcome of this novel and valuable dissertation research may shed light on the neural mechanisms of attention deficits in adults post TBI, suggest the neurobiological targets for treatment of this severe and common condition, and may also provide the important neural foundation for future research to develop effective rehabilitation strategies to improve attention processing in adults post TBI.

CHAPTER 2

GENERAL METHODOLOGY

2.1 Participants

A total of 139 young adults (ranging from 18 through 33 years of age) are initially involved in this dissertation research. All potential subjects are recruited from New Jersey Institute of Technology (NJIT) and Rutgers New Jersey Medical School (Rutgers NJMS) through study flyers. For each of the potential subject, an onsite screening is conducted for eligibility check. During the eligibility screening visit, the general demographical information (i.e., age, gender, education level, participant parents' education level), current status and history of medical conditions are gathered from each person. Specific and general inclusion/exclusion criteria for this dissertation research are given below.

In particular, specific inclusion criteria for the patient group are: having a history of one or multiple sports- and/or recreational activity-related TBIs clinically confirmed at least 6 months prior to study enrollment; having no head injury which caused overt focal brain damage; having no history of diagnosis with attention-deficit/hyperactivity disorder (ADHD) prior to the first onset TBI. In addition, patient subjects who used prescribed psychostimulants to treat TBI-induced symptoms such as attention deficits are required to undergo a washout period for at least 24 h for short-acting and 48 h for long-acting stimulants prior to the scanning procedure (the length of the washout period was determined by the half-life of the medication). Specific inclusion criteria for the control group are: having no history of TBI; having no history of diagnosed ADHD; T-score < 60 for both the inattentiveness and hyperactivity/impulsivity subscales in Conner's Adult

ADHD Self-Reporting Rating Scales (CAARS) (The CAARS scales quantitatively measure the presence and severity of ADHD symptoms in adults, and provide a multiple-informant assessment with self-report and observer ratings) (Epstein, 2006), which are administered during study assessments, with higher scores indicate greater behavioral concerns. General inclusion criteria for both subject groups are: native or fluent speakers of English, strongly right-handed measured using Edinburgh Handedness Inventory (The Edinburgh Handedness Inventory is a measurement scale used to assess the dominance of a person's right or left hand in everyday activities, which can be used by an observer assessing the person, or by a person self-reporting hand use.) (Oldfield, 1971). General exclusion criteria for both groups are: having a history or current diagnosis of neurological and psychiatric disorders such as generalized anxiety disorder, major depression, obsessive-compulsive disorder, autism spectrum disorder, substance use disorder, conduct disorder, and learning disorders; received treatment with any non-stimulant psychotropic medication within the month prior to testing; MRI constraints such as metal implants, claustrophobia, etc.

Among the 139 adults, 20 do not match the inclusion criteria and thus are excluded from the further study visit. Among the 119 young adults who are eligible for the study participation, 56 are individuals with TBI, including 29 male patients and 27 female patients. Sixty-three are demographically matched normal controls (NC), including 35 males and 28 females. A second onsite visit is then scheduled for all these 119 subjects to collect imaging data. This dissertation research receives Institutional Reviewed Board Approvals at NJIT and Rutgers. Written informed consents are provided by all participants after the nature of the study and its procedures are carefully explained.

Detailed demographic characteristics regarding age, gender, race/ethnicity and education level for each of the 119 participants are summarized in Table 2.1.

Table 2.1 Demographic Characteristics of All Participants (Continued)

Sub ID	Grp	Age	Gen	R/E	EYC	Sub ID	Grp	Age	Gen	R/E	EYC
B001	NC	26	M	Black	18	B012	NC	21	M	Asian	16
A004, B013	NC	24	M	Asian	16	A003, B015	NC	24	M	Asian	16
A021, B027	NC	25	M	Asian	n/a	B031	NC	27	M	Asian	18
B033	NC	27	M	Asian	17	A045, B034	NC	22	M	Caucasian	16
B038	NC	24	M	Asian	16	B044	NC	25	M	Asian	16
B046	NC	24	M	Asian	16	A087, B051	NC	18	M	Black	12
B052	NC	24	M	Asian	16	B058	NC	23	M	Caucasian	14
B059	NC	24	M	Asian	16	B060	NC	18	M	Black	12
B086	NC	20	M	Caucasian	14	B089	NC	20	M	Asian	14
B090	NC	22	M	Caucasian	15	B096	NC	24	M	Asian	17
B109	NC	18	M	Hispanic	12	B110	NC	20	M	Caucasian	13
B115	NC	19	M	Asian	12	B009	NC	26	F	Asian	17
A052, B010	NC	21	F	Caucasian	15	A020, B016	NC	22	F	Asian	16
A058, B025	NC	18	F	Caucasian	12	A043, B028	NC	23	F	Caucasian	15
,B036	NC	19	F	Black	13	B037	NC	28	F	Asian	16
A082, B045	NC	19	F	Caucasian	12	A023, B049	NC	19	F	Caucasian	14
B050	NC	24	F	Asian	16	B054	NC	20	F	More than one	14
B056	NC	23	F	Asian	17	B087	NC	20	F	Hispanic	14
B088	NC	24	F	Caucasian	17	B091	NC	22	F	Caucasian	16
B092	NC	22	F	More than one	15	B094	NC	26	F	Caucasian	20
B108	NC	20	F	More than one	13	B112	NC	20	F	Black	13
B113	NC	20	F	Caucasian	13	B114	NC	20	F	Caucasian	13
B117	NC	20	F	Hispanic	13	A005, B014	NC	24	M	Caucasian	18
A006	NC	25	M	Asian	16	A010	NC	22	M	Asian	14
A011	NC	26	M	Asian	16	A015, B022	NC	26	M	Asian	17
A028	NC	23	F	Caucasian	16	A041	NC	22	M	Asian	16
A042	NC	18	F	Caucasian	12	A050, B032	NC	23	F	More than one	15
A051	NC	19	M	Black	13	A073	NC	21	M	Caucasian	15
A079	NC	19	M	Caucasian	13	A083	NC	21	M	Black	14

Table 2.1 (Continued) Demographic Characteristics of All Participants

Sub ID	Grp	Age	Gen	R/E	EYC	Sub ID	Grp	Age	Gen	R/E	EYC
A098	NC	18	F	Hispanic	13	A099	NC	20	M	Caucasian	14
A100	NC	21	F	Caucasian	14	A002	NC	27	F	Asian	16
A014	NC	33	M	Caucasian	18						
B002	TBI	27	F	Asian	20	A036, B003	TBI	18	F	Caucasian	13
A032, B006	TBI	18	F	Caucasian	13	A059, B017	TBI	18	F	Asian	n/a
A068, B039	TBI	21	F	Caucasian	15	A069, B043	TBI	21	F	More than one	15
B069	TBI	22	F	Caucasian	15	B072	TBI	22	F	Caucasian	15
B076	TBI	21	F	Caucasian	13	B079	TBI	26	F	Asian	16
B081	TBI	23	F	Black	14	B097	TBI	18	F	Black	12
B102	TBI	22	F	More than one	15	B104	TBI	19	F	Caucasian	12
B107	TBI	22	F	Caucasian	15	B116	TBI	20	F	Asian	13
B118	TBI	21	F	More than one	14	B119	TBI	23	F	Caucasian	16
B120	TBI	23	F	Caucasian	12	B122	TBI	21	F	Black	14
B123	TBI	21	F	Caucasian	14	A060, B019	TBI	21	M	Caucasian	14
A066, B021	TBI	21	M	Caucasian	14	A067, B023	TBI	26	M	Asian	15
A040, B024	TBI	19	M	Caucasian	13	A071, B026	TBI	20	M	Caucasian	13
B030	TBI	21	M	Asian	14	B035	TBI	21	M	Caucasian	13
A081, B040	TBI	23	M	Black	15	B041	TBI	22	M	Black	15
A080, B042	TBI	22	M	Asian	16	A085, B048	TBI	23	M	Latino	15
B055	TBI	23	M	Asian	17	A078, B061	TBI	21	M	Others	15
B062	TBI	21	M	Caucasian	14	A086, B065	TBI	19	M	Asian	13
B071	TBI	22	M	Caucasian	15	B073	TBI	26	M	Asian	16
B098	TBI	20	M	Caucasian	13	B101	TBI	19	M	Black	12
B103	TBI	21	M	Caucasian	13	B106	TBI	20	M	Caucasian	13
B111	TBI	21	M	Black	14	B121	TBI	23	M	More than one	15
A030	TBI	18	F	Black	12	A034	TBI	19	F	Asian	14
A035	TBI	21	F	Caucasian	14	A046	TBI	18	F	Caucasian	12
A054	TBI	26	M	Caucasian	13	A057	TBI	22	F	Caucasian	16
A063	TBI	22	F	Caucasian	15	A072	TBI	19	M	Caucasian	13
A074	TBI	18	M	Caucasian	13	A075	TBI	18	M	Black	12
A077	TBI	20	M	Black	14	A084	TBI	21	M	Black	14

Sub ID: Subject ID number; Grp: group type; Gen: gender; R/E: race/ethnicity; EYC: the number of completed education years; NC: normal controls; TBI: traumatic brain injury; M: male; F: female (Subject ID starts with letter "A" and "B" denotes participants who involved in the functional near-infrared spectroscopy study and multimodal magnetic resonance imaging study, respectively.)

2.2 General Techniques of Functional Near-Infrared Spectroscopy

2.2.1 Functional Near-Infrared Spectroscopy Instrument

Major fNIRS system usually consists four components, including the NIRS unit, headcap, navigation sensor, and user interface device (Figure 2.1).

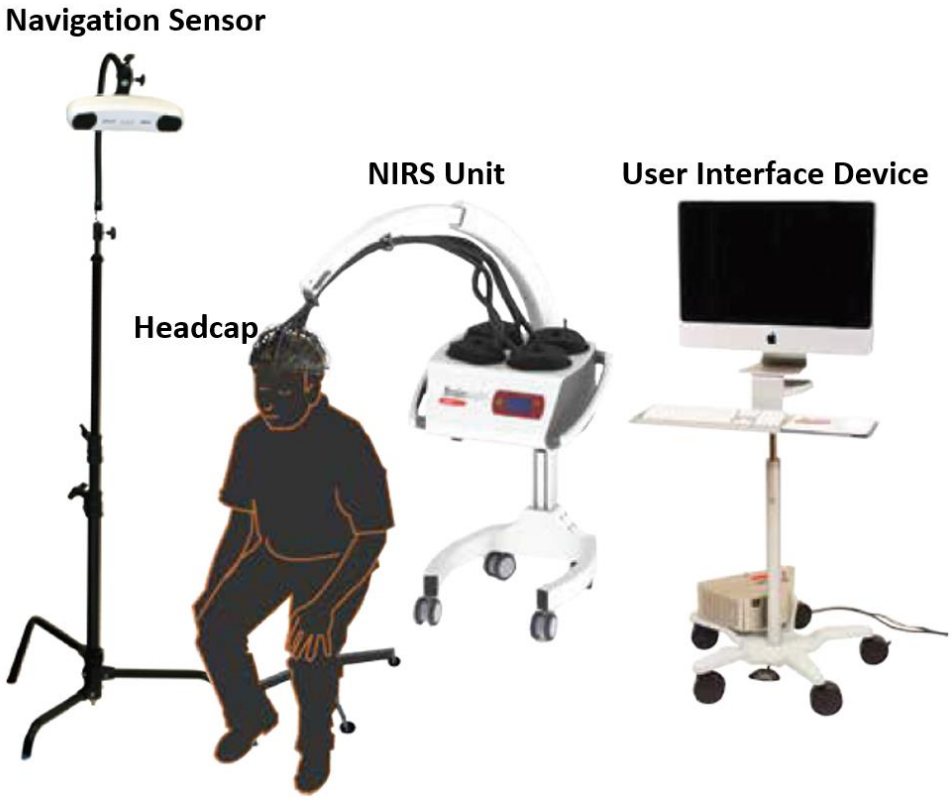

Figure 2.1 Main components of fNIRS instrument.
(Source: Brainsight NIRS User Manual v2.3)

The NIRS unit contains the electronic devices, allowing to manage the optical modules, acquire and process the NIRS data and interface with external control devices. The optical module generates the NIR light that is channeled into the head and measure the resulting light scattered within the brain. The headcap is designed to rigidly hold the NIRS optodes on the head. The navigation sensor system helps for the appropriate

localization and co-registration of optodes. The user interface device offers the graphical visualization for the setup.

2.2.2 Basic Principles of Functional Near-Infrared Spectroscopy Data Generation and Acquisition Parameters

fNIRS allows non-invasive measurement of cerebral oxygenation levels utilizing continuous NIR light (usually between 650 and 950 nm) (Hibino et al., 2013; Kontos et al., 2014; Rodriguez Merzagora et al., 2014). NIR light is emitted into the head and undergoes random scattering and absorption processes in the tissue, with a fraction propagates through the brain tissue on a banana-shaped path back to the surface where is then detected by a photodetector (Figure 2.2).

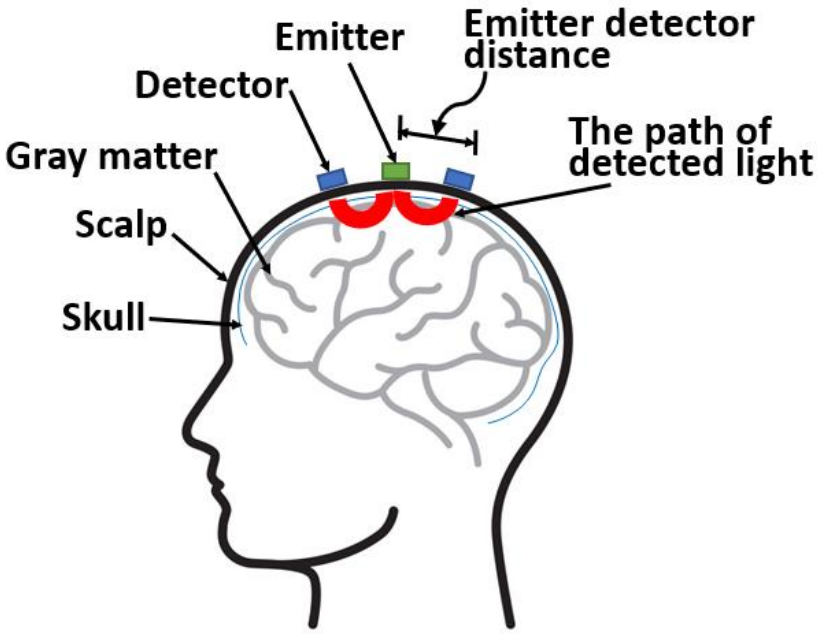

Figure 2.2 Principle of fNIRS measurement.

Most parts of the tissue and largely water are relatively transparent to light in the NIRS range, allowing the emitted light to penetrate the skull and reach sufficient depth (Okada et al., 1997). Some chromophores such as oxy-hemoglobin (OxyHb), deoxy-hemoglobin (DeoxyHb) are strong absorbers for NIR light with their concentrations changing with metabolism and blood flow. Optical imaging at centimeter depths is afforded by the relationship of the absorption spectra of water, OxyHb and DeoxyHb, the three primary absorbers in tissue at near-infrared wavelengths. The water spectrum at those wavelengths permits a "spectral window" in the background absorption allowing investigators to see the hemoglobin (Figure 2.3). Moreover, within this window, the spectra of OxyHb and DeoxyHb are distinct enough to allow spectroscopy and recovery of separate concentrations of both types of molecules.

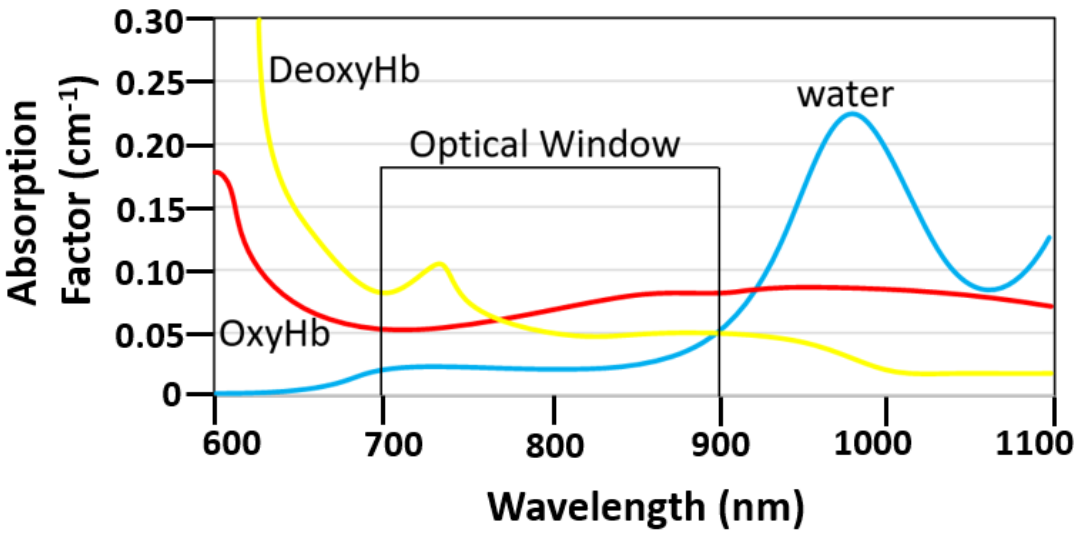

Figure 2.3 Absorption spectra of oxygenated hemoglobin and deoxygenated hemoglobin.

The modified Beer-Lambert Law (MBLL) (Baker et al., 2014) is utilized for measuring the attenuation changes in light at two or more wavelengths, allowing for calculating the hemoglobin concentration changes. Unlike the traditional approach that

quantify the absorption coefficient within purely absorbing samples, the MBLL adds a differential path-length factor (DPF) to account for the increased path-length of light through the sample due to the highly scattering tissue by using the following equation (Rajashree Doshi, 2013; Baker et al., 2014):

$$\boldsymbol{OD = Log(I_0/I) = \varepsilon \cdot c \cdot L \cdot DPF} \quad (2.1)$$

where OD is the optical density; I_0 is the light intensity of incident light; I is the light intensity of transmitted light; ε is the extinction coefficient of hemoglobin; c is the concentration of hemoglobin; L is the length of distance between source-detector pair; and DPF is the differential path-length factor.

The fNIRS instrument we implement in this dissertation research is the TechEn's continuous-wave 6 (CW6) real time system (http://www.nirsoptix.com/publications.html). CW NIR lights of 690 nm and 830 nm wavelengths are used to obtain quantitative estimates of relative changes primarily in OxyHb and DeoxyHb during functional activity. CW technology is used widely for functional measurements because of the large number of source and detector channels, low cost, non-ionizing radiation, portability, and ease of setup for patient use. It provides real-time data acquisition and display, which have dramatically advanced the state of NIRS technology. Continuous real-time data acquisition of the entire head is achieved by incorporating eight source lasers and sixteen detectors in this CW6 system architecture, along with novel software and digital signal processing. The very fast, real-time output sample rate of the CW6 offers significantly higher resolution than previous systems, and generally provides for superior dynamic range. The

demodulated output sampling rate is 50 Hz. A total of eight connectors for auxiliary signals and triggers from external devices are also provided. This allows integration of E-Prime, a physiological instrument, with the CW6 by saving the data in the same file for display and analysis.

2.3 General Techniques of Multimodal Magnetic Resonance Imaging

2.3.1 Magnetic Resonance Imaging Scanners

Major components of MRI scanners (Figure 2.4) consist of the main static magnetic field, radiofrequency (RF) coils, gradient coils, shimming coils, and computer control system (Scott A. Huettel).

Figure 2.4 MRI scanner.

In particular, the main static magnetic field is generated by a series of electromagnetic coils which carry very large currents around the scanner, allowing to align certain nuclei within the human body (e.g., hydrogen nuclei) for the mapping of tissue properties. RF coils are utilized for producing MR signals by generating and receiving electromagnetic fields at the resonant frequencies of the atomic nuclei within the static magnetic field. This is based on the understanding that most atomic nuclei of interest for MRI studies have resonant frequencies in the RF portion of the electromagnetic spectrum. Gradient coils provide the spatial information for MR imaging. A gradient coil caused the MR signal to become spatially dependent in a controlled fashion, so that different locations in space contribute differently to the measured signal over time. Three gradient coils which typically oriented along the cardinal directions (x, y, and z) relative to the static magnetic field are used to modify the strength of the magnetic field. The direction represented by z is parallel to the main field, while x and y are perpendicular to the main field and to each other. Shimming coils can produce multiple order magnetic fields in order to generate compensatory magnetic fields that correct for the inhomogeneity in the static magnetic field. Computer control system is used to coordinate all hardware components (e.g., gradient coils, RF coils) for digitizing, decoding, and displaying MR images. In addition, specialized software requirements are also needed for collection and analysis of MRI images by sending instructions to the scanner hardware via a graphic user interface (Figure 2.5).

Figure 2.5 Graphic user interface for MRI data collection.

2.3.2 Basic Principles of Magnetic Resonance Signal Generation

MR signal generation depends on the following physical principles. Atomic nuclei with the nuclear magnetic resonance (NMR) property have an intrinsic characteristic called spin. When placed in a static strong magnetic field, these nuclei precess around an axis that is either parallel to the magnetic field (low-energy) or antiparallel to the magnetic field (high-energy). When RF pulse are applied to the magnetized nuclei, some low-energy nuclei will absorb the energy from the system and change to the high-energy state, effectively converting the longitudinal magnetization (parallel to the magnetic field) into transverse magnetization (this process is called excitation). Once the RF pulses are turned off, excited nuclei will return to the low-energy state by releasing the absorbed energy. The emitted energy which will be picked up by the receiver coil provides the MR signal data and will be eventually transformed into images (Scott A. Huettel).

As known, MRI does not use projection, reflection or refraction mechanisms commonly used in optical imaging methods to form image. For MR image formation, the spatial information of the protons contributing MR signal is determined by the spatial frequency and phase of their magnetization. Spatially varying magnetic field is generated by using the gradient coils. Spins at different location in the strong magnetic field thus precess at unique frequencies, allowing to reconstruct MR images. In general, construction of a sequence of three-dimensional MR images includes three steps, the initial selection of a two-dimensional slice (using the z-gradient), the pre-application of one spatial gradient during phase encoding (using the y-gradient), and the application of another gradient for frequency encoding (using the x-gradient) during acquisition of the MR signal (Scott A. Huettel). In specific, slice selection allows to restrict the MR signal recorded in the detector coils to one two-dimensional slice at a time. The key element of slice selection is to ensure that there is a match between the precession frequency of the spins within the desired slice and the RF excitation pulse. A positive spatial gradient (G_Z) along the z direction gives a continuous change in the strength of the magnetic field (stronger towards the back of the scanner allowing spins toward more rapidly and weaker at the front of the scanner where spins would precess more slowly). An excitation RF pulse which contains the same frequency range as the precession frequencies of spins in a particular band (specific brain region) within the gradient field (Scott A. Huettel). A slice with a desired thickness was created by calculating the bandwidth for the excitation pulse using the formula:

$$\Delta \boldsymbol{Z} = {}^{\Delta \boldsymbol{\omega}}/_{\boldsymbol{\gamma G_Z}} \qquad (2.2)$$

where ω is the center frequency; γ is a constant value (i.e., for hydrogen: $\gamma = 42.58\ MHz/Tesla$); and G_Z is the z-gradient. Then two additional gradients (frequency-encoding gradients/x-gradients and phase-encoding gradients/y-gradients) which cause spins at different spatial locations to precess at different rates were applied.

2.3.3 Functional Magnetic Resonance Imaging Technique

Functional MRI, with the concept builds on the earlier MRI scanning technology and the discovery of properties of oxygen-rich blood, capitalizes on magnetic differences between oxygenated and deoxygenated blood during neuronal activation and rest. This technique relies on an endogenous measure called blood-oxygenation-level-dependent (BOLD) contrast (Scott A. Huettel). In particular, a stimulus (i.e., visual, vibration, motor activity) causes neuronal activity that increases the cerebral blood flow, cerebral blood volume, and oxygen delivery. Blood flow increases to a greater extent than necessary simply to provide oxygen and glucose for the increased energy production, resulting in a local reduction in deoxygenated blood. While oxygenated blood is isomagnetic, deoxygenated blood is slightly paramagnetic relative to brain tissue, and thus slightly distorts the magnetic field in its vicinity. These microscopic field inhomogeneities associated with the presence of deoxyhemoglobin lead to the shortening of the relaxation time within the tissue voxel and is also called static dephasing. Thus, variations in regional tissue oxygenation due to changes in oxygen uptake and altered blood supply caused by localized brain activity can thereby be mapped by the MRI scanner. This ability to probe functional changes within the intact brain is based on physical principles of NMR and the intrinsic effects of blood oxygenation on the MR signal due to the magnetic properties of the DeoxyHb. The idea of BOLD contrast is firstly introduced by Ogawa and colleagues in 1990 in a rat model

(Ogawa et al., 1990), with a follow up work which shows the association between intrinsic blood oxygenation changes in normal physiology and neural activity changes, providing evidence of functional MRI as an effective tool to examine brain activity patterns (Ogawa et al., 1992).

The most common imaging sequence used for functional MRI is echo planar imaging (EPI). In EPI, imaging data are acquired by sampling during a train of rapid field gradient reversals following RF excitation of protons. The type of contrast that is generated is determined by whether a spin echo or gradient echo preparation is used, as well as sequence parameters, such as echo time (TE), sequence repetition time (TR), and flip angle. For functional MRI studies, gradient echo preparation is typically used since it confers a signal advantage over spin echo preparation.

2.3.4 Structural Magnetic Resonance Imaging Technique

Structural MRI provides information to qualitatively and quantitatively describe the shape, size, and integrity of GM and WM structures in the brain. In brief, MRI signal varies across tissue types because GM contains more cell bodies (e.g., neurons and glial cells) than WM, which is primarily composed of long-range nerve fibers (myelinated axons), along with supporting glial cells. Morphometric techniques measure the volume or shape of GM structures, such as subcortical nuclei or the hippocampus, and the volume, thickness, or surface area of the cerebral neocortex. Macrostructural WM integrity can also be measured using volumes of normal and abnormal WM, providing indications of inflammation, edema, or demyelination, complementing microstructural diffusion weighted MRI to provide a comprehensive picture of WM integrity (https://www.mrsolutions.com/applications/preclinical-imaging/anatomical-imaging/).

Many pulse sequences are available, emphasizing different aspects of normal and abnormal brain tissue. By modifying sequence parameters such TR and TE, for example, anatomical images can emphasize contrast between GM and WM or between brain tissue and cerebrospinal fluid (http://fmri.ucsd.edu/Howto/3T/structure.html).

2.3.5 Diffusion Tensor Imaging Technique

DTI is an MRI-based neuroimaging technique which makes it possible to estimate the location, orientation, and anisotropy of the brain's WM tracts. The architecture of the axons in parallel bundles and their myelin shield facilitate the diffusion of the water molecules along their main direction. When applies diffusion gradients in at least six non-collinear directions, it is possible to calculate, for each pixel, a diffusion tensor that describes this diffusion anisotropy. The fiber's direction is indicated by the tensor's main eigenvector (https://www.imagilys.com/brain-imaging-neuroimaging-techniques/).

Diffusion-weighted images are routinely accomplished by applying strong pulsed "diffusion" gradients during the evolution of the MR signal (Holdsworth and Bammer, 2008). Typically, the diffusion-weighted signal is generated by a spin echo with diffusion gradients straddling the 180-degree refocusing pulse, after which the signal is read out with the more or less standardized EPI trajectory. The reduction in signal can be related to the amount of diffusion that is occurring in the tissue and how much diffusion sensitivity the diffusion gradients add to the spin echo sequence. The amount of diffusion sensitivity is a function of the gradient-related parameters: strength, duration, and the period between diffusion gradients, and is represented by the b-value.

FA is a common measurement used in DTI studies and ranges from 0, isotropic movement of water molecules (e.g., cerebrospinal fluid), to 1, anisotropic movement of

water molecules (e.g., fiber bundles) (https://en.wikipedia.org/wiki/Fractional_anisotropy). It can be computed for each voxel to express the preference of water to diffuse in an isotropic or anisotropic manner. The mathematical principel for FA calculation is shown below in Equation (2.3), where D_x, D_y, and D_z represent the three principal axes of the diffusion tensor:

$$FA = \frac{\sqrt{(D_x - D_y)^2 + (D_y - D_z)^2 + (D_z - D_x)^2}}{\sqrt{2({D_x}^2 + {D_y}^2 + {D_z}^2)}} \tag{2.3}$$

FA values approaching 1 indicate that nearly all of the water molecules in the voxel are diffusing along the same preferred axis, while FA values approaching 0 indicated that the water molecules are equally likely to diffuse in any direction.

2.4 Multimodal Magnetic Resonance Imaging Data Acquisition Protocols

A 3-Tesla 32 Channel Siemens TRIO (Siemens Medical Systems) scanner at the Rutgers University Brain Imaging Center is used for multimodal MRI data acquisition. Acquisition protocols exceed Biomedical Informatics Research Network recommendations (http://www.nbirn.net/), which ensure the image quality and stability.

Functional MRI data are collected using a gradient echo-planar sequence with the flowing parameters: TR = 1000 ms, TE = 28.8 ms; field of view (FOV) =, voxel size = 1.5mm×1.5mm ×2.0mm, number of slices = 300.

The structural MRI data were collected using a magnetization prepared rapid gradient echo sequence with the following parameters: TR = 1900 ms, TE = 2.52 ms, flip

angle = 9°; FOV = 350mm×263mm×350 mm, voxel size = 1.0mm×1.0mm ×1.0mm, number of slices = 176.

DTI data were acquired using an EPI pulse sequence with the following parameters: TR= 7700 ms, TE= 103 ms, FOV = 220mm×220mm×138 mm, voxel size = 2.0mm×2.0mm ×2.5mm, number of slices = 55, b-value = 700 s/mm^2 along 30 independent directions, as well as a reference volume without diffusion-weighting (b = 0 s/mm^2).

2.5 Experimental Task Utilized in Projects 1 and 2

During data acquisition of Project 1 and 2, each subject performed a visual sustained attention task (VSAT), which is designed to assess individual's behavioral capacity of sustained attention (defined as the ability to maintain the focus of cognitive activity over time on a given task or stimulation) (Li et al., 2012a; De La Fuente et al., 2013; Li et al., 2013; Xia et al., 2014; Wu et al., 2018b). The VSAT is an enhanced continuous performance test (CPT), which has been widely validated for its capability of measuring sustained attention abilities (Barkley RA, 1990; Halperin et al., 1990; Rubia et al., 2009; Schneider et al., 2010; Tana, 2010). To achieve maximal measurement power in a relatively brief period, block design is used for the VSAT, with each stimulus formed by a three-digit stimulus set. Block designs have superior measurement characteristics in a given time period relative to event-related designs (at a cost of experimental flexibility). Multi-digit stimuli evoke more attentional demands than single-digit stimuli. In addition, to increase the power for detecting differences across inattentive symptoms, a sufficient long block length (30 seconds) is given in this block designed VSAT to maximize variability between task and non-task blocks (Li et al., 2012a).

The VSAT design is shown in Figure 2.6. It consists of five task blocks (marked as "T") interleaved by five rest blocks (marked as "R"). Each block lasts for 30 seconds.

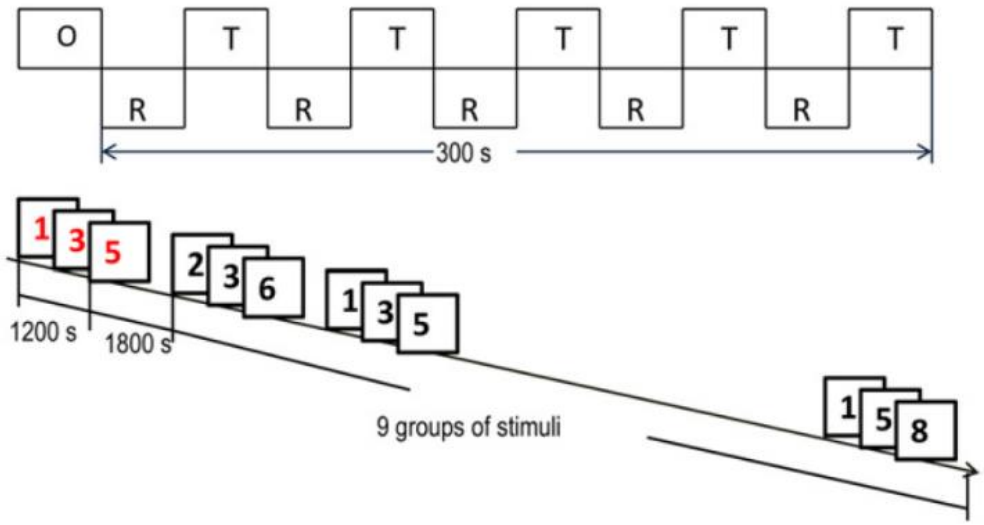

Figure 2.6: VSAT design structure and the sequence of one task block. (O: initial fixation period; R: 30 seconds' rest block; s: seconds; T: 30 seconds task block (Li et al., 2012a; Wu et al., 2018b).

During the rest blocks, the participant was instructed to keep their eyes open and to remain as relaxed and motionless as possible. In each of the five task blocks, a red cross appeared in the center of the computer screen and lasts for 800 milliseconds. Then a target sequence of three-digit sets (1-3-5, 2-5-8, 3-7-9, 5-2-7 and 6-1-8, respectively) were shown in red at the rate of one digit per 400 milliseconds. After a 1.0-second delay during which participants were required to remember the current target sequence, nine sequences of three digits, ranging from 1 to 9, appeared in black in a pseudo-random order at the rate of 400 milliseconds per digit. A 1.8 second response period ensued after each sequence. In this response period, the subject was asked to press the left button of a response box with the forefinger of their right hand as fast as possible when the stimulus sequence (black ones) matched the target sequence (red ones), and to press the right button with the middle finger

otherwise. The duration of the entire task was 5 minutes. A set of task training blocks was provided to each participant to ensure that they understood the requirements of the task (Li et al., 2012a).

The VSAT was implemented by the E-prime 2.0 software (https://pstnet.com/products/e-prime/). It allowed to synchronize the start time point of visual stimuli presentation with the fNIRS or MRI data collection. A logfile including information regarding the onset times of the stimuli, the reaction times and the real-time response of the subject was obtained during the task, allowing to compute the number of correct responses, errors of omission and commission and mean hit reaction time of each subject. An omission error is committed whenever the subject does not respond to the nontarget stimulus and is used for measuring subject's inattention; a commission error is committed whenever the subject gives an incorrect response to a non-target stimulus and is used for measuring subject's impulsivity (Wu et al., 2018b). Before the data collection in Project 1 and 2, participants were provided a set of task training blocks to ensure that they understood the requirements of the task.

2.6 Statistical Methods Implemented in Projects 1, 2, and 3

2.6.1 Chi-square Test of Independence

Chi-square test of independence is a statistical test that used to determine if there is a significant relationship between two or more nominal (categorical) variables. It is based on the difference between the observed frequency in the data and the expected frequency if there was no relationship between the variables. The calculation of the Chi-square test of independence is shown as:

$$\chi^2 = \sum \frac{(O_i - E_i)^2}{E_i} \tag{2.4}$$

where O_i is the observed frequency of an outcome; E_e is the expected frequency if no relationship existed between the variables.

2.6.2 Independent Sample T-test

The independent sample t-test is a parametric test that compares two independent groups on the mean value of a continuous and normally distributed variable. The test statistic t is computed as:

$$t = \frac{\overline{x}_1 - \overline{x}_2}{s_p \sqrt{(\frac{1}{n_1} + \frac{1}{n_2})}} \tag{2.5}$$

with

$$s_p = \sqrt{\frac{(n_1 - 1){s_1}^2 + (n_2 - 1){s_2}^2}{n_1 + n_2 - 2}} \tag{2.6}$$

where $\overline{x}_1$ and $\overline{x}_2$ are the means of two samples; n_1 and n_2 are the size of two samples (i.e., number of observations); s_1 and s_2 are the standard deviation of two samples; and s_p is the pooled standard deviation. The calculated t value is then compared to the critical t value from a t distribution table with degrees of freedom (equals to $n_1 + n_2 - 2$) and chosen confidence level.

2.6.3 One-way Analysis of Variance and One-way Analysis of Covariance

The one-way analysis of variance (ANOVA) is used to determine whether there are any significant differences between two or more independent groups on a dependent variable. The test statistic F is computed as:

$$F = \frac{variance\ between\ groups}{variance\ due\ to\ sampling\ error} = \frac{MS_{between-groups}}{MS_{within-groups}} \tag{2.7}$$

$$MS_{between-groups} = \frac{SS_{between-groups}}{df_{between-groups}} \tag{2.8}$$

$$MS_{within-groups} = \frac{SS_{within-groups}}{df_{within-groups}} \tag{2.9}$$

where SS is the sum of squares; df is the degree of freedom.

The one-way analysis of covariance (ANCOVA) is an extension of the one-way ANOVA to incorporate a covariate. The one-way ANOVA looks for differences in the group means, whereas the one-way ANCOVA looks for differences in adjusted means (i.e., adjusted for the covariate), which allows to examine the influence of an independent variable on a dependent variable while removing the effect of the covariate factor. In particular, the one-way ANCOVA first conducts a regression of the independent variable (i.e., the covariate) on the dependent variable. The residuals (the unexplained variance in the regression model) are then subject to an ANOVA in order to test whether

the independent variable still influences the dependent variable after the influence of the covariate(s) has been removed.

2.6.4 Pearson's Correlation Analysis

The Pearson's correlation analysis is a bivariate analysis which is used for determining the empirical relationship between two variables. It utilizes the Pearson's correlation coefficient to represent the correlation strength. Pearson's correlation coefficient is a measure of the linear correlation between two variables with a value between -1 and 1, where -1 indicates a total negative linear correlation, 0 is no linear correlation, and 1 is stands for a total positive linear correlation. It is defined as:

$$\rho_{X,Y} = \frac{cov(X,Y)}{\sigma_X \sigma_Y} = \frac{E[(X-\mu_X)(Y-\mu_Y)]}{\sigma_X \sigma_Y} \tag{2.10}$$

where μ_X, μ_Y are the mean of X and Y; σ_X, σ_Y are the standard deviation of X and Y.

CHAPTER 3

PROJECT 1: FUNCTIONAL NEAR-INFRARED SPECTROSCOPY STUDY

3.1 Introduction

Over the last two decades, increasingly neuroimaging studies have started to demonstrate functional brain abnormalities in TBI patients, and their associations with attention-related deficits following TBI. Specifically, multiple task-based functional MRI studies have demonstrated significantly increased activations in dorsolateral and anterior MFG, DLPFC, and ventrolateral PFC in patients with TBI compared to group-matched healthy controls when performing visual working memory, executive control, and cognitive rehablitation tasks (Scheibel et al., 2007; Turner and Levine, 2008; Kohl et al., 2009; Zhang et al., 2010). Another functional MRI study reports significantly reduced neural activations in posterior parietal cortex and frontal eye fields prefrontal cortex during attentional disengagement in adults with mild TBI, relative to group-matched controls (Mayer et al., 2009). Abnormal activation in the anterior cingulate cortex is also observed in patients with TBI relative to controls, when performing cognitive control tasks (Soeda et al., 2005; Sozda et al., 2011). In addition, increased resting-state functional connectivity (FC) in the posterior cingulate gyrus and decreased connectivity in frontal and parietal regions are reported in adolescent athletes with concussion, relative to controls (Borich et al., 2015). Greater activation in the posterior cerebellum and its association with additional demand for inhibitory control are

reported in a functional MRI study in children with mild TBI, relative to matched controls (Krivitzky et al., 2011). Furthermore, altered hemodynamic responses and functional connectivities associated with temporal, insular cortices, and subcortical areas are demonstrated in children and adults with TBI relative to controls in other functional MRI studies (Saluja et al., 2015; Zhou, 2017; Li et al., 2019). Nevertheless, significantly decreased and/or no significant change in frontal areas are also reported in multiple functional MRI studies in patients with TBI (Soeda et al., 2005; Sanchez-Carrion et al., 2008; Krivitzky et al., 2011; Kontos et al., 2014).

fNIRS is a non-invasive, portable neuroimaging technique which utilizes near-infrared light propagating diffusely through the scalp and brain, for functional monitoring and imaging of human brain hemodynamics (Irani et al., 2007; Ferrari and Quaresima, 2012; Shin et al., 2016; Scarapicchia et al., 2017; Siddiqui et al., 2017). It detects optical property changes of cerebral cortex, based on the different absorption characteristics of OxyHb and DeoxyHb. This neuroimaging modality works with a portable and wearable device, which is less sensitive to head motion and allows more flexibility in subject setup during the experiment, without scanner environmental constraints. This optical imaging technique thus has provided notable contributions in newborn infants' studies (Ferrari and Quaresima, 2012; Siddiqui et al., 2017) full-body behaviors (such as body exercise) examination studies (Scarapicchia et al., 2017) and many other studies in brain disorders (Irani et al., 2007). By employing fNIRS in TBI studies, significantly reduced brain

activation in bilateral frontal areas are demonstrated in patients with sports-related TBI during performances of spatial design memory, digit-symbol substitution (symbol match), and working memory tasks (Kontos et al., 2014). Increased activation in the medial frontal regions are observed in patients with severe TBI during performances of multiple cognitive rehabilitation tasks (Hibino et al., 2013). Meanwhile, fNIRS studies also demonstrate increased brain activation in left prefrontal areas in TBI patients during verbal working memory processing (Rodriguez Merzagora et al., 2014). However, none of the existing fNIRS studies have directly investigated attention processing brain mechanisms in TBI. Throughout the current neuroimaging studies in TBI, inconsistency of the findings can be mainly caused by the differences of the imaging and analytic techniques and heterogeneity of the study cohorts in terms of demographic characteristics, pathoanatomic and physical mechanisms of the injuries.

Project 1 focused on understanding the neurophysiological underpinings of TBI induced attention deficits by utilizing fNIRS. fNIRS data from the TBI participants and the group-matched controls were collected during performance of the VSAT. Based on the findings of previous studies in TBI (Soeda et al., 2005; Scheibel et al., 2007; Turner and Levine, 2008; Kohl et al., 2009; Mayer et al., 2009; Zhang et al., 2010; Krivitzky et al., 2011; Sozda et al., 2011; Hibino et al., 2013; Kontos et al., 2014; Rodriguez Merzagora et al., 2014; Borich et al., 2015; Saluja et al., 2015; Zhou, 2017; Li et al., 2019), we hypothesized that functional brain alterations in frontal and occipital brain regions would

be observed in the group of TBI subjects. We further expected that these brain functional abnormalities would significantly contribute to TBI induced inattention in those affected individuals.

3.2 Project Specific Participants

Among the total of 119 participants, 56 performed the fNIRS experiment, including 29 NC and 27 with TBI. Two controls (1 male and 1 female) did not complete the data collection and were excluded from further analysis. This attrition leaves a total of 27 patients and 27 group-matched NC for group-level analysis of Project 1. Demographic characteristics of these 54 subjects are summarized in Table 3.1.

Table 3.1 Demographic, Clinical, and Task Performance Measures in the Groups of NC and TBI (Continued)

	NC (N=27)	**TBI (N=27)**	
	Mean (SD)	**Mean (SD)**	**p**
Age (years)	21.5 (2.50)	20.5 (2.28)	0.117
Education (years)	14.6 (1.68)	13.9 (1.178)	0.075
Mother's education (years)	15.6 (1.96)	15.8 (2.53)	0.715
Father's education (years)	16.3 (2.72)	15.5 (2.78)	0.315
Conners' Adult ADHD Rating Scale (T score)			
Inattentive	46.7 (6.31)	56.6 (17.6)	**0.009**
Hyperactive/impulsive	42.7 (6.56)	54.1 (14.7)	**0.001**
ADHD Total	40.2 (5.57)	49.4 (12.2)	**0.001**
	N (%)	**N (%)**	**p**
Male	16 (59.3)	16 (59.3)	1.00
Right-handed	27 (100)	27 (100)	1.00
Race/ Ethnicity			0.773
Caucasian	12 (44.4)	14 (51.9)	
Black or African American	3 (11.1)	5 (18.5)	
Asian	9 (33.3)	5 (18.5)	

Table 3.1 (Continued) Demographic, Clinical, and Task Performance Measures in the Groups of NC and TBI

	N (%)	**N (%)**	**p**
Hispanic/Latino	1 (3.70)	1 (3.70)	
More than one race	1 (3.70)	1 (3.70)	
Others	1 (3.70)	1 (3.70)	
fNIRS task performance measures			
Accuracy rate	0.993 (0.012)	0.984 (0.041)	0.284
Omission error rate	0.002 (0.009)	0.006 (0.019)	0.313
Commission error rate	0.005 (0.009)	0.010 (0.024)	0.329
Reaction time(ms)	525 (163)	524 (157)	0.979

NC: normal control; TBI: sports-related concussion; ADHD: attention-deficit hyperactivity disorder; Accuracy rate: number of correct response/number of requested response; Omission error rate: number of missed response/number of requested response; Commission error rate: number of wrong responses/number of requested responses; ms: milliseconds; p: level of significance;.

3.3 Project Specific Experimental Setup

Task responsive hemodynamic responses are recorded using a CW optical imaging fNIRS system (CW6; TechEn Inc., Milford, MA) at a high temporal resolution of 50 Hz. Near-infrared light with wavelengths of 690 and 830 nm are delivered via 8 source optodes to 16 detector optodes. Three types of customized rubber headcaps are designed, which allow the light emitters and detectors to be placed with an inter-optode distance of 30 mm and 10 mm. Diagrammatic drawing of the headcap design and the setup on subject's head are shown in Figure 3.1.

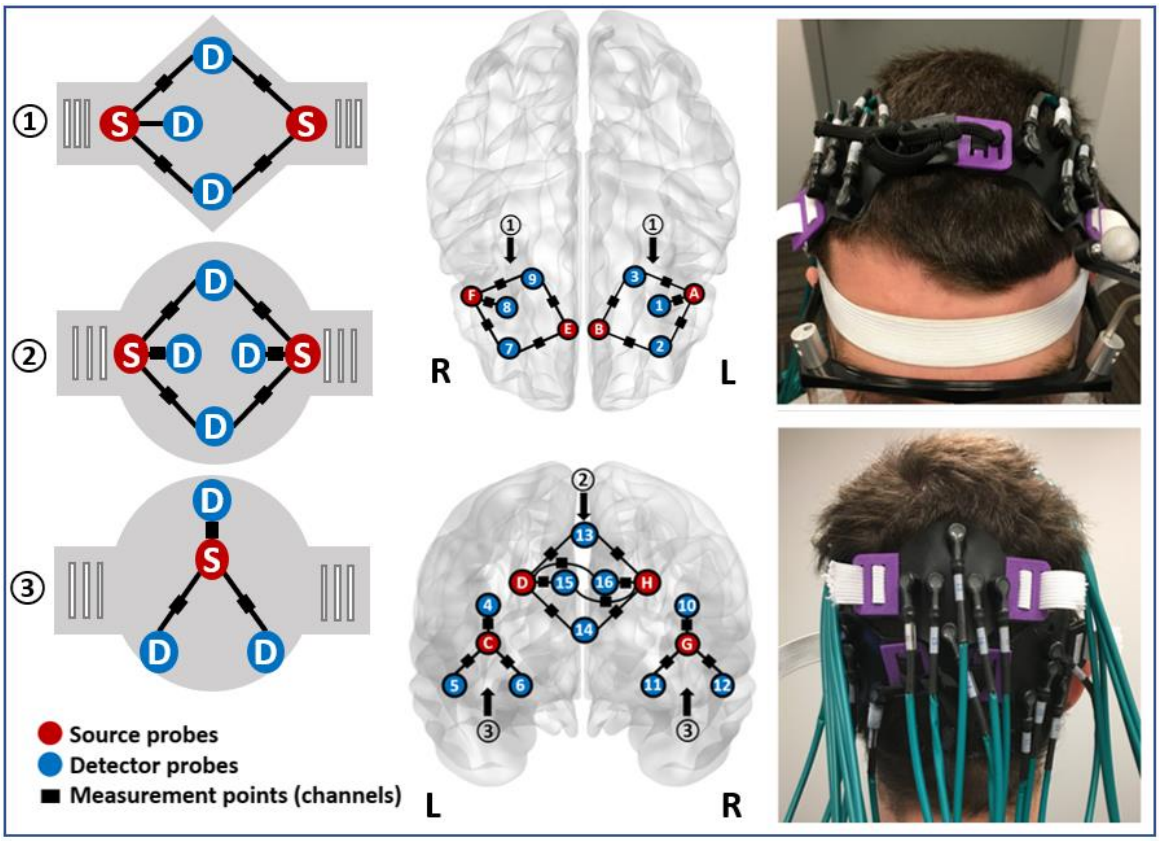

Figure 3.1 Head cap design and its setup on subject.

The long separation source-detector channel (30 mm) provides reasonable sensitivity of the near-infrared light to the cortex for measuring the concentration changes in hemoglobin (Li et al., 2011; Strangman et al., 2013), and signals obtained by using short separation channels (10 mm) contribute to the removal of systemic interference occurring in the superficial layers of the head (Gagnon et al., 2012). The layout of the three headcaps generates a total of 24 source-detector channels, including 18 long separation and 6 short separation channels, to cover 6 brain areas as the regions of interest (ROIs). The 6 ROIs are located on the Montreal Neurological Institute (MNI) coordinates of [-44, 23, 49] (left

middle frontal gyrus (MFG.L.)), [45, 23, 49] (right middle frontal gyrus (MFG.R.)), [-4, -94, 14] (left calcarine gyrus (CG.L.)), [4, -94, 14] (right calcarine gyrus (CG.R.)), [-36, -83, -10] (left inferior occipital cortex (IOC.L.)) and [44, -83, -10] (right inferior occipital cortex (IOC.R.)). The selection of these 6 brain areas as ROIs are based on the following reasons. First, previous neuroimaging studies have largely and consistently reported these 6 ROIs to have significant involvement during the visual attention processing (Fan et al., 2005; Wang et al., 2009; Schneider et al., 2010; Bonnelle et al., 2011; Cocchi et al., 2012; Li et al., 2012a; De La Fuente et al., 2013; Hu et al., 2013; Xia et al., 2014; Wu et al., 2018b). Second, anatomical locations of these 6 ROIs can be detected by the fNIRS machine.

Diagrammatic drawing of the experimental setup and data acquisition are shown in Figure 3.2. During the data acquisition, each participant was instructed to sit in front of a laptop. An optical position sensor and a neuronavigation system (Rouge Research Inc.'s Neuronavigation System with Brainsight software, Montreal, Quebec, Canada) were utilized to accomplish the registration of real locations of optodes on the subject's head. Three typical landmarks (nasion, left pre-auricular, right pre-auricular) were registered with a coil tracker and a pointer tool to help identify the locations of optodes.

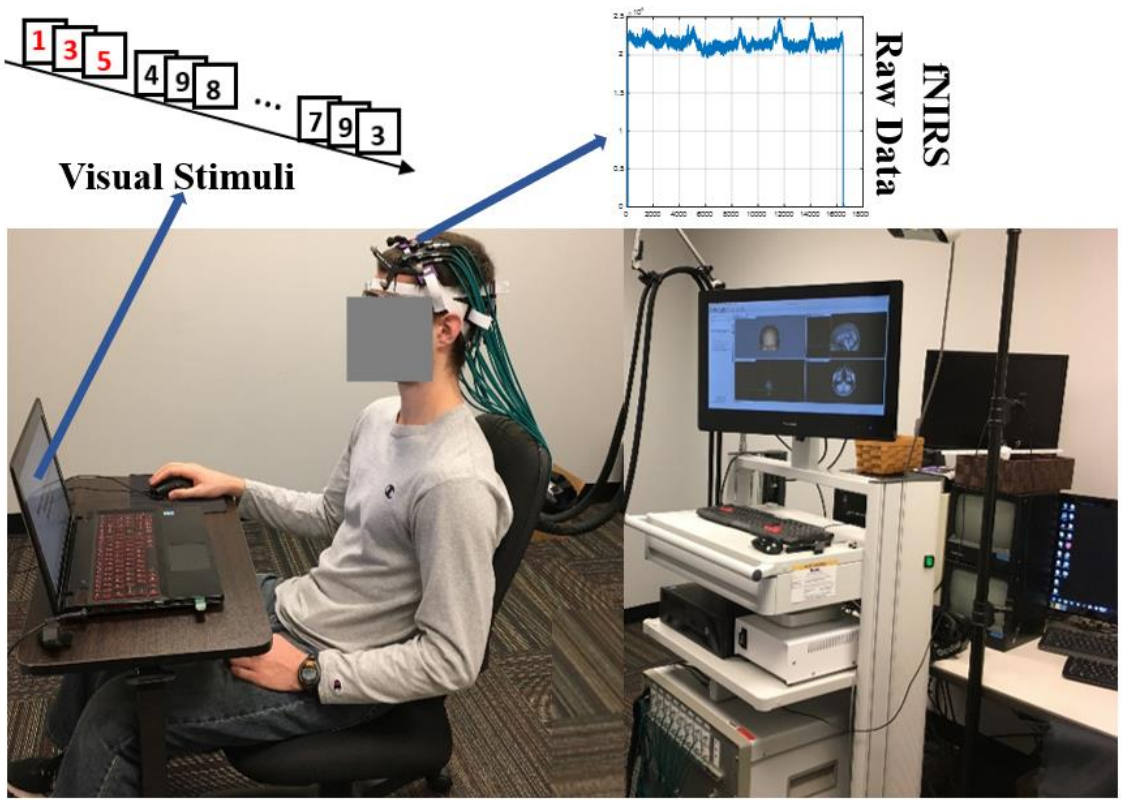

Figure 3.2 FNIRS Experimental setup and data acquisition.

3.4 Individual Level Data Analyses

The diagrammatic drawing of individual-level date preprocessing is shown in Figure 3.3. In particular, extra time points that went beyond the five-minute cognitive task were trimmed out. The raw light intensity values were converted to optical density values; a temporal-filter was applied using a bandpass filter between 0.01Hz and 0.15Hz to remove baseline fluctuations and other physiological noise (such as cardiac (1-2Hz) and respiration (0.2-0.4Hz)) in the data (Tong et al., 2012; Tong et al., 2013; Tong et al., 2016). The general principle for temporal filtering is the Fourier transform and inverse Fourier transform which use the following definitions (https://en.wikipedia.org/wiki/Fourier_transform):

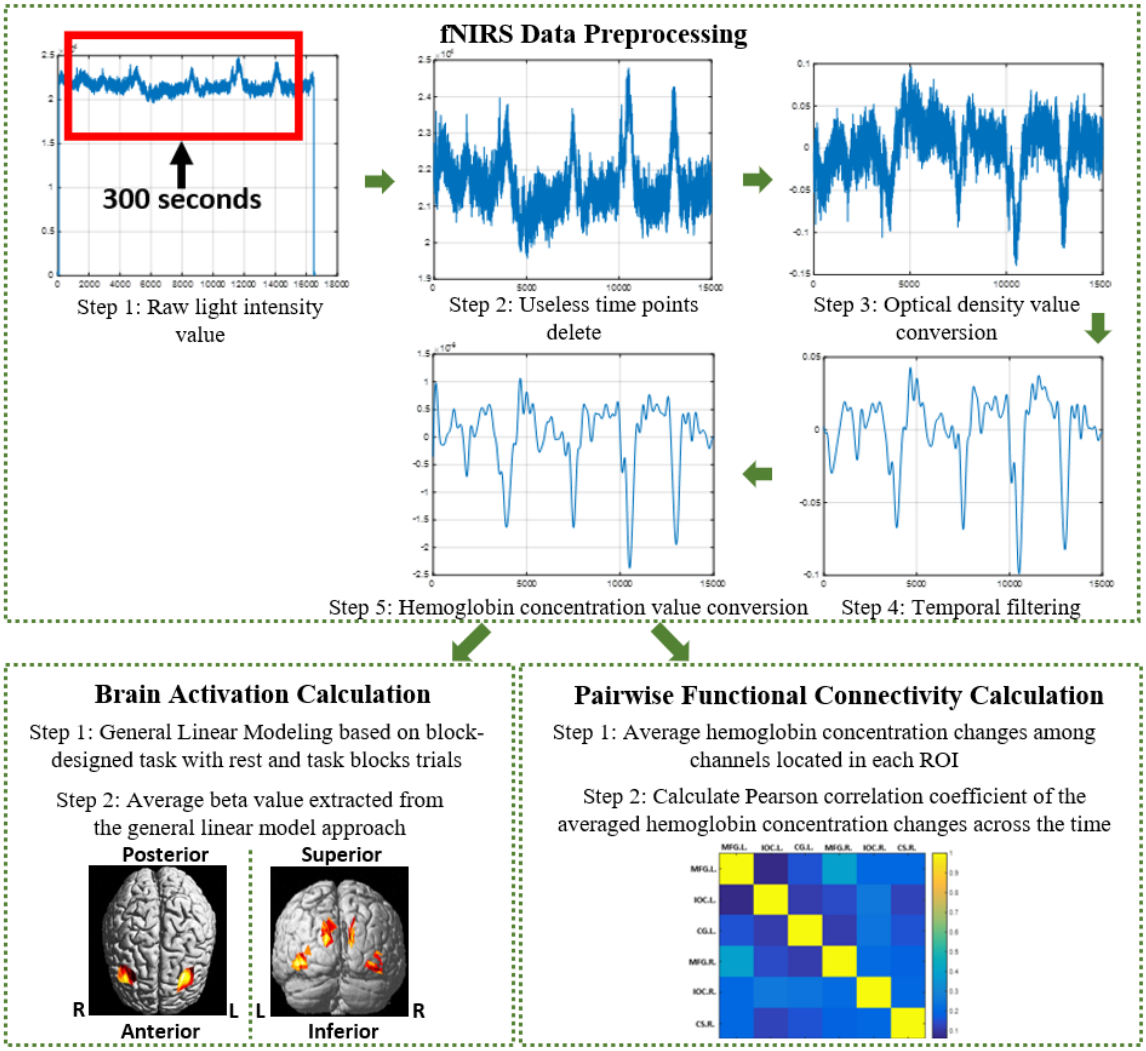

Figure 3.3 Diagrammatic drawing of individual-level fNIRS data processing.

$$\boldsymbol{F(x) = \int_{-\infty}^{\infty} f(\xi) e^{-2\pi i x \xi}\, dx} \tag{3.1}$$

$$\boldsymbol{f(\xi) = \int_{-\infty}^{\infty} F(x) e^{2\pi i x \xi}\, d\xi} \tag{3.2}$$

where the independent variable x represents time; transform variable ξ represents the frequency.

Finally, the optical density values are converted to changes in hemoglobin concentration values, based on the MBLL (Equation 2.1) (Kocsis et al., 2006). A general linear model (GLM) was further implemented in order to model the beta estimates of different types of task-responsive activation. The basic formula for the analysis is:

$$\boldsymbol{y(t) = \beta_0 + \beta_1 x_1(t) + \beta_2 x_2(t) + \cdots + \beta_n x_n(t) + \varepsilon(t)} \quad (3.3)$$

where $y(t)$ represents the value of the observed data; β_i is the variable weighting of each regressor $x_i(t)$; and $\varepsilon(t)$ is the residual noise in the data or error in the measurement.

The regional cortical activation magnitude in each ROI was estimated by averaging coefficients extracted from all long separation channels. FC refers to the functionally integrated relationship among two or more anatomically distinct time-series (Friston, 2011), and is useful to discover and compare patterns within and between groups. To calculate pairwise FC, hemoglobin concentration changes across the time series (duration was 300s) were first averaged among all long separation channels located in each ROI. The Pearson's correlation coefficients (Equation 2.10) were calculated for representing the strength of pairwise FC between two given ROIs.

3.5 Reliability and Reproducibility Test

Considering that fNIRS technique is novel in the field of TBI, especially for assessing the ability of visual attention processing. Thus, in order to ensure an acceptable level of accuracy, reliability and reproducibility were tested in Project 1. In particular, 12 subjects (8 males, 4 females) in TBI group and 12 group-matched NCs were randomly chosen from the whole project sample. Each of these 24 participant was asked to perform the VSAT twice (stimuli were randomized and counter-balanced). Study test-retest stability was assessed using the interclass correlation coefficient (ICC) (Shrout and Fleiss, 1979) of all the 6 ROIs in the 24 subjects. For each ROI, the average value of the BOLD signal of all the responsive channels was regarded as a rater. An ICC is a numerical value between 0 and 1, which estimates the ratio of variances (Shrout and Fleiss, 1979):

$$\boldsymbol{ICC} = \frac{\boldsymbol{Var}(\boldsymbol{subjects})}{\boldsymbol{Var}(\boldsymbol{subjects}) + \boldsymbol{Var}(\boldsymbol{error})} \tag{3.4}$$

where $subjects$ are defined as the between-subject differences; and $error$ are defined as the within-subject differences of the measurements acquired at the two time points (Shrout and Fleiss, 1979). A higher ICC value represents a better study test-retest stability. A commonly used threshold for acceptable test-retest stability is ICC $\geq$ 0.75 (Landis and Koch, 1977). The ICC values of our ROIs are 0.965 for the MFG.L., 0.986 for the MFG.R.,

0.942 for the CG.L., 0.884 for the CG.R., 0.988 for the IOC.L. and 0.896 for the IOC.R.. These results demonstrate high test-retest reliability of the fNIRS technique for examining functional brain properties in individuals with TBI.

3.6 Group Level Data Analyses

For group analyses, comparisons of clinical and demographic characteristics were first carried out using chi-squares test (Equation 2.4) for discrete variables such as gender, and independent sample t-test (Equations 2.5 and 2.6) for continuous variables including other clinical and demographic measures, the ROI-based cortical activation magnitude, and the FC measures.

In addition, in each diagnostic group, Pearson correlation analysis (Equation 2.10) was conducted between the ROI-based brain imaging measures and clinical symptom measures (T scores of the inattentive and hyperactive-impulsive indices from the CAARS). Multiple comparisons were corrected using the false discovery rates (FDR) (Benjamini, 1995) at $\alpha = 0.05$.

3.7 Results

3.7.1 Demographic, Clinical and Behavioral Measures

Demographic measures did not show significant between-group differences (Table 3.1). All participants achieved > 80% responding accuracy when performing the VSAT during

fNIRS acquisition. There were no significant between-group differences presented in the fNIRS task performance measures.

3.7.2 Brain Imaging Measures

As shown in Figure 3.4, significant task-responsive BOLD activations were observed in all the 6 ROIs in both control and patient groups. Group comparisons of cortical activations showed that relative to controls, patients post TBI had significantly increased cortical activation in the MFG.L. ($t = 2.15$; $p = 0.036$).

Distinct patterns of the FC maps and weighted connectivity matrices among the 6 ROIs in two groups were showed in Figure 3.5, where FC between the CG.L. and IOC.R. ($t = 2.13$; $p = 0.038$) and that between the CG.R. and the IOC.R. ($t = 2.54$; $p = 0.014$) were significantly increased (marked in blue color) in adults post TBI, relative to healthy controls.

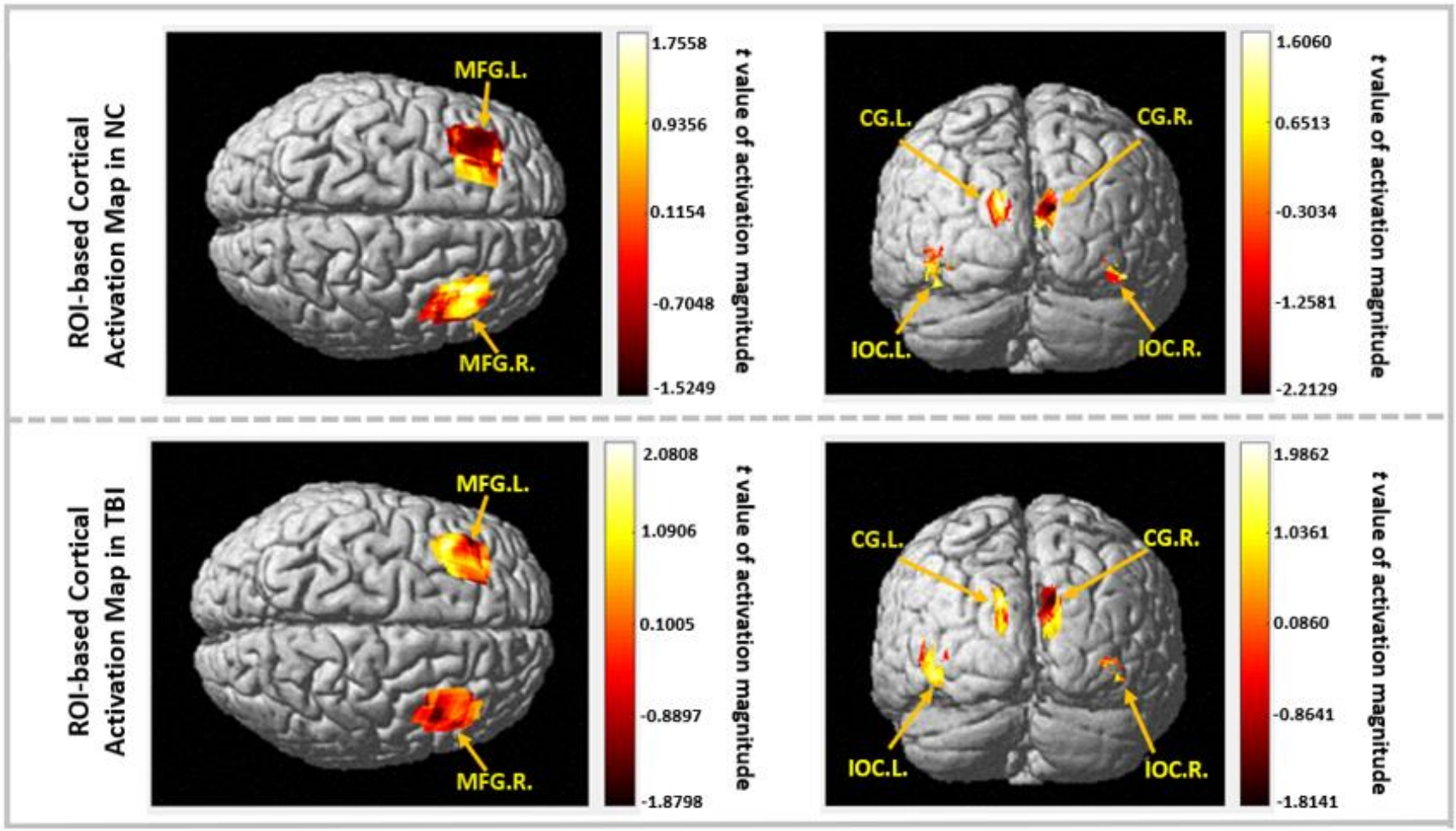

Figure 3.4 ROI based cortical activation map and functional connectivity matrix in the NC and TBI groups: (A) Cortical activation maps in the 6 ROIs in frontal and occipital regions for the control and patient groups;

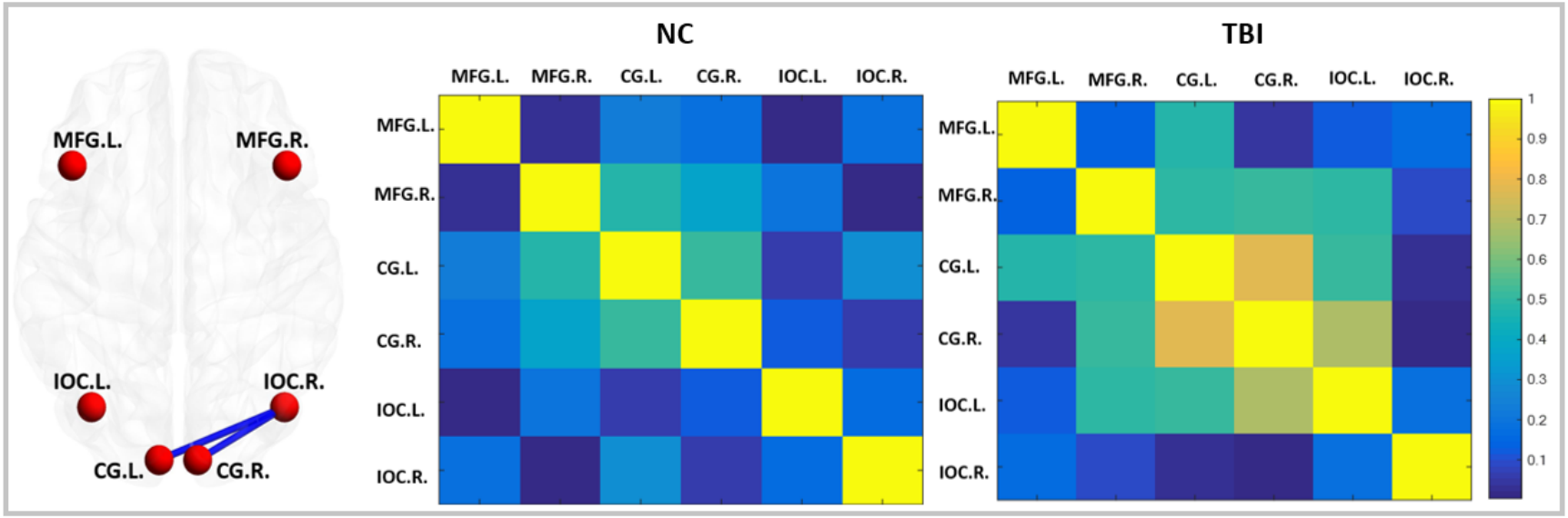

Figure 3.5 Differentiated pairwise functional connectivity between the groups of NC and TBI and weighted functional connectivity matrices of the two groups. (ROI: regions of interest; fNIRS: functional Near-Infrared Spectroscopy; NC: normal control; TBI: sports-related concussion; MFG.L.: left middle frontal gyrus; MFG.R.: right middle frontal gyrus; CG.L.: left calcarine gyrus; CG.R.: right calcarine gyrus; IOC.L.: left inferior occipital cortex; IOC.R.: right inferior occipital cortex) (Wu et al., 2018b)

3.7.3 Associations between Brain and Behavioral Measures

The measurements on brain-behavior associations showed distinct group-specific patterns. In particular, the MFG.L. activation magnitude and hyperactive/impulsive symptom severity measures demonstrated a significant negative correlation in controls ($r = -0.419$, $p = 0.030$), whereas a trend of positive correlation in patients ($r = 0.351$, $p = 0.073$). The MFG.L. activation magnitude and inattentive symptom severity measures showed a trend of negative correlation in controls ($r = -0.357$, $p = 0.068$), but no significant or trend of correlation in patients ($r = 0.122$, $p = 0.545$). Meanwhile, right side CG-IOC connectivity and hyperactive/impulsive symptom severity measures were significantly positively correlated in the patient group ($r = 0.456$, $p = 0.017$), but not in the controls ($r = 0.099$, $p = 0.624$). (Table 3.2 and Figure 3.6).

Table 3.2 Significant Associations Between Brain Imaging Measures and Clinical Symptom Measures in Groups of NC and TBI

Group	Brain imaging Measures	ADHD Symptom Measure	
		T_I	T_H
		(r) p	(r) p
NC	Brain Activation of left MFG	(-0.357) **0.068**†	(-0.419) **0.030***
	Brain Activation of right MFG	(-0.170) 0.397	(-0.483) **0.011***
	Brain Connectivity between left MFG & left IOC	(0.484) **0.011***	(0.553) **0.003***
TBI	Brain Activation of left MFG	(0.122) 0.545	(0.351) **0.073**†
	Brain Activation of right MFG	(-0.380) **0.051**†	(-0.417) **0.031***
	Brain Connectivity between left MFG & right CG	(0.270) 0.174	(0.539) **0.004***
	Brain Connectivity between right MFG & right CG	(0.356) **0.068**†	(0.517) **0.006***
	Brain Connectivity between right CG & left IOC	(0.117) 0.560	(0.412) **0.033***
	Brain Connectivity between right CG & right IOC	(0.249) 0.211	(0.456) **0.017***

NC: normal control; TBI: sports-related concussion; ADHD: attention-deficit hyperactivity disorder; MFG: Middle Frontal Gyrus; IOC: Inferior Occipital Cortex; CG: Calcarine Gyrus; ADHD: attention-deficit hyperactivity disorder; T_I: T score of the inattentive symptoms; T_H: T score of the hyperactive/impulsive symptoms; r: strength of correlation; p: level of significance; *: significant correlation; †: trend of significant correlation.

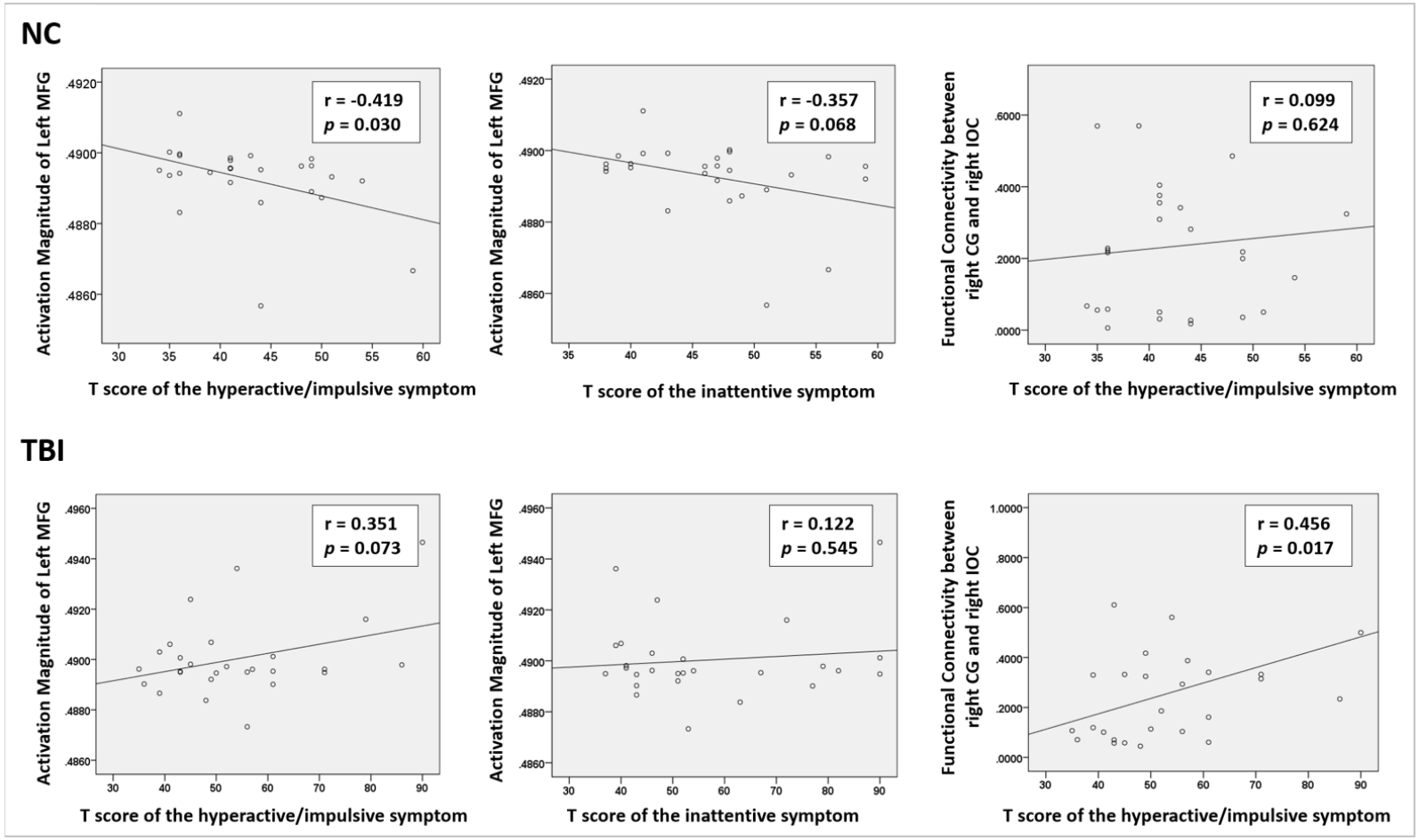

Figure 3.6 Distinct group-specific patterns of the brain-behavior associations in the NC and TBI groups. (NC: normal control; TBI: Traumatic Brain Injury; MFG: middle frontal gyrus; CG.: calcarine gyrus; IOC: inferior occipital cortex; r: strength of correlation; p: level of significance) (Wu et al., 2018b)

3.8 Discussion

In Project 1, we utilized fNIRS as a non-invasive, portable optical imaging technique for assessing brain activations responding to visual sustained attention processing. Results showed that relative to the group-matched NC, patients post TBI had significantly increased regional activations in the middle frontal lobe and between-regional hyper-communications among bilateral occipital areas during visual sustained attention processing, which were strongly associated with their elevated hyperactive/impulsive symptoms. Consistent findings regarding functional abnormalities in frontal lobe in patients with TBI during performance of cognitive tasks that involved significant amount of attention load were reported in existing studies (Scheibel et al., 2007; Turner and Levine, 2008; Kohl et al., 2009; Zhang et al., 2010; Hibino et al., 2013; Rodriguez Merzagora et al., 2014). Together with these existing findings, the direct investigation of attention processing in patients with TBI in Project 1 suggests that increased activation demand in the left middle frontal cortex is involved for the TBI patients to appropriately perform the sustained attention task, which in turn suggests that this region as a key component of abnormality associated with inattention in TBI (Wu et al., 2018b).

Furthermore, assessments on brain-behavior associations in this study showed distinct group-specific patterns in the TBI patients and the group-matched controls. Specifically, left middle frontal lobe activation magnitude and hyperactive/impulsive symptom severity score showed a significantly negative correlation in controls, whereas a

trend of positive correlation in patients. Regional brain activation magnitude in the left MFG and inattentive symptom severity score showed a trend of negative correlation in controls, but not in patients. In addition, right side CG-IOC connectivity was significantly positively correlated with the hyperactive/impulsive symptom severity score in the patient group, but not in the controls. These findings may confirm the essential role of functional integrity in the frontal and occipital cortices in normal visual attention processing and provide important evidence on the significant involvement of these cortical regions and their functional communications for TBI-induced attention deficits (Wu et al., 2018b).

In summary, results of Project 1 provided important insights into the brain mechanisms of TBI induced inattention, which highlighted the strong involvements of altered neuronal activities and interactions in middle frontal and occipital areas that may significantly contribute to the inattentive behaviors in young adults with TBI. Although it is greatly beneficial especially in subjects with attention deficits due to its setup flexibility and insensitivity to head motion, the fNIRS technique lacks sufficient penetration depth to reach subcortical structures and had limited numbers of sensors to cover the whole brain (Kontos et al., 2014; Wu et al., 2018b). Due to such technical limitations, other brain regions involved in the attention processing pathway, such as parietal cortex, thalamus, and brainstem, were not investigated in this Project.

CHAPTER 4

PROJECT 2: FUNCTIONAL MAGNETIC RESONANCE IMAGING STUDY

4.1 Introduction

Large numbers of existing functional neuroimaging studies, utilizing conventional brain properties such as regional brain activity and pairwise FC, have provided evidences regarding altered patterns of these characteristics and significant role which they play in attention-related cognitive and behavioral deficits following TBI, relative to non-injured people. As reviewed in Chapter 3, abnormal patterns of these typical brain functional measures in wide spread cortical area including frontal, parietal, temporal, insular lobes and subcortical regions, as well as their impacts to TBI-induced cognitive and behavioral impairments have been extensively reported in TBI patients, relative to control subjects, by utilizing multiple neuroimaging techniques including resting-state and task-based functional MRI (Soeda et al., 2005; Scheibel et al., 2007; Turner and Levine, 2008; Kohl et al., 2009; Mayer et al., 2009; Zhang et al., 2010; Krivitzky et al., 2011; Sozda et al., 2011; Borich et al., 2015; Saluja et al., 2015; Zhou, 2017; Li et al., 2019) and fNIRS (Hibino et al., 2013; Kontos et al., 2014; Rodriguez Merzagora et al., 2014).

Although existing studies which focused on local changes in brain functional patterns following TBI have elucidated evidences regarding functional disruption following this syndrome, these typical measures have limited capacity to characterize the

functional human brain as a high performance parallel information processing system. Graph theoretic techniques (GTT) is a powerful technique which can characterize the regional and global topological characteristics of functional brain networks. It has been proved as a very effective and informative way for exploring brain function and cognitive/behavioral performances (Li et al., 2012b; Farahani et al., 2019). However, to date, there are only limited studies involving the application of GTT in TBI. Among these studies, many of them assessed resting-state brain FC network properties, with Yan et al., reported significantly higher clustering coefficient, across local network communication efficiency, and connectivity strength (Yan et al., 2017); Messe et al., demonstrated significantly lower network modularity, significant nodal strength increasement in the precentral gyrus and right middle temporal gyrus limbic system, and reduction in the bilateral superior frontal gyri, inferior frontal operculum and thalamus, in mild TBI patients, when compared with controls (Messe et al., 2013); and Pandit et al., found reduced overall connectivity, longer average path lengths, and reduced network efficiency (Pandit et al., 2013); and reduced overall connectivity strength and degree distribution change (Nakamura et al., 2009) in patients with mild to severe TBI, relative to controls. So far, only one study investigated topological properties of task-based functional network. In particular, compared with controls, patients with TBI showed increased FC, and higher values of local efficiency of cognitive task-switching network (Caeyenberghs et al., 2012).

Little is known about the TBI-induced abnormalities in the interactions among the regions of task-evoked functional networks in TBI patients.

With this perspective, in Project 2, we implemented the GTT to examine alterations of the functional topological patterns, responding to sustained attention processing in young adults with TBI, relative to matched controls. Topological measures including efficiency, degree and network hub were selected to examine and quantify characteristics of the network. In addition, the association between altered functional brain networks properties and inattentive and hyperactive/impulsive behaviors following TBI were also assessed. Based on the findings of existing TBI studies conducted by our research teams and others (Soeda et al., 2005; Scheibel et al., 2007; Turner and Levine, 2008; Kohl et al., 2009; Mayer et al., 2009; Nakamura et al., 2009; Zhang et al., 2010; Krivitzky et al., 2011; Sozda et al., 2011; Caeyenberghs et al., 2012; Hibino et al., 2013; Messe et al., 2013; Pandit et al., 2013; Kontos et al., 2014; Rodriguez Merzagora et al., 2014; Borich et al., 2015; Saluja et al., 2015; Yan et al., 2017; Zhou, 2017; Li et al., 2019), we hypothesize that altered topological characteristics of the functional brain network for visual attention processing would be observed in adults with TBI, relative to matched controls. We further expect that these functional abnormalities would significantly correlate with inattentive and/or hyperactive behaviors post TBI.

4.2 Project Specific Participants

Among the total of 119 participants, 89 performed the functional MRI experiment. Forty-four are TBI patients, including 23 male TBI patients and 21 female TBI patients, and 45 are group-matched NC, including 23 males and 22 females. Twenty-six (11 controls and 15 TBI patients) of them overlap with participants involved in Project 1. All these 89 subjects involved in the group level analysis of Project 2. Demographic characteristics are summarized in Table 4.1.

Table 4.1 Demographic Characteristics and Clinical Diagnostic Measurements in the Groups of NC and TBI (Continued)

	NC (N=45)	**TBI (N=44)**	
	Mean (SD)	**Mean (SD)**	**p**
Age	22.25 (2.72)	21.58 (1.97)	.186
Education year	14.91 (1.95)	14.20 (1.55)	.064
Mother's education year	15.20 (2.63)	15.64 (2.72)	.450
Father's education years	15.53 (3.18)	15.53 (2.75)	1.00
CAARS scores			
Inattentive raw scores	4.64 (2.76)	9.25 (6.14)	**<.001**
Inattentive T-scores	45.76 (6.38)	56.98 (14.84)	**<.001**
Hyperactive/impulsive raw scores	5.07 (2.71)	9.27 (5.68)	**<.001**
Hyperactive/impulsive T-scores	42.51 (5.81)	52.80 (14.38)	**<.001**
	N (%)	**N (%)**	**p**
Male	23 (51.11)	23 (52.27)	.913
Right-handed	45 (100)	44 (100)	1.000
Race/Ethnicity			.219
Caucasian	14 (31.91)	21 (46.67)	
Black or African American	4 (8.51)	7 (17.78)	
Asian	20 (44.68)	10 (22.22)	
Hispanic/Latino	3 (6.38)	2 (4.44)	
More than one race	4 (8.51)	4 (8.88)	

Table 4.1 (Continued) Demographic Characteristics and Clinical Diagnostic Measurements in the Groups of NC and TBI

fMRI Task performance measures			
Accuracy rate	0.99 (0.04)	0.99 (0.01)	0.304
Omission error rate	0.01 (0.03)	0.001 (0.005)	0.131
Commission error rate	0.003 (0.01)	0.005 (0.01)	0.623
Correct response reaction time(ms)	608.27 (132.13)	605.24 (14.013)	0.917

NC: normal control; TBI: sports-related concussion; CAARS: Conner's Adult ADHD Self-Reporting Rating Scales Accuracy rate: number of correct response/number of requested response; Omission error rate: number of missed response/number of requested response; Commission error rate: number of wrong responses/number of requested responses; ms: milliseconds; p: level of significance.

4.3 Project Specific Experimental Setup

Before entering the MRI scan room, a pre-metal check was completed for ensuring the safety of the experiment. Each participant was then positioned on a moveable examination table. Earplugs were offered to attenuate scanner noise. Head motion was restrained with positioning pads. A bolster was set under the knees to help stay still and maintain the correct position during imaging. A head coil which capable of sending and receiving radio waves was placed above the participant's head. A mirror was positioned on the head coil, allowing each participant to see the visual stimuli that were performed by screen of a computer-guided projector. A two-button response box was given to each subject, allowing them to press for responding to the given cognitive task. In addition, a squeeze ball was given to each participant before the MRI scan, allowing them to alert the technologist if they would like to talk while the MRI machine is working.

4.4 Individual Level Data Analyses

4.4.1 Preprocessing

The preprocessing pipeline of individual level data is shown in Figure 4.1. For each individual, task-based fMRI data pre-processing was carried out using functional MRI Expert Analysis Tool (FEAT)/FSL (www.fmrib.ox.ac.uk/fsl). The first step was to exclude data set which include heavy head motion. Severe head motion in functional MRI data can cause position shifts of the brain structures and induce artifacts in the BOLD signals (Xia et al., 2014). Previous studies have demonstrated significantly impact on the BOLD signal due to heavy head movements (Power et al., 2012; Van Dijk et al., 2012). Thus, for the initial quality check, measurements of the six translation and rotation parameters of the functional MRI data set were calculated from the rigid body transformation (Jenkinson and Smith, 2001; Jenkinson et al., 2002). For those participants who performed heavy head motion during the functional MRI scan, that is, having consecutive motion larger than 2.0 mm for translation and 0.5 degree for rotation, data were excluded from further analyses.

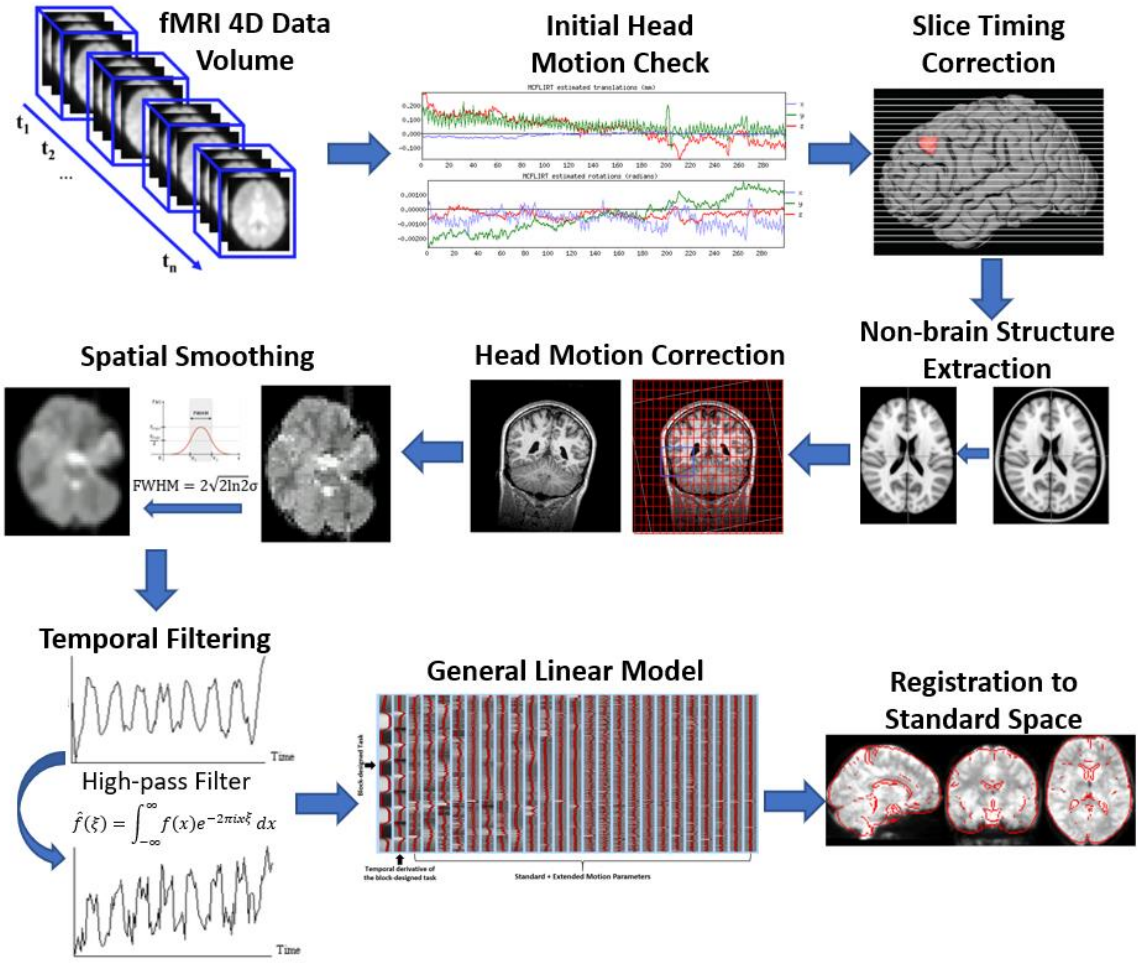

Figure 4.1 Individual-level preprocessing pipeline of functional MRI data.

For all the remaining data which passed the initial head motion severity check, slice timing was corrected, non-brain structures were extracted, head motion was corrected, images were smoothed with an 8-mm full-width-at-half-maximum Gaussian spatial filter, a high-pass temporal filter of 1/75 Hz was implemented to remove low-frequency noise. The voxel-based brain activation map in response to the visual stimuli of the VSAT in each individual and the average maps for each diagnostic group were then generated using the FMRIB's Improved Linear Model (FILM) tool from FEAT (www.fmrib.ox.ac.uk/fsl).

Finally, the functional MRI data were registered to the ICBM152_T1_2mm template in the MNI space (Jenkinson and Smith, 2001; Jenkinson et al., 2002).

4.4.2 Seed Regions (Nodes) Detection

A total of 114 spherical seed ROIs were identified based on the combination (union) of the brain clusters that were significantly activated ($Z > 2.3$) in the average activation maps in the groups of NC and TBI. This combined activation map was parcellated according to the structural and FC-based Brainnetome atlas (Fan et al., 2016), which parcellated the brain into 210 cortical and 36 subcortical subregions. The Brainnetome atlas provides a fine-grained, cross-validated atlas and contains information on both anatomical and functional connections (Fan et al., 2016). The seed regions are spheres (radius = 4 mm) identified from the coordinates of the local activation peaks containing at least 100 contiguous voxels surrounding the peak voxel. The size of the seed regions is determined based on the estimation of average cortical thickness of adult human brain (Power et al., 2011; Wig et al., 2014). Detailed information of the 114 seed ROIs are listed in Table 4.2.

Table 4.2 Node Regions of Interest for Functional Brain Network Construction (Continued)

Node ID	Anatomical Regions	Brodmann's Area	Abbreviation	MNI coordinates		
				x	y	z
1	L. Basal ganglia, globus pallidus		BG_L_6_2	-22	-2	4
2	L. Basal ganglia, ventromedial putamen		BG_L_6_4	-23	7	-4
3	L. Basal ganglia, dorsal caudate		BG_L_6_5	-14	2	16
4	L. Basal ganglia, dorsolateral putamen		BG_L_6_6	-28	-5	2
5	R. Basal ganglia, globus pallidus		BG_R_6_2	22	-2	3
6	R. Basal ganglia, ventromedial putamen		BG_R_6_4	22	8	-1
7	R. Basal ganglia, dorsolateral putamen		BG_R_6_6	29	-3	1
8	L. Cingulate gyrus, caudodorsal	24	CG_L_7_5	-5	7	37
9	R. Cingulate gyrus, pregenual	32	CG_R_7_3	5	28	27
10	L. Fusiform gyrus, medioventral	37	FuG_L_3_2	-31	-64	-14
11	L. Fusiform gyrus, lateroventral	37	FuG_L_3_3	-42	-51	-17
12	R. Fusiform gyrus, medioventral	37	FuG_R_3_2	31	-62	-14
13	R. Fusiform gyrus, lateroventral	37	FuG_R_3_3	43	-49	-19
14	L. Inferior frontal gyrus, dorsal	44	IFG_L_6_1	-46	13	24
15	L. Inferior frontal gyrus, opercular	44	IFG_L_6_5	-39	23	4
16	L. Inferior frontal gyrus, ventral	44	IFG_L_6_6	-52	13	6
17	R. Inferior frontal gyrus, dorsal	44	IFG_R_6_1	45	16	25
18	R. Inferior frontal sulcus		IFG_R_6_2	48	35	13
19	R. Inferior frontal gyrus, caudal	45	IFG_R_6_3	54	24	12
20	R. Inferior frontal gyrus, opercular	44	IFG_R_6_5	42	22	3
21	R. Inferior frontal gyrus, ventral	44	IFG_R_6_6	54	14	11
22	L. Dorsal agranular insula	16	INS_L_6_3	-34	18	1
23	L. Dorsal granular insula	16	INS_L_6_5	-38	-8	8
24	L. Dorsal dysgranular insula	16	INS_L_6_6	-38	5	5

Table 4.2 (Continued) Node Regions of Interest for Functional Brain Network Construction

25	R. Dorsal agranular insula	16	INS_R_6_3	36	18	1
26	R. Dorsal dysgranular insula	16	INS_R_6_6	38	5	5
27	L. Inferior parietal lobule, rostrodorsal	39	IPL_L_6_2	-38	-61	46
28	L. Inferior Parietal Lobule, rostrodorsal	40	IPL_L_6_3	-51	-33	42
29	L. Inferior parietal lobule, caudal	40	IPL_L_6_4	-56	-49	38
30	L. Inferior parietal lobule, rostroventral	40	IPL_L_6_6	-53	-31	23
31	R. Inferior parietal lobule, rostrodorsal	39	IPL_R_6_2	39	-65	44
32	R. Inferior parietal lobule, rostrodorsal	40	IPL_R_6_3	47	-35	45
33	R. Inferior parietal lobule, caudal	40	IPL_R_6_4	57	-44	38
34	R. Inferior parietal lobule, rostroventral	39	IPL_R_6_5	53	-54	25
35	L. Inferior temporal gyrus, extreme lateroventral	37	ITG_L_7_2	-51	-57	-15
36	L. Inferior temporal gyrus, ventrolateral	37	ITG_L_7_5	-55	-60	-6
37	L. Inferior temporal gyrus, caudolateral	20	ITG_L_7_6	-59	-42	-16
38	R. Inferior temporal gyrus, extreme lateroventral	37	ITG_R_7_2	53	-52	-18
39	R. Inferior temporal gyrus, ventrolateral	37	ITG_R_7_5	54	-57	-8
40	R. Inferior temporal gyrus, caudolateral	20	ITG_R_7_6	61	-40	-17
41	L. Middle occipital gyrus	18	LOcC_L_4_1	-31	-89	11
42	L. lateral occipital cortex	18	LOcC_L_4_2	-46	-74	3
43	L. Occipital polar cortex	17	LOcC_L_4_3	-18	-99	2
44	L. Inferior occipital gyrus	19	LOcC_L_4_4	-30	-88	-12
45	L. Middle frontal gyrus, dorsal	8	MFG_L_7_1	-27	43	31
46	L. Inferior frontal junction	8	MFG_L_7_2	-42	13	36
47	L. Middle frontal gyrus	9	MFG_L_7_3	-28	56	12
48	L. Middle frontal gyrus, ventral	6	MFG_L_7_4	-41	41	16
49	L. Middle frontal gyrus, ventrolateral	6	MFG_L_7_5	-33	23	45
50	L. Middle frontal gyrus, ventrolateral	9	MFG_L_7_6	-32	4	55
51	R. Middle frontal gyrus, dorsal	8	MFG_R_7_1	30	37	36

Table 4.2 (Continued) Node Regions of Interest for Functional Brain Network Construction

52	R. Inferior frontal junction	8	MFG_R_7_2	42	11	39
53	R. Middle frontal gyrus	9	MFG_R_7_3	28	55	17
54	R. Middle frontal gyrus, ventral	6	MFG_R_7_4	42	44	14
55	R. Middle frontal gyrus, ventrolateral	6	MFG_R_7_5	42	27	39
56	R. Middle frontal gyrus, ventrolateral	9	MFG_R_7_6	34	8	54
57	R. Middle frontal gyrus, lateral	10	MFG_R_7_7	25	61	-4
58	L. Middle temporal gyrus, caudal	21	MTG_L_4_1	-65	-30	-12
59	L. Anterior superior temporal sulcus	22	MTG_L_4_4	-58	-20	-9
60	R. Middle temporal gyrus, caudal	21	MTG_R_4_1	65	-29	-13
61	R. Middle temporal gyrus, dorsolateral	37	MTG_R_4_3	60	-53	3
62	R. Anterior superior temporal sulcus	22	MTG_R_4_4	58	-16	-10
63	L. Orbital gyrus, lateral	11	OrG_L_6_3	-23	38	-18
64	L. Orbital gyrus, lateral	12/47	OrG_L_6_6	-41	32	-9
65	R. Orbital gyrus, orbital	12/47	OrG_R_6_2	40	39	-14
66	R. Orbital gyrus, lateral	11	OrG_R_6_3	23	36	-18
67	R. Orbital gyrus, lateral	12/47	OrG_R_6_6	42	31	-9
68	L. Postcentral gyrus (upper limb, head and face region)	1/2/3	PoG_L_4_1	-50	-16	43
69	L. Postcentral gyrus (tongue and larynx region)	1/2/3	PoG_L_4_2	-56	-14	16
70	L. Postcentral gyrus	2	PoG_L_4_3	-46	-30	50
71	L. Postcentral gyrus (trunk region)	1/2/3	PoG_L_4_4	-21	-35	68
72	R. Postcentral gyrus	2	PoG_R_4_3	48	-24	48
73	L. Precentral gyrus (head and face region)	4	PrG_L_6_1	-49	-8	39
74	L. Precentral gyrus, caudal dorsolateral	6	PrG_L_6_2	-32	-9	58
75	L. Precentral gyrus (upper limb region)	4	PrG_L_6_3	-26	-25	63
76	L. Precentral gyrus (trunk region)	4	PrG_L_6_4	-13	-20	73
77	L. Precentral gyrus (tongue and larynx region)	4	PrG_L_6_5	-52	0	8
78	L. Precentral gyrus, caudal ventrolateral	6	PrG_L_6_6	-49	5	30

Table 4.2 (Continued) Node Regions of Interest for Functional Brain Network Construction

79	R. Precentral gyrus, caudal dorsolateral	6	PrG_R_6_2	33	-7	57
80	R. Precentral gyrus (tongue and larynx region)	4	PrG_R_6_5	54	4	9
81	R. Precentral gyrus, caudal ventrolateral	6	PrG_R_6_6	51	7	30
82	L. Rostroposterior superior temporal sulcus	22	pSTS_L_2_1	-54	-40	4
83	L. Caudoposterior superior temporal sulcus	22	pSTS_L_2_2	-52	-50	11
84	R. Rostroposterior superior temporal sulcus	22	pSTS_R_2_1	53	-37	3
85	R. Caudoposterior superior temporal sulcus	22	pSTS_R_2_2	57	-40	12
86	R. Lateral superior occipital gyrus	19	LOcC_R_2_2	29	-75	36
87	R. Middle occipital gyrus	18	LOcC_R_4_1	34	-86	11
88	R. Lateral occipital cortex	18	LOcC_R_4_2	48	-70	-1
89	R. Occipital polar cortex	17	LOcC_R_4_3	22	-97	4
90	R. Inferior occipital gyrus	19	LOcC_R_4_4	32	-85	-12
91	L. Superior frontal gyrus, medial	8	SFG_L_7_1	-5	15	54
92	L. Superior frontal gyrus, dorsolateral	6	SFG_L_7_4	-18	-1	65
93	L. Superior frontal gyrus, medial	6	SFG_L_7_5	-6	-5	58
94	L. Superior frontal gyrus, medial	9	SFG_L_7_6	-5	36	38
95	R. Superior frontal gyrus, medial	8	SFG_R_7_1	7	16	54
96	R. Superior frontal gyrus, dorsolateral	6	SFG_R_7_4	20	4	64
97	R. Superior frontal gyrus, medial	6	SFG_R_7_5	7	-4	60
98	R. Superior frontal gyrus, medial	9	SFG_R_7_6	6	38	35
99	L. Superior parietal lobule, lateral	5	SPL_L_5_3	-33	-47	50
100	L. Superior parietal lobule, postcentral	7	SPL_L_5_4	-22	-47	65
101	L. Superior parietal lobule, intraparietal	7	SPL_L_5_5	-27	-59	54
102	R. Superior parietal lobule, lateral	5	SPL_R_5_3	35	-42	54
103	R. Superior parietal lobule, intraparietal	7	SPL_R_5_5	31	-54	53
104	L. Superior temporal gyrus	41/42	STG_L_6_2	-54	-32	12
105	L. Superior temporal gyrus, caudal	22	STG_L_6_4	-62	-33	7

Table 4.2 (Continued) Node Regions of Interest for Functional Brain Network Construction

106	L. Thalamus, medial pre-frontal		Tha_L_8_1	-7	-12	5
107	L. Thalamus, pre-motor		Tha_L_8_2	-18	-13	3
108	L. Thalamus, sensory		Tha_L_8_3	-18	-23	4
109	L. Thalamus, posterior parietal		Tha_L_8_5	-16	-24	6
110	L. Thalamus, caudal temporal		Tha_L_8_7	-12	-22	13
111	L. Thalamus, lateral pre-frontal		Tha_L_8_8	-11	-14	2
112	R. Thalamus, medial pre-frontal		Tha_R_8_1	7	-11	6
113	R. Thalamus, pre-motor		Tha_R_8_2	12	-14	1
114	R. Thalamus, lateral pre-frontal		Tha_R_8_8	13	-16	7

4.4.3 Functional Network Analysis

In order to construct the visual sustained attention processing network, the time series of the total of 114 spherical seed regions from each participant were firstly extracted. A wavelet-based approach was then implied to denoise the functional MRI time series signals. This algorithm provides multi-frequency information about signals and are known to be effective at identifying non-stationary events caused by motion and detecting transient phenomena, such as spikes (Mallat, 1998). Specifically, each voxel time series was decomposed in the wavelet domain, using the Maximal Overlap Discrete Wavelet Transform (MODWT). The corresponding MODWT coefficients were then reconstructed to the time series signal in each voxel and averaged within each seed region for further analysis. The FC matrix was further constructed using the absolute values of the Pearson's correlation coefficients (Equation 2.10), and was converted into a binary graph, by using the network cost as threshold. The network cost is defined as:

$$\boldsymbol{C_G = \frac{K}{N(N-1)/2}} \tag{4.1}$$

where N and K are the total number of nodes and edges respectively; $N(N-1)/2$ represents the number of all possible subnetworks in the graph G (Latora and Marchiori, 2001).

The current study used the absolute values of the functional correlation coefficients, with the understanding that strong functional connections of brain regions in both positive and negative ways represent strong regional interactions for sensory and cognitive information transferring during the task (Meunier et al., 2014; Wang et al., 2017). The network topological properties were investigated over a wide range of the cost values from 0.1 to 0.5, with increments of 0.01, which was widely suggested to allow the small-world properties to be properly estimated and the sub-networks to be connected with enough discriminatory power in FC (Watts and Strogatz, 1998; Bullmore and Sporns, 2009; Xia et al., 2014). Global efficiency, $E_{glob}(G)$ and local-efficiency, $E_{loc}(G)$ are defined using the following:

$$\boldsymbol{E_{glob}(G) = \frac{1}{N(N-1)} \sum_{i \neq j \in G} \frac{1}{l_{ij}}} \tag{4.2}$$

and

$$\boldsymbol{E_{loc}(G) = \frac{1}{N} \sum_{i \in G} E_{glob}(G_i)} \tag{4.3}$$

where l_{ij} is the shortest path length between node i and j; $E_{glob}(G_i)$ is the global efficiency of the sub-network G_i that is constructed by the set of nodes that are immediate neighbors of node i (Latora and Marchiori, 2001). The graph is considered a small-world network if it met the criteria: $E_{glob}(G_{regular}) < E_{glob}(G) < E_{glob}(G_{random})$ and $E_{loc}(G_{random}) <$

$E_{loc}(G) < E_{loc}(G_{regular})$, where $E_{glob}(G_{regular})$, $E_{glob}(G_{random})$, $E_{loc}(G_{regular})$ and $E_{loc}(G_{random})$ represent the global and local-efficiency of the node- and edge-matched regular and random networks, respectively (Achard and Bullmore, 2007).

Nodal-efficiency, $E_{nodal}(G, i)$, is a local measurement, allowing to evaluate the communication efficiency between a node I and all other nodes in the network G (Latora and Marchiori, 2001). It is determined as following:

$$\boldsymbol{E_{nodal}(G) = \frac{1}{N-1}\sum_{j \in G}\frac{1}{l_{ij}}} \quad (4.4)$$

where l_{ij} is the shortest path length between node i and j.

Network hubs in each diagnostic group were also investigated. Degree and BC were utilized to determine whether a node acts as a network hub. The definition of degree of a node is the number of edges connected to that node, while the BC of node is defined by the number of all the shortest paths between two nodes that pass through a node (Sporns et al., 2007). In each individual, the average values of the degree and BC measures of each node over the network cost range of 0.1 to 0.4 were calculated and then normalized by converting into z scores using a normal distribution. The network hubs in each group were identified by estimating the grand sample means of degree and BC in each diagnostic group. These standardized values were then tested with a normal distribution. A node i is

defined as an acting network hub if 1 - $\Phi(Z_i) < \alpha$, where $\Phi(\cdot)$ is the standard normal cumulative distribution function, and α=0.05 is the level of significance (Li et al., 2012b).

4.5 Group Level Data Analyses

The demographical, clinical variables and fMRI task performance measures were compared between the groups of controls and TBI patients using chi-square tests (Equation 2.4) for discrete variables (i.e., gender) and/or independent sample t-tests (Equations 2.5 and 2.6) for continuous variables.

Group comparisons of the functional brain network topological measures, including efficiency measures $E_{glob}(G)$, $E_{glob}(G)$, $E_{glob}((G,i))$ at each i, and network hub measures D_i and BC_i at each i, were carried out using the one-way ANCOVA between the groups of controls and TBI, with gender as a fixed-effect covariate and age, participant's education level, participant parents' education level as random-effect covariates (Equations 2.7, 2.8 and 2.9).

Pearson's correlation analysis (Equation 2.10) was applied in the controls and TBI groups, respectively, to determine the association between the inattentive and hyperactive/impulsive symptoms (measured using the raw and T scores of the DSM-IV inattentive and hyperactive/impulsive indices) and the brain network measures that showed significant alterations in the TBI group relative to controls. Multiple comparisons were corrected using the FDR (Benjamini, 1995) at $\alpha = 0.05$.

4.6 Results

4.6.1 Demographic, Clinical and Behavioral Measures

Demographic and task performance measures showed no significant between-group differences (Table 4.1). All participants achieved > 95 % responding accuracy when performing the VSAT during functional MRI data acquisition.

4.6.2 Brain Network Topological Measures

Figure 4.2 shows the locations of a total of 114 seed ROIs, which were selected from a combination (union) of the brain clusters that are significantly activated in the average activation maps derived from the TBI and NC groups.

As shown in Figure 4.3, we observed that the locations of the global and local efficiency curves of both groups were between the corresponding curves of the random and regular graphs within the range 0.1=cost=0.4, known as a small-world regime (Achard and Bullmore, 2007)

The network global- and local-efficiency measures did not significantly differ between the groups of controls and TBI patients. Relative to controls, adults with TBI showed significantly higher nodal-efficiency in left postcentral gyrus ($F=9.793$, $p=0.014$).

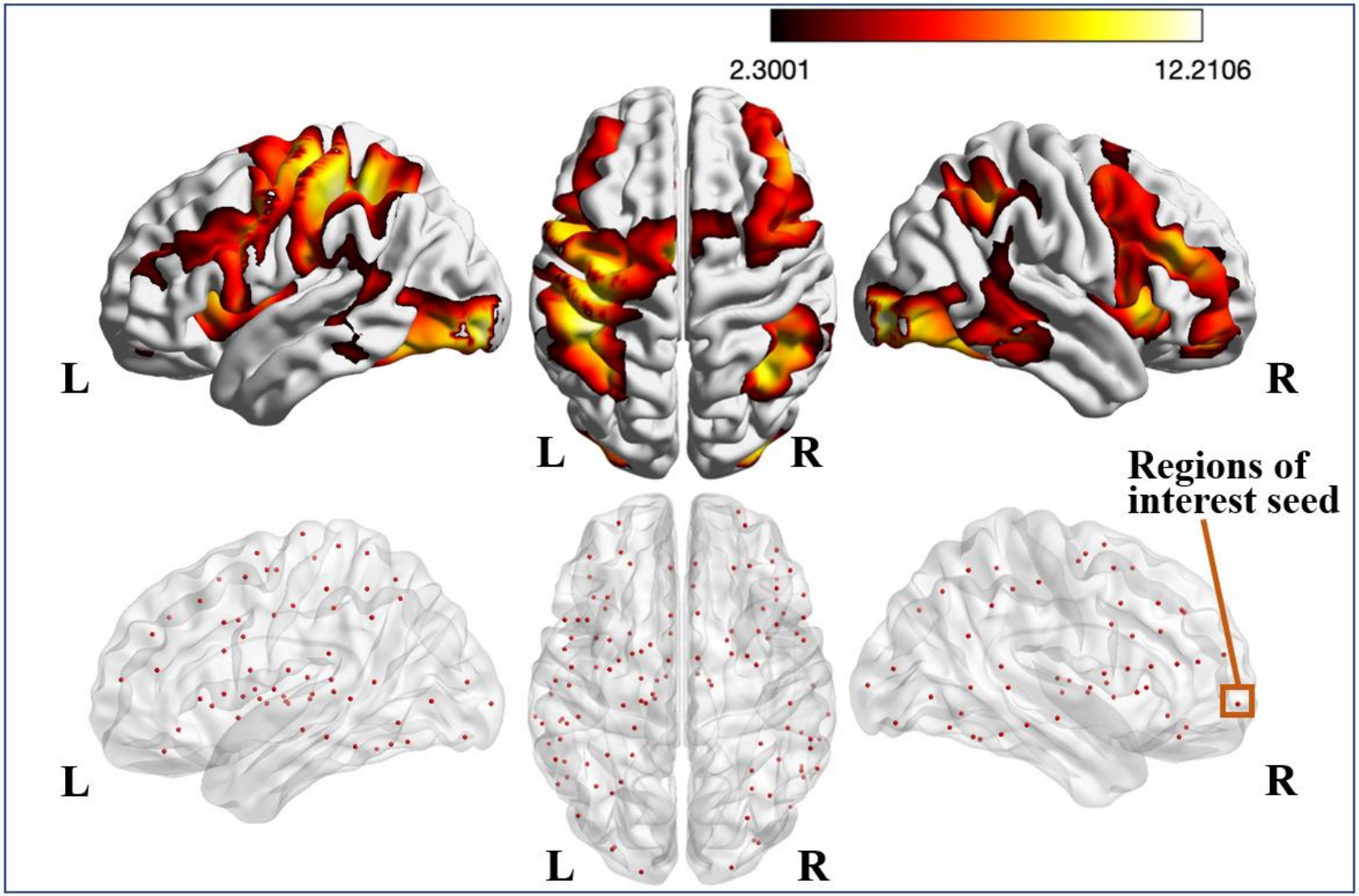

Figure 4.2 Node locations of the functional brain network. (L: left hemisphere; R: right hemisphere).

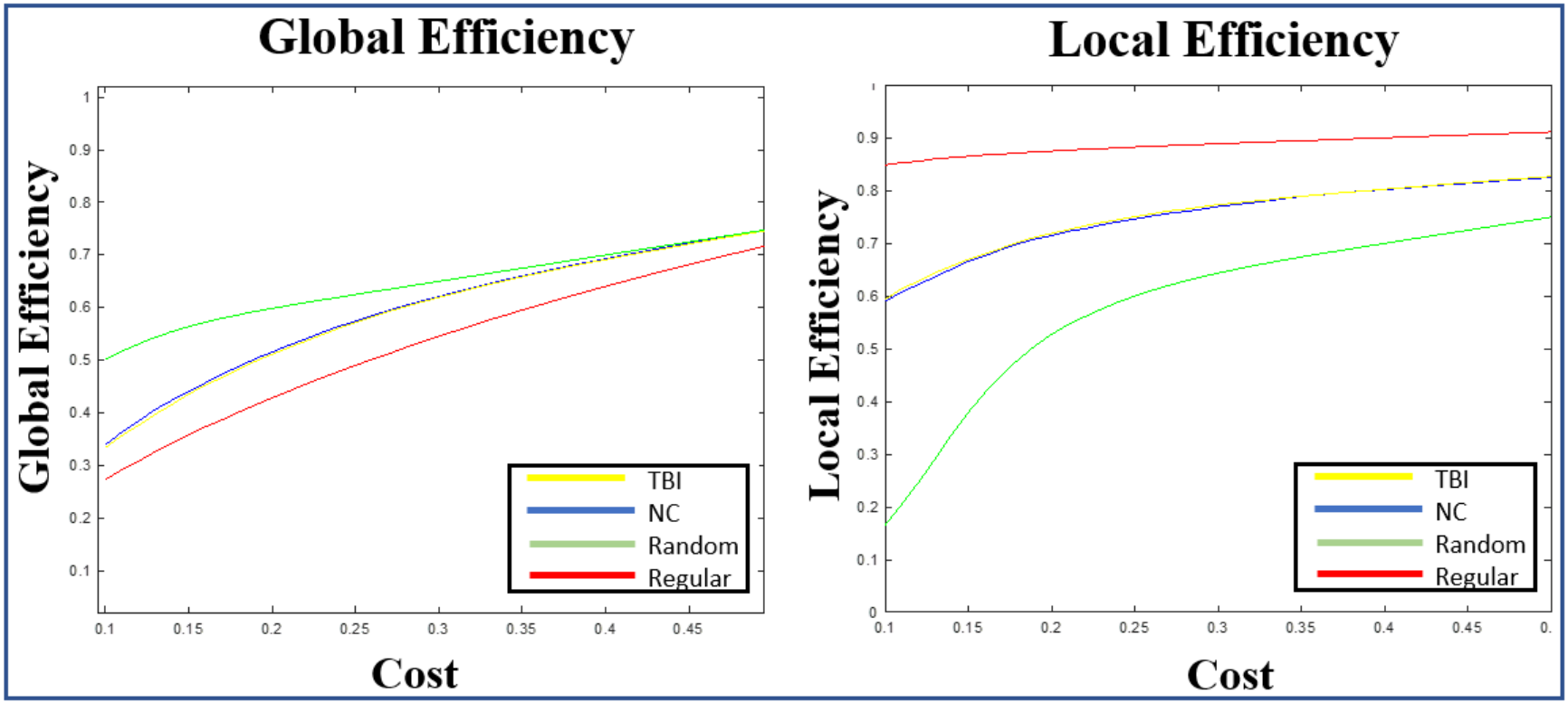

Figure 4.3 The global and local efficiency curves of both NC and TBI groups. (NC: normal controls; TBI: traumatic brain injury)

Figure 4.4 and Table 4.3 detailed the anatomical regions and locations of the network hubs that were detected using average “degree” and “between-centrality” meaures over the small-world regime in both groups.

Group comparisons showed that compared to controls, the group of TBI had significantly higher degree in the left postcentral gyrus ($F=9.407$, $p=0.021$). Distinct patterns of acting network hub distribution were observed between the two diagnostic groups in the left hemisphere, with the group of NC showed acting network hubs in inferior frontal gyrus, precetral gyrus and insular gyrus, however, that were not found in the group of TBI. In addition, the left postcentral gyrus was shown as acting network hub in the TBI, but not in controls. The distribution pattern in the right hemisphere were the same of two groups, with both NC and TBI patients showed acting network hubs in the MFG, inferior fronal gyrus, insular gyrus, inferior parietal lobule, and superior parietal lobule (SPL).

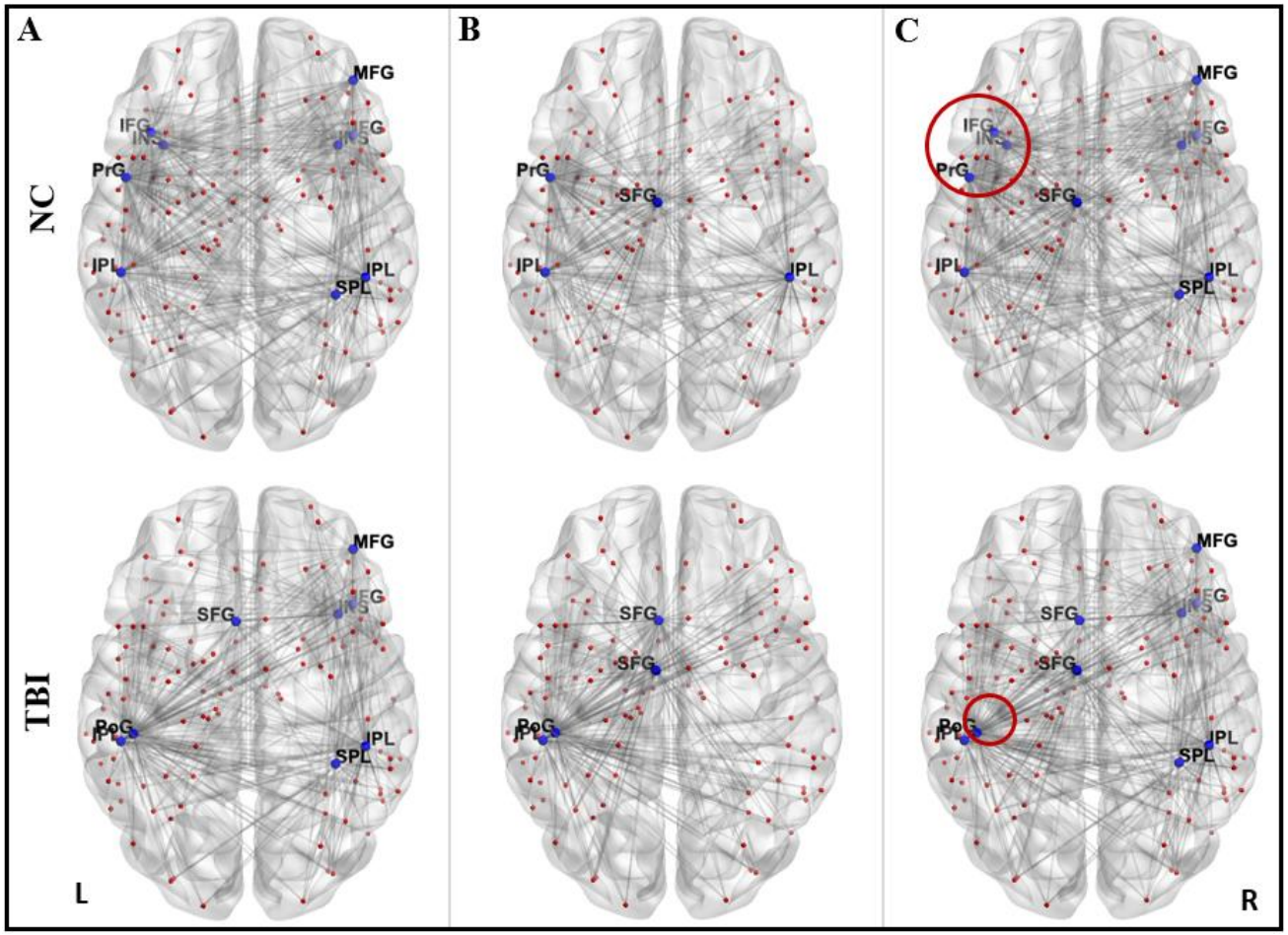

Figure 4.4 Network hubs in the group of controls and TBI. (A) Hubs identified with only betweenness centrality measure; (B) Hubs identified with only degree measure; (C) Combination of hubs identified using degree and betweenness centrality measures, with group-unique features circled in red.

Table 4.3 Acting Network Hubs in the Groups of NC and TBI

Node ID	Anatomical Region	Brodmann's Area	Normal Control		Traumatic Brain Injury	
			Betweenness Centrality	Degree	Betweenness Centrality	Degree
15	**L. Inferior Frontal Gyrus**	**44**	√			
20	R. Inferior Frontal Gyrus	45	√		√	
22	**L. Insular Gyrus**		√			
25	R. Insular Gyrus		√		√	
28	L. Inferior Parietal Lobule	40	√	√	√	√
32	R. Inferior Parietal Lobule	40	√	√	√	
54	R. Middle Frontal Gyrus	9/46	√		√	
70	**L. Postcentral Gyrus**	**2**			√	√
78	**L. Precentral Gyrus**	**6**	√	√		
102	R. Superior Parietal Lobule	5	√		√	

BOLD fonts indicate the nodes that showed different roles in the normal control and traumatic brain injury groups

4.6.3 Associations between Brain and Behavioral Measures

Figure 4.5 shows the nodes where the degrees were significantly correlated with inattentive and hyperactive/impulsive behavioral measures.

Specifically, left pre- and post-central gyrus played important roles in inattentive and hyperactive/impulsive behaviors in the group of TBI, with a significant negative correlation was found between the degree of left postcentral gyrus and T scores of inattentive and hyperactive/impulsive combined symptoms (r=-0.331, p=0.028). In addition, the degree of precentral gyrus was significantly negatively correlated with T scores of inattentive and hyperactive/impulsive combined symptoms (r=-0.300, p=0.048).

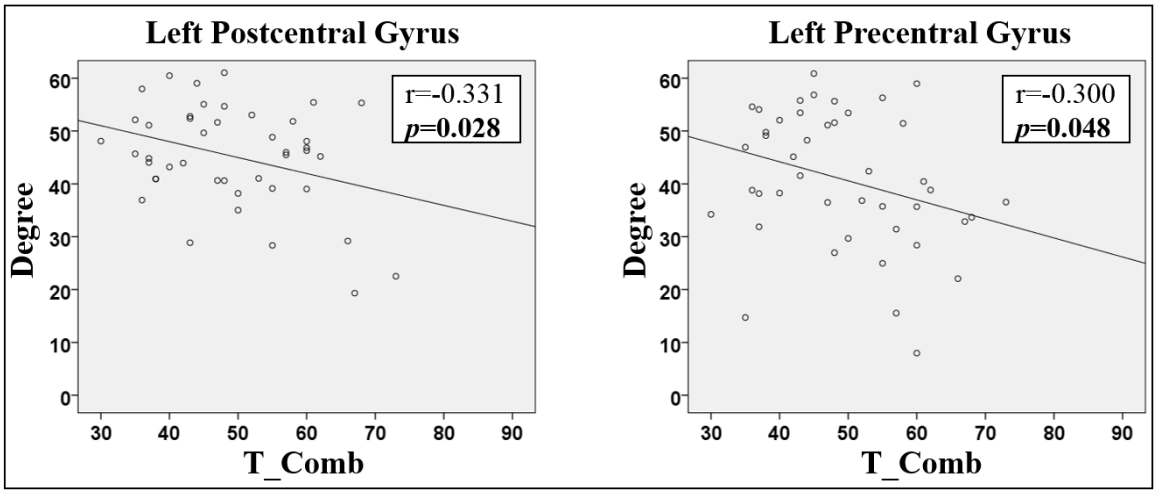

Figure 4.5 Regions that showed significant correlations between their nodal degree and the clinical symptom measures in the TBI group. (T_Comb: T scores of inattentive and hyperactive/impulsive combined symptoms)

4.7 Discussion

To our best knowledge, this is the first study which investigated associations between functional network topology of visual sustained attention processing and inattention and hyperactivity/impulsivity behaviors following TBI, by utilizing a graph theoretical approach. Although brain networks of both groups showed economical small-world topology, altered network hub patterns, degree, and efficiency were demonstrated in patients with TBI.

We found that network hubs in the left inferior frontal gyrus, precentral gyrus, which observed in the networks of NC, were essentially absent from the networks of the TBI group. Furthermore, lower degree of left precentral gyrus was significantly associated with higher inattentive and hyperactive/impulsive symptom scores in adults with TBI. Current finding is consistent with previous evidences which showed abnormal topological properties of functional network regarding significantly decreased nodal strength and edge diversity in frontal regions in TBI patients (Messe et al., 2013). In addition, exisiting neuroimaging studies have pointed to both functional and structural brain dysruptions of frontal cortex in people with TBI reltive to controls, and these alterations have been linked to cognitve and behavioral impairments. Specifically, a task-based functional MRI study demonstrated significantly increased inferior frontal gyrus activations in patients with TBI compared to group-matched healthy controls when performing executive control tasks

(Turner and Levine, 2008). Another functional MRI study reported significantly reduced neural activations in frontal eye fields and ventrolateral prefrontal cortex during attentional disengagement in adults with mild TBI, relative to group-matched controls (Mayer et al., 2009). Our recent fNIRS study reported significantly increased middle frontal activity in patients with TBI and its missing association with hyperactive/impulsive behavior, relative to matched controls (Wu et al., 2018b). Significantly decreased resting-state FC in frontal and parietal regions were also demonstrated in adolescent athletes with concussion, relative to controls (Borich et al., 2015). Moreover, consistent findings regarding functional abnormalities in frontal lobe in patients with TBI during performance of cognitive tasks that involved significant amount of attention load were reported in existing studies (Scheibel et al., 2007; Turner and Levine, 2008; Kohl et al., 2009; Zhang et al., 2010; Hibino et al., 2013; Rodriguez Merzagora et al., 2014). In terms of structural neuroimaging studies, a voxel-based morphometry study reported significant GM atrophy in the inferior frontal gyrus and its significant associations with attention deficits in young adults with TBI, relative to age and gender matched controls (Gale et al., 2005). A DTI study reported significantly reduced FA in dorsalateral prefrontal cortex and its linkage to predict executive functioning in TBI patients, relative to controls (Lo et al., 2009). Inaddition, persistent GM intensity reduction and WM disruption associated with frontal lobe, as well as their significantly associations with inattention-related post-consussion symptoms were reported in individuals with mild TBI, relative to healthy controls (Munivenkatappa et al.,

2014; Dean et al., 2015). Together with these existing results, our findings suggest that severe functional impairments in the frontal cortex may play an important role in TBI induced inattention and hyperactivity/impulsivity in adult patients.

We also observed that the left postcentral gyrus acted as a network hub for visual sustained attention processing in the TBI group, but not in controls. Moreover, the TBI group showed significantly higher degree and nodal-efficiency in the left postcentral gyrus, relative to controls and the higher postcentral degree in TBI patients was significantly correlated with lower inattentive and hyperactive symptom scales. In previous TBI studies, functional and structural alterations in parietal regions were consistently reported. Specifically, significantly increased SPL activation during attention processing (McAllister et al., 1999; Bonnelle et al., 2011) and significantly increased FC within the parietal lobe during resting state (Lu et al., 2019) were found in patients with TBI. Recent structural MRI studies reported significantly increased cortical thickness of medial SPL in patients with chronic mild TBI (Wang et al., 2015; Shao et al., 2018). Consistently higher parietal cortical thickness in patients with acute-through-chronic mild TBI (over a 3-month interval since the onset of brain injury), when compared to group-matched controls were also observed (Govindarajan et al., 2016). It is known that the parietal cortex plays an important role in sensory information transformation and attentional modulation (Behrmann et al., 2004; Han et al., 2004; Hutchinson et al., 2009; Szczepanski et al., 2010; Wu et al., 2016). Structural alterations associated with this region have been linked to

visual attentional information processing (Behrmann et al., 2004; Bisley and Goldberg, 2010). The parietal cortex is a critical component of attention network (Han et al., 2004), and plays an important role in sensory information transformation and attentional modulation (Behrmann et al., 2004; Han et al., 2004; Hutchinson et al., 2009; Szczepanski et al., 2010; Wu et al., 2016). Therefore, current findings regarding the parietal cortex as a super active hub for visual sustained attention processing in the TBI group, as well as the role it plays in inattentive and hyperactive behaviors may suggest the importance of optimal parietal function for the recovery of TBI induced inattention and hyperactivity/impulsivity.

Moreover, topological abnormalities of other cortical regions including the missing network hub of the insular gyrus were observed in TBI patients, relative to controls. Insula is a critical component of the salience network (Bonnelle et al., 2012), which is responsible for integrating external and internal processes and controlling cognitive functions (Platel et al., 1997; Bamiou et al., 2003). Evidences have pointed altered structural and functional brain patterns, as well as their important role played in attention performance associated with insula in TBI studies (Yasuno et al., 2014; Saluja et al., 2015; Zhou, 2017; Li et al., 2019). Together with our findings, the altered functional topological properties associated with insular cortices we observed in Project 2 might indicate the critical role of this region played for visual sustained attention processing.

This project has an issue that need to be further discussed. The sample includes both male and female subjects. Although it is unclear whether the neuropathological

underpinnings of TBI have gender differences, clinical studies have reported different outcomes in male and female TBI patients (Covassin et al., 2007; Colvin et al., 2009; Covassin et al., 2012; Covassin et al., 2013; Sandel et al., 2017; Tanveer et al., 2017). To partially remove gender-related effect, the gender was added as a covariate in the group-level analysis.

In summary, this study showed hypo-functionally interacting in frontal cortex and hyper-functionally interacting in the parietal cortex for visual sustained attention processing in young adults with TBI, and the prior one might play an important role in inattention and hyperactivity behaviors following TBI, while the latter one might indicate a compensatory mechanism for the recovery of these TBI-induced behavioral impairments. In addition, it is clear from the present results that assessment of the functional brain networks provides new insights into the understanding of inattention and hyperactivity/impulsivity changes following TBI.

CHAPTER 5

PROJECT 3: STRUCTURAL MAGNETIC RESONANCE IMAGING AND DIFFSION TENSOR IMAGING STUDY

5.1 Introduction

In the literature, attention-related neurocognitive consequences in those with TBI have been associated with widespread structural alterations of brain. Specifically, a voxel-based morphometry study reported significantly reduced GM concentration in frontal, temporal and parietal cortices and their significant associations with attention deficits in young adults with TBI (Gale et al., 2005). Significant GM volumetric atrophy in cingulate gyrus was observed in adults with TBI, without showing linkages with neurocognitive and behavioral impairments in the TBI subjects (Yount et al., 2002). An DTI study linked increased FA of the anterior corona radiata to increased attentional control ability in adults with mild TBI (Niogi et al., 2008b). Significantly higher FA of the posterior CC was observed in patients with mTBI relative to matched controls, and was linked with poorer inhibitory control capacity (Bazarian et al., 2007). A recent longitudinal structural MRI study and a DTI study reported persistent GM intensity reduction and WM disruption in frontal cortex in individuals with mild TBI relative to healthy controls, which were significantly associated with inattention-related post-consussion symptoms (Munivenkatappa et al., 2014; Dean et al., 2015). Besides these, structural alterations in

other brain regions, such as temporal lobe, thalamus, hippocampus and fornix, were reported and found to link with cognitive/behavioral impairments related to decision making, processing speed, visual tracking and working memory, in adolescents and adults with TBI (Tate and Bigler, 2000; Fujiwara et al., 2008; Maruta et al., 2010; Yallampalli et al., 2013). However, a recent DTI study demonstrated no significant WM abnormality in athletes after sports-related concussion, relative to matched controls (Churchill et al., 2017). The significant inconsistency of findings from the existing structural and functional neuroimaging studies in TBI can be partially resulted from technical differences in data acquisitions and analyses, and sample-related biases such as differences in injury mechanism, post-injury stage, varying age ranges, and gender ratios.

Indeed, gender-specific patterns of behavioral and neurocognitive alterations induced by TBI have been largely documented (Donders and Hoffman, 2002; Barr, 2003; Donders and Woodward, 2003; Covassin et al., 2006; Covassin et al., 2007; Colvin et al., 2009; Covassin et al., 2012; Covassin et al., 2013; Sandel et al., 2017; Tanveer et al., 2017), resulting in contradictory results with some reported significantly worse performances of visual, verbal memory and executive control domains in females with TBI, relative to male TBI patients (Covassin et al., 2007; Colvin et al., 2009; Covassin et al., 2012; Covassin et al., 2013; Sandel et al., 2017; Tanveer et al., 2017), however, others demonstrated better performances in females (Donders and Hoffman, 2002; Barr, 2003; Donders and Woodward, 2003; Covassin et al., 2006) or no substantial gender differences (Zuckerman

et al., 2012). Several existing neuroimaging studies have attempted to investigate gender-related brain mechanisms associated with TBI (Fakhran et al., 2014; Hsu et al., 2015; McGlade et al., 2015; Shao et al., 2018; Sollmann et al., 2018; Wang et al., 2018). Specifically, a DTI study reported significantly decreased FA in bilateral uncinate fasciculi in males with TBI relative to females TBI patients and controls (Fakhran et al., 2014). A structural MRI study found significantly increased cortical thickness in the left caudal anterior cingulate cortex in females with TBI, compared to male patients (Shao et al., 2018). A resting-state functional MRI study reported significantly increased connectivity between the orbitofrontal cortex (OFC) and parietal, occipital and cerebellum areas as well as significantly decreased connectivity between the OFC and temporal, insular regions in females with TBI relative to males TBI patients (McGlade et al., 2015). Another resting-state functional MRI study found increased intrinsic FC in motor network, ventral stream network, executive function network, cerebellum network and decreased connectivity in visual network in males with TBI relative to females TBI patients (Wang et al., 2018). Again, findings from these investigations on gender-related brain alterations in TBI are far from converging.

Motivated to further investigate the interactions between TBI-induced structural brain alterations and cognitive/behavioral impairments, as well as their gender-specific patterns, structural MRI and DTI data from young adults with TBI and matched NC were acquired for this study. Behavioral measures including inattention and

hyperactivity/impulsivity, which are among the most frequently reported domains impacted by TBI (Levin et al., 2004; Sinopoli et al., 2011; Biederman et al., 2015), were also collected from every subject. Gender distributions are balanced in both groups. Based on findings of previous studies conducted by our team and other researchers (Gale et al., 2005; Mayer et al., 2009; McGlade et al., 2015; Wu et al., 2018b), we hypothesized that injury induced structural alterations associated with frontal, parietal and occipital cortices, regions well-recognized to play important roles in attentional and inhibitory deployment, would significantly contribute to inattentive and hyperactive/impulsive behaviors in affected individuals. We further expected that these structural brain abnormalities would demonstrate gender-specific patterns.

5.2 Project Specific Participants

All 89 participants who performed the functional MRI experiment in Project 2 involved in Project 3, including 44 TBI patients (23 male TBI patients and 21 female TBI patients), and 45 group-matched NC (23 males and 22 females). Structural MRI and DTI data were acquired. Demographic characteristics of the 89 participants are summarized in Table 5.1.

After individual-level neuroimaging data analysis, 4 subjects were excluded from further data analysis due to excessive head motions (with any of the 6 realignment parameters > 2.5 mm). Therefore, a total of 85 subjects (including 43 controls and 42 TBI patients) were involved in group-level analyses.

Table 5.1 Demographic and Clinical Characteristics in the groups of NC and TBI

	NC (N=45)	**TBI (N=44)**	
	Mean (SD)	**Mean (SD)**	**p**
Age	22.25 (2.72)	21.58 (1.97)	.186
Education year	14.91 (1.95)	14.20 (1.55)	.064
Mother's education year	15.20 (2.63)	15.64 (2.72)	.450
Father's education year	15.53 (3.18)	15.53 (2.75)	1.00
CAARS scores			
Inattentive raw scores	4.64 (2.76)	9.25 (6.14)	**<.001**
Inattentive T-scores	45.76 (6.38)	56.98 (14.84)	**<.001**
Hyperactive/impulsive raw scores	5.07 (2.71)	9.27 (5.68)	**<.001**
Hyperactive/impulsive T-scores	42.51 (5.81)	52.80 (14.38)	**<.001**
	N (%)	**N (%)**	**p**
Male	23 (51.11)	23 (52.27)	.913
Right-handed	45 (100)	44 (100)	1.00
Race/ Ethnicity			.219
Caucasian	14 (31.91)	21 (46.67)	
Black or African American	4 (8.51)	7 (17.78)	
Asian	20 (44.68)	10 (22.22)	
Hispanic/Latino	3 (6.38)	2 (4.44)	
More than one race	4 (8.51)	4 (8.88)	

NC: normal controls; TBI: traumatic brain injury; N: number of subjects; SD: standard deviation; p: level of significance; CAARS: Conner's Adult ADHD Self-Reporting Rating Scales.

5.3 Individual Level Data Analyses

5.3.1 Individual Level Structural Magnetic Resonance Imaging Data Analysis

For each subject, structural MRI data was motion corrected and then processed using an automated surface reconstruction model in the FreeSurfer v.6.0 software package (https://surfer.nmr.mgh.harvard.edu/). All of the steps were done using the recommended standard parameters (Dale et al., 1999). To estimate regional cortical thickness and surface area values, non-brain tissues were removed using a hybrid watershed/surface deformation

procedure. Each volume was registered to the Talairach atlas using an affine registration method. Intensity variations caused by magnetic field inhomogeneities are corrected. A cutting plane was defined to separate the left and right hemispheres and to remove the cerebellum and brain stem. Two surfaces between the GM and WM (called WM surface) and between the GM and cerebrospinal fluid (called pial surface) were generated using the triangular tessellation technique. The GM/WM border surface was then inflated to an average spherical surface to locate both the pial surface and the GM/WM boundary. Cortical thickness is measured as the average of two distances including the distance from each white surface vertex to their corresponding closet point on the pial surface and vice versa. Surface area is quantified by averaging the surrounding triangular face of the surface representation with vertex coordinates. Cortical parcellation was provided based on the Desikan-Killiany atlas (Desikan et al., 2006). According to our hypotheses, cortical GM ROIs included all the subregions of bilateral frontal (22 subregions), parietal (10 subregions), and occipital (8 subregions) cortices. Cortical thickness and surface area values of these 40 bilateral cortical ROIs were included in group-level analyses.

5.3.2 Individual Level Diffusion Tensor Imaging Data Analysis

DTI data of each subject was preprocessed using the Diffusion Toolbox from FMRIB Software Library (FSL) version 5.0.9 (Jenkinson et al., 2012). Eddy-current induced geometrical distortions and head motion were estimated and corrected. Voxel-based

whole-brain FA maps were then created by fitting a diffusion tensor model. For DTI data, ROI-based and tractography-based analyses were conducted in each subject.

For ROI-based analysis, each voxel-based FA map was first non-linearly aligned to the 1×1×1 mm MNI152 space (a normalized and averaged brain atlas developed by the Montreal Neurologic Institute). According to our hypotheses, four WM ROIs were extracted, including the bilateral SLF (which connects frontal, parietal and occipital lobes), and bilateral superior FOF (sFOF) (which interconnects frontal and occipital lobes), based on the Johns Hopkins University human brain WM tractography atlas (Mori and van Zijl, 2007), and then mapped to each individual's voxel-based FA image. Figure 5.1A demonstrate the SLF and sFOF ROIs in the left hemisphere. The mean FA value of each WM ROI were included in group-level analyses.

For tractography-based analysis, three cortical seeds were first determined in each hemisphere, including the frontal, parietal and occipital cortices parcellated from the structural MRI data of each subject using Desikan-Killiany atlas (Desikan et al., 2006), and then linearly registered to the native diffusion space. Within each voxel of each seed, two crossing fibers were estimated using the FSL/BEDPOSTX toolbox (Behrens et al., 2007). Probabilistic tractography in each pair of the three seeds was conducted with the following parameters: 5000 individual pathways were drawn on the principle fiber direction of each seed voxel within the ROI, with a step length of 0.5mm and maximum travel steps of 2000 for each sample pathway. Curvature threshold of 0.2 was set to exclude implausible

pathways. Figure 5.1B depict the three WM tracts in left hemisphere generated in this step. The FA and volume of each tract were then extracted and involved in the group-level analyses.

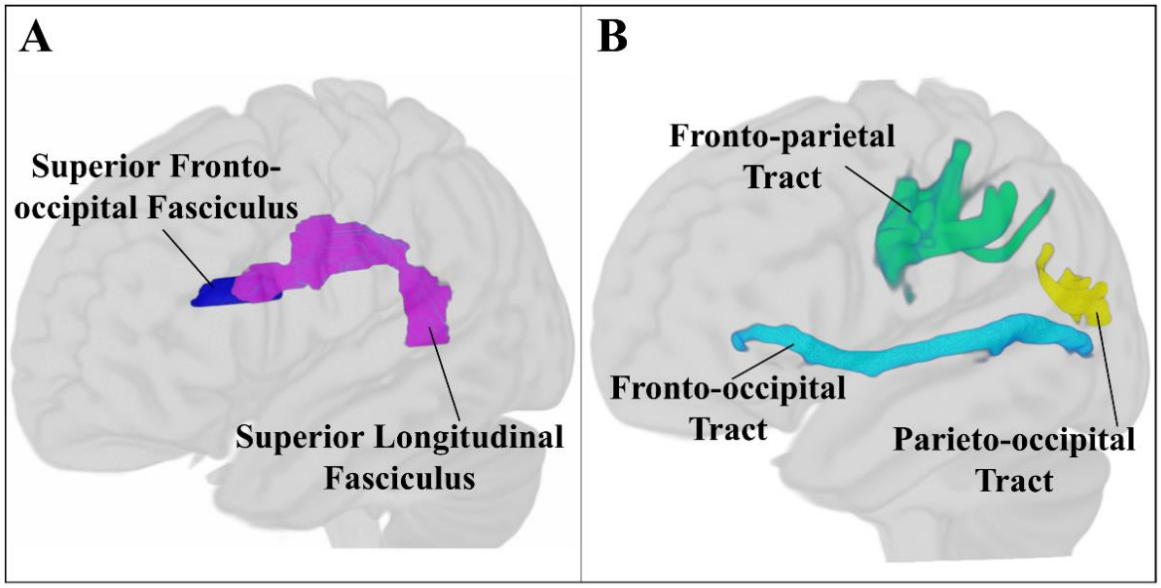

Figure 5.1 WM ROIs selected based on Johns Hopkins University human brain WM tractography atlas and WM tracts generated from probabilistic tractography analysis (displayed only in the left hemisphere).

5.4 Group Level Data Analyses

The demographical and clinical variables were compared between controls and TBI patients, and then between males and females in each diagnostic group, using chi-square tests (Equation 2.4) for discrete variables (i.e., gender) and independent sample t-test (Equations 2.5 and 2.6) for continuous variables.

Neuroimaging measures (including cortical thickness and surface area values of 40 bilateral cortical ROIs, FA of 4 WM ROIs, and FA of 6 tractography-based WM measures) were compared using one-way ANCOVA (Equations 2.7, 2.8 and 2.9) between controls and TBI patients, by controlling age, participant's and their parents' education levels as covariates. For the anatomical measures which showed significantly between-group differences, post-hoc t-tests were further conducted to examine gender-specific comparisons between the groups of TBI and controls. For each analysis, the threshold of significant difference, $p \leq 0.05$, was determined after controlling multiple comparisons using the FDR (Benjamini, 1995).

Furthermore, Pearson's correlation analysis was conducted between the inattentive and hyperactive/impulsive symptom scores and the neuroimaging measures which show significant between-group differences and gender-specific patterns.

5.5 Results

5.5.1 Demographic, Clinical and Behavioral Measures

Relative to NC, TBI patients showed significantly higher raw and T scores for inattentive and hyperactive/impulsive symptoms measured by the CAARS subscales, while no between-group differences were observed in any demographic measures (Table 5.1). In

addition, between-gender comparisons in the NC and TBI groups did not show significant differences in any clinical/demographic measures.

5.5.2 Brain Imaging Measures

Relative to controls, TBI patients had significantly increased regional cortical thickness in the right SPL (F=6.954, p=0.050). Post-hoc analysis further showed that males with TBI had significantly increased cortical thickness of right SPL when compared to male controls (t=2.729, p=0.009) (Tables 5.2 and 5.3).

Meanwhile, TBI patients showed significantly higher FA of the left SLF ROI (F=5.137, p=0.039), when compared to controls. Post-hoc analysis further showed that females with TBI have a trend of significantly higher FA of the left SLF ROI (t=2.048, p=0.053) compared to females in the NC group. Compared to controls, the TBI group also showed significantly higher FA of the left sFOF (F=5.820, p=0.039). We did not observe between-group differences in the 6 tractography-based WM measures.

Table 5.2 Neuroanatomical Measures Which Show Significant Differences Between the Groups of NC and TBI

	Neuroanatomical Measures	NC Mean (SD)	TBI Mean (SD)	F-value	p-value after FDR correction
NC v.s. TBI	CT of right superior parietal lobule	2.278 (0.121)	2.347 (0.131)	6.954	**0.050**
	FA of left superior longitudinal fasciculus ROI	0.504 (0.035)	0.518 (0.020)	5.137	**0.039**
	FA of left superior fronto-occipital fasciculus ROI	0.539 (0.044)	0.565 (0.042)	5.820	**0.039**

NC: normal controls; TBI: traumatic brain injury; SD: standard deviation; CT: regional cortical thickness; FA: fractional anisotropy; FDR: false discovery rate.

Table 5.3 Neuroanatomical Measures Which Show Significant or A Trend of Significant Between-Group Differences in Males and Females

	Neuroanatomical Measures	NC Mean (SD)	TBI Mean (SD)	t-value	p-value after FDR correction
NC_M v.s. TBI_M	CT of right superior parietal lobule	2.273 (0.149)	2.385 (0.130)	-2.729	**0.009**
	FA of left superior longitudinal fasciculus ROI	0.514 (0.034)	0.528 (0.017)	-1.688	0.101
	FA of left superior fronto-occipital fasciculus ROI	0.545 (0.047)	0.571 (0.041)	-1.959	0.101
NC_F v.s. TBI_F	CT of right superior parietal lobule	2.283 (0.086)	2.304 (0.121)	-0.679	0.501
	FA of left superior longitudinal fasciculus ROI	0.491 (0.034)	0.509 (0.017)	-2.048	**0.053**†
	FA of left superior fronto-occipital fasciculus ROI	0.532 (0.041)	0.559 (0.043)	-1.997	**0.053**†

NC_M: male normal controls; TBI_M: male traumatic brain injury patients; NC_F: female normal controls ; TBI_F: female traumatic brain injury patients; SD: standard deviation; CT: regional cortical thickness; FA: fractional anisotropy; FDR: false discovery rate; †: trend of significant difference.

5.5.3 Associations between Brain and Behavioral Measures

Greater regional cortical thickness of right SPL was significantly correlated with increased inattentiveness measured by the CAARS inattentive subscale in all male participants (r=0.389, p=0.011), especially in males of the TBI group (r=0.629, p=0.004). Meanwhile, higher FA of the left sFOF ROI was significantly correlated with decreased hyperactive/impulsive behaviors measured by the CAARS hyperactive/impulsive subscale in females of the patient group (r=-0.629, p=0.007) (Figure 5.2).

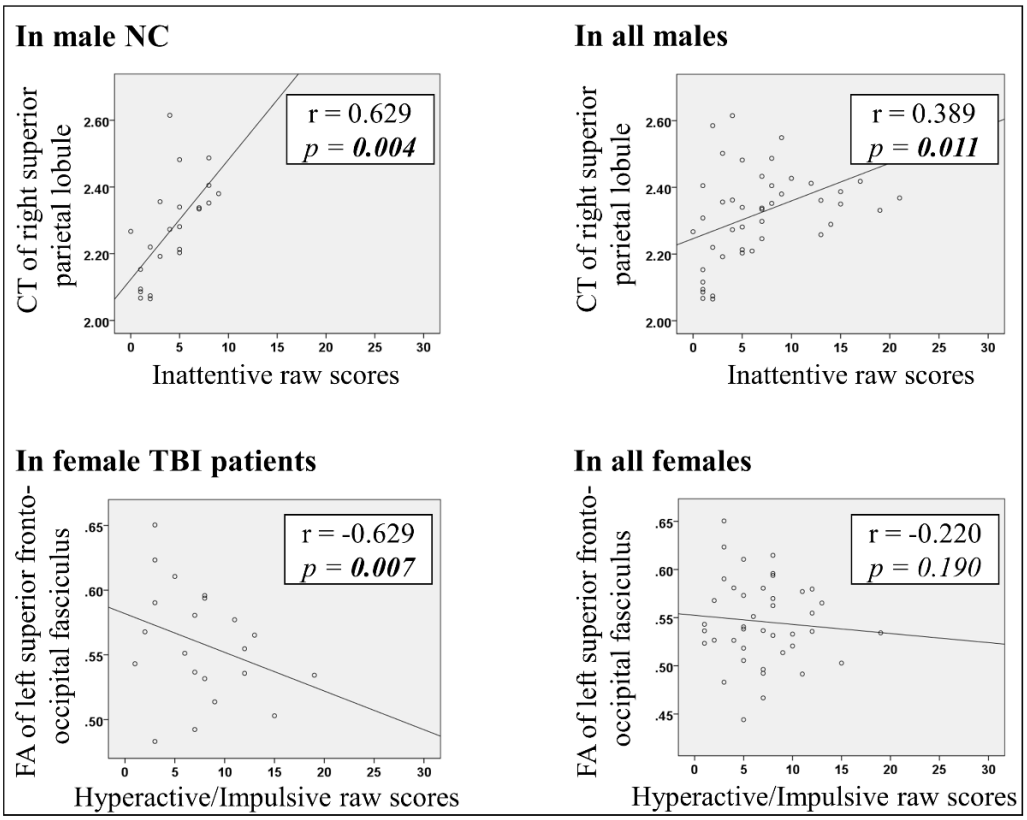

Figure 5.2 Associations between neuroanatomical measures and inattentive and hyperactive/impulsive symptom scores. (NC: normal controls; TBI: traumatic brain injury; CT: cortical thickness; FA: fractional anisotropy; r: strength of correlation; p: level of significance)

5.6 Discussion

To our knowledge, this is the first study which assessed both GM and WM structural alterations, their relationship with inattentive and hyperactive/impulsive behaviors, as well as their gender-differentiated patterns in young adults with TBI.

We observed significantly increased cortical thickness in right SPL in the TBI group, when compared to controls. Structural alterations in parietal regions have been consistently reported in previous TBI studies. Recent structural MRI studies reported significantly increased cortical thickness of medial SPL in patients with chronic mTBI(Wang et al., 2015; Shao et al., 2018), and consistently higher parietal cortical thickness in patients with acute-through-chronic mTBI (over a 3-month interval since the onset of brain injury), when compared to group-matched controls (Govindarajan et al., 2016). Although the biological mechanisms of such phenomena are still unclear, the underlying cellular process during the post TBI neuroinflammation stage may partially contribute to increased cortical thickness in affected brain regions (Dall'Acqua et al., 2017; Xiong et al., 2018).

Besides the main finding of significantly increased cortical thickness in right SPL in the group of TBI, our post hoc analysis showed that this TBI-higher-than-NC pattern regarding to cortical thickness of right SPL was mainly driven by the extremely greater right SPL cortical thickness in males with TBI relative to males in the NC group. Meanwhile, we observed significant correlation between greater regional cortical thickness

of right SPL and increased inattentiveness in males of the entire sample, but not in females. SPL is a major subregion of posterior parietal cortex, which plays an important role in sensory information transformation and attentional modulation (Behrmann et al., 2004; Han et al., 2004; Hutchinson et al., 2009; Szczepanski et al., 2010; Wu et al., 2016). Structural alterations associated with this region have been found to contribute to visual attentional disorders such as neglect (Behrmann et al., 2004; Bisley and Goldberg, 2010). Functional neuroimaging studies in patients with TBI have reported increased SPL activation during attention processing (McAllister et al., 1999; Bonnelle et al., 2011) and increased FC within the parietal lobe during resting state (Lu et al., 2019). Although gender differences associated with SPL structural alterations have not been reported in human-based TBI studies, , animal studies have consistently observed more aggressive neuroinflammatory profile in male mice compared to female mice in multiple brain injury models (Bodhankar et al., 2015; Villapol et al., 2017). Together with findings from these existing studies, our results may further suggest that compared to that in females, TBI-induced cortical abnormalities in SPL are more vulnerable to contribute to increased inattentive behaviors in males.

Results of the current study also showed that compared to the controls, subjects with TBI had significantly higher FA of left SLF and sFOF. SLF is a large bundle of association fibers in each hemisphere connecting the parietal, occipital and temporal lobes with ipsilateral frontal cortices, which is an essential component for higher level cognitive

processes (Schmahmann et al., 2008); while sFOF is initiated from a compact fascicle at the level of the anterior horn of the lateral ventricle and terminated at the parietal region via the lower part of caudate (Bao et al., 2017), and is suggested to play an important role in inhibitory control (Depue et al., 2016). Increased FA in SLF was previously reported in youth with TBI, when compared to controls (Babcock et al., 2015). Although its biological mechanism is still unclear, studies suggest that prolonged TBI-reactive WM intracellular processes may partially stimulate axon regenerations, and result in increased FA (Schwartz et al., 2003; Lipton et al., 2012; Armstrong et al., 2016).

In addition, the gender-specific post hoc analysis further reported that the TBI-higher-than-NC pattern regarding to FA of left sFOF and left SLF, respectively, were both mainly led by higher FA of the ROIs in females with TBI relative to females in the NC group. And higher FA of left sFOF was significantly correlated with decreased hyperactive/impulsive behaviors in females of the patient group. So far, only a few studies have investigated gender-differences in TBI-induced structural brain alterations and their associations with the clinical/behavioral outcomes, related to ability of processing speed, working memory and executive function (Fakhran et al., 2014; Shao et al., 2018; Sollmann et al., 2018). Although there is lack of directly comparable results, previous studies have consistently observed strong associations between increased regional WM FA and better performance on processing speed, and awareness in TBI patients (Farbota et al., 2012; Edlow et al., 2016; Yin et al., 2019). Adding into existing studies, our findings suggest that

improved WM integrity in left SLF and sFOF can happen due to TBI-reactive WM intracellular processes and axon regenerations, which may partially modulate the inhibitory control function and contribute to better inhibitive behaviors, especially in females with TBI.

There are some issues of this study that need to be further discussed. First, this study assessed both group-wise and gender-specific patterns of the TBI-related structural brain alterations. Although a total of 85 subjects (with both genders included) were involved in group-level comparisons, each post hoc gender-specific analysis was conducted within roughly a half of the entire sample, which is a relatively smaller sample size and may cause reduced statistical power. Future studies can focus on investigating sex effect in TBI, by recruiting a larger study sample. Second, one participant with TBI had been taking short-acting medications for inattentive symptoms, while all others were medication naive. An at least 24-hour wash-out period was instructed to this subject, before the MRI procedure. Nevertheless, there is no evidence from existing studies demonstrating significant impact of any short-acting stimulants to GM or WM brain structures (Phillips et al., 2008).

In summary, this study demonstrated male-dominated pattern of significantly increased right SPL cortical thickness and female-dominated pattern of significantly higher FA in the left SLF and sFOF in patients with TBI, when compared to controls. Moreover, TBI-induced cortical abnormalities in SPL may significantly contribute to increased

inattentive behaviors in males, while increased WM integrity in left SLF and sFOF may play an important role in better inhibitive control in females with TBI.

CHAPTER 6

CONCLUSION AND FUTURE RESEARCH DIRECTIONS

6.1 Dissertation Research Conclusion

In order to identify the neurobiological mechanisms associated with attention deficits in adults post TBI, in this dissertation research, non-invasive, powerful and robust neuroimaging techniques including the fNIRS, functional MRI, structural MRI and DTI were implemented in three pioneer projects for systematically investigating both functional and structural brain alterations in patients with TBI, relative to group-matched healthy controls. In addition, associations between these abnormal brain patterns and neurocognitive consequences following TBI (especially inattention and hyperactivity/impulsivity behaviors) were further analyzed.

Results of Project 1 showed differentiated brain functional properties in respond to visual attention processing, including the significantly increased middle frontal lobe activation and hyper-communication within occipital lobes in the TBI group, relative to controls. Distict brain-behavior association patterns in the two groups were also observed, with the significant correlation between middle frontal lobe activation and hyperactivity/impulsivity behaviors only observed in the control group, whereas the association between within occipital lobe FC and hyperactivity/impulsivity behaviors only observed in the TBI group. Key contributions of Project 1 includes the following two

aspects. First, it indicates the fNIRS technique as a reliable technique for evaluating cerebral oxygenation changes during visual attention processing in TBI patients. Second, it highlights the strong involvement of altered neuronal activities and interactions in frontal and occipital areas that contribute to the inattention and hyperactivity/impulsivity behaviors in young adults with TBI.

Project 2 is one of the pioneer studies which investigates the topological characteristics of visual attention network in individuals with and without TBI, and is also the first one which further examines the associations between these altered brain network topological patterns with inattention and hyperactivity/impulsivity behaviors following TBI. Major findings of Project 2 include the hypo-functionally interacting in frontal cortex and hyper-functionally interacting in the parietal cortex. According to the results of brain-behavior association analysis, the prior finding might indicate an important role which the frontal lobe plays in inattention and hyperactivity/impulsivity behaviors following TBI, while the hyperfunction in the parietal lobe might indicate a compensatory mechanism for the recovery of these behavioral impairments. More than that, findings regarding the abnormal brain functional properties in frontal lobe which we observed in Project 2 are consistent with those found in Project 1. This finding thus highlights the frontal lobe as a critical region which may significantly contribute to attention-related behavioral deficits following TBI.

Project 3 investigated the neurobiological substrates associated with TBI-induced attention deficits in the anatomical division. Results demonstrated significantly increased cortical thickness in the parietal lobe and significantly increased WM integrity associated with frontal, parietal and occipital cortices in patients with TBI, when compared to controls. Findings of these structural alterations may serve as the anatomical basis for the functional abnormalities associated with corresponding brain areas observed in Projects 1 and 2. In addition, results of brain-behavior association analysis further suggest the role which the parietal lobe may play in inattention following TBI, as well as the involvement of the interactions among frontal, parietal and occipital cortices in inhibitive control post TBI.

Together, this hypothesis-driven dissertation research consistently reports altered brain functional and structural patterns in frontal, parietal and occipital cortices, as well as their significant associations in attention deficits post TBI, which may suggest these abnormalities as vital biomarkers for improving prognosis, and diagnosis of this syndrome. In addition, as a pioneer work which systimatically investigated the neurobiological basis of the most significant long-term neurocognitive consequence post TBI, findings of this dissertation research may manifest its pivotal position for guiding effective rehabilitation strategies for treatment and interventions of this major public health concern.

6.2 Future Research Directions

Future directions of this dissertation research are suggested mainly in two sections. First, there is no denying that DTI is the most extensively used technique worldwide to study the microstructural properties of WM *in vivo* (Basser and Jones, 2002; Mori and Zhang, 2006; Mukherjee et al., 2008). Microstructural WM disruptions induced by TBI, together with their consequences regarding neurocognitive and behavioral deficits have been widely reported in this research field (Croall et al., 2014; Yuh et al., 2014; Oehr and Anderson, 2017). However, traditional DTI metrics such as the FA represents basic statistical descriptions of diffusion cannot quantify neurite-specific measures such as their density and orientation dispersion (Eva M. Palacios, 2018). In 2012, Zhang and colleagues enables the *in vivo* mapping of these measures with the development of the neurite orientation dispersion and density imaging (NODDI) (Zhang et al., 2012).

NODDI is a practical diffusion MRI technique for estimating the microstructural complexity of dendrites and axons in vivo on clinical MRI scanners. Such indices of neurites relate more directly to and provide more specific markers of brain tissue microstructure than standard indices from DTI, such as FA. Mapping these indices over the whole brain on clinical scanners presents new opportunities for understanding brain development and disorders. So far, clinical studies have been carried out using NODDI for applications including normal brain development and ageing (Billiet et al., 2015; Chang et al., 2015; Nazeri et al., 2015), neurological disorders (Kunz et al., 2014; Lemkaddem et al.,

2014; Owen et al., 2014; Winston et al., 2014; Eaton-Rosen et al., 2015; Timmers et al., 2015) and brain connectivity (Lemkaddem et al., 2014). A few numbers of neuroimaging studies have also implemented this novel technique in the TBI field and report abnormal WM properties on NODDI such as neurite density and orientation dispersion index in TBI patients, relative to controls (Eva M. Palacios, 2018; Wu et al., 2018a; Mallott et al., 2019). Together, further studies with the implementation of this novel and powerful technique may greatly enhance the capacity for TBI diagnosis, prognosis and treatment monitoring.

Second, previous TBI studies have shown that TBI-induced forces can directly damage the neurons, axons, dendrites, glia, and blood vessels in a focal, multifocal, or diffuse pattern and initiate a dynamic series of complex cellular, inflammatory, mitochondrial, neurochemical, and metabolic alterations (McKee and Daneshvar, 2015; Kinder et al., 2019). Although this dissertation research focuses on a chronic stage after brain injury which is appropriate for investigating long-term consequences in affected individuals, the meaning with respect to assess brain development and behavioral performances during the whole process post TBI could not be excluded. Future studies with longitudinal assessments at acute, subacute, and chronic time points are highly recommended to better understand the neurobiological mechanisms associated with TBI induced long-term cognitive and behavioral deficits.

REFERENCES

Achard, S., & Bullmore, E. (2007). Efficiency and cost of economical brain functional networks. *PLoS Comput Biol* 3**,** e17.

Adams, J.H., Doyle, D., Ford, I., Gennarelli, T.A., Graham, D.I., & Mclellan, D.R. (1989). Diffuse axonal injury in head injury: definition, diagnosis and grading. *Histopathology* 15**,** 49-59.

Amyot, F., Kenney, K., Moore, C., Haber, M., Turtzo, L.C., Shenouda, C., Silverman, E., Gong, Y., Qu, B.X., Harburg, L., Lu, H.Y., Wassermann, E.M., & Diaz-Arrastia, R. (2018). Imaging of cerebrovascular function in chronic traumatic brain injury. *J Neurotrauma* 35**,** 1116-1123.

Anderson, V., Catroppa, C., Morse, S., Haritou, F., & Rosenfeld, J. (2005). Attentional and processing skills following traumatic brain injury in early childhood. *Brain Inj* 19**,** 699-710.

Arfanakis, K., Haughton, V.M., Carew, J.D., Rogers, B.P., Dempsey, R.J., & Meyerand, M.E. (2002). Diffusion tensor MR imaging in diffuse axonal injury. *AJNR Am J Neuroradiol* 23**,** 794-802.

Armstrong, R.C., Mierzwa, A.J., Marion, C.M., & Sullivan, G.M. (2016). White matter involvement after TBI: Clues to axon and myelin repair capacity. *Exp Neurol* 275 Pt 3**,** 328-333.

Astafiev, S.V., Shulman, G.L., Metcalf, N.V., Rengachary, J., Macdonald, C.L., Harrington, D.L., Maruta, J., Shimony, J.S., Ghajar, J., Diwakar, M., Huang, M.X., Lee, R.R., & Corbetta, M. (2015). Abnormal white matter blood-oxygen-level-dependent signals in chronic mild traumatic brain injury. *J Neurotrauma* 32**,** 1254-1271.

Babcock, L., Yuan, W., Leach, J., Nash, T., & Wade, S. (2015). White matter alterations in youth with acute mild traumatic brain injury. *J Pediatr Rehabil Med* 8**,** 285-296.

Baker, W.B., Parthasarathy, A.B., Busch, D.R., Mesquita, R.C., Greenberg, J.H., & Yodh, A.G. (2014). Modified Beer-Lambert law for blood flow. *Biomed Opt Express* 5**,** 4053-4075.

Bamiou, D.E., Musiek, F.E., & Luxon, L.M. (2003). The insula (Island of Reil) and its role in auditory processing. Literature review. *Brain Res Brain Res Rev* 42**,** 143-154.

Bao, Y., Wang, Y., Wang, W., & Wang, Y. (2017). The superior fronto-occipital fasciculus in the human brain revealed by diffusion spectrum imaging tractography: An anatomical reality or a methodological artifact? *Front Neuroanat* 11**,** 119.

Barkley Ra, D.G., Mcmurray Mb (1990). Comprehensive evaluation of attention deficit disorder with and without hyperactivity as defined by research criteria. *J Consult Clin Psychol* 58, 775-789.

Barr, W.B. (2003). Neuropsychological testing of high school athletes. Preliminary norms and test-retest indices. *Arch Clin Neuropsychol* 18**,** 91-101.

Basser, P.J., & Jones, D.K. (2002). Diffusion-tensor MRI: theory, experimental design and data analysis - a technical review. *NMR Biomed* 15**,** 456-467.

Bazarian, J.J., Zhong, J., Blyth, B., Zhu, T., Kavcic, V., & Peterson, D. (2007). Diffusion tensor imaging detects clinically important axonal damage after mild traumatic brain injury: a pilot study. *J Neurotrauma* 24**,** 1447-1459.

Behrens, T.E., Berg, H.J., Jbabdi, S., Rushworth, M.F., & Woolrich, M.W. (2007). Probabilistic diffusion tractography with multiple fibre orientations: What can we gain? *Neuroimage* 34**,** 144-155.

Behrmann, M., Geng, J.J., & Shomstein, S. (2004). Parietal cortex and attention. *Curr Opin Neurobiol* 14**,** 212-217.

Benjamini, Y.H., Yosef (1995). Controlling the false discovery rate: a practical and powerful approach to multiple testing. *Journal of the Royal Statistical Society, Series B.* 57**,** 289-300.

Bergeson, A.G., Lundin, R., Parkinson, R.B., Tate, D.F., Victoroff, J., Hopkins, R.O., & Bigler, E.D. (2004). Clinical rating of cortical atrophy and cognitive correlates following traumatic brain injury. *Clin Neuropsychol* 18**,** 509-520.

Biederman, J., Feinberg, L., Chan, J., Adeyemo, B.O., Woodworth, K.Y., Panis, W., Mcgrath, N., Bhatnagar, S., Spencer, T.J., Uchida, M., Kenworthy, T., Grossman, R., Zafonte, R., & Faraone, S.V. (2015). Mild traumatic brain injury and attention-deficit hyperactivity disorder in young student athletes. *J Nerv Ment Dis* 203**,** 813-819.

Bigler, E.D. (2004). Neuropsychological results and neuropathological findings at autopsy in a case of mild traumatic brain injury. *J Int Neuropsychol Soc* 10**,** 794-806.

Bigler, E.D., Blatter, D.D., Anderson, C.V., Johnson, S.C., Gale, S.D., Hopkins, R.O., & Burnett, B. (1997). Hippocampal volume in normal aging and traumatic brain injury. *AJNR Am J Neuroradiol* 18**,** 11-23.

Billiet, T., Vandenbulcke, M., Madler, B., Peeters, R., Dhollander, T., Zhang, H., Deprez, S., Van Den Bergh, B.R., Sunaert, S., & Emsell, L. (2015). Age-related microstructural differences quantified using myelin water imaging and advanced diffusion MRI. *Neurobiol Aging* 36**,** 2107-2121.

Bisley, J.W., & Goldberg, M.E. (2010). Attention, intention, and priority in the parietal lobe. *Annu Rev Neurosci* 33**,** 1-21.

Blumbergs, P.C., Scott, G., Manavis, J., Wainwright, H., Simpson, D.A., & Mclean, A.J. (1994). Staining of amyloid precursor protein to study axonal damage in mild head injury. *Lancet* 344**,** 1055-1056.

Bodhankar, S., Lapato, A., Chen, Y., Vandenbark, A.A., Saugstad, J.A., & Offner, H. (2015). Role for microglia in sex differences after ischemic stroke: importance of M2. *Metab Brain Dis* 30**,** 1515-1529.

Bonnelle, V., Ham, T.E., Leech, R., Kinnunen, K.M., Mehta, M.A., Greenwood, R.J., & Sharp, D.J. (2012). Salience network integrity predicts default mode network function after traumatic brain injury. *Proc Natl Acad Sci U S A* 109**,** 4690-4695.

Bonnelle, V., Leech, R., Kinnunen, K.M., Ham, T.E., Beckmann, C.F., De Boissezon, X., Greenwood, R.J., & Sharp, D.J. (2011). Default mode network connectivity predicts sustained attention deficits after traumatic brain injury. *J Neurosci* 31**,** 13442-13451.

Borich, M., Babul, A.N., Yuan, P.H., Boyd, L., & Virji-Babul, N. (2015). Alterations in resting-state brain networks in concussed adolescent athletes. *J Neurotrauma* 32**,** 265-271.

Bramlett, H.M., & Dietrich, W.D. (2015). Long-term consequences of traumatic brain injury: current status of potential mechanisms of injury and neurological outcomes. *J Neurotrauma* 32**,** 1834-1848.

Brouwer, W.H., Ponds, R.W., Van Wolffelaar, P.C., & Van Zomeren, A.H. (1989). Divided attention 5 to 10 years after severe closed head injury. *Cortex* 25**,** 219-230.

Brouwer, W.H., Withaar, F.K., Tant, M.L., & Van Zomeren, A.H. (2002). Attention and driving in traumatic brain injury: a question of coping with time-pressure. *J Head Trauma Rehabil* 17**,** 1-15.

Brown, M., Baradaran, H., Christos, P.J., Wright, D., Gupta, A., & Tsiouris, A.J. (2018). Magnetic resonance spectroscopy abnormalities in traumatic brain injury: A meta-analysis. *J Neuroradiol* 45**,** 123-129.

Bullmore, E., & Sporns, O. (2009). Complex brain networks: graph theoretical analysis of structural and functional systems. *Nat Rev Neurosci* 10**,** 186-198.

Byrnes, K.R., Wilson, C.M., Brabazon, F., Von Leden, R., Jurgens, J.S., Oakes, T.R., & Selwyn, R.G. (2014). FDG-PET imaging in mild traumatic brain injury: a critical review. *Front Neuroenergetics* 5**,** 13.

Caeyenberghs, K., Leemans, A., Heitger, M.H., Leunissen, I., Dhollander, T., Sunaert, S., Dupont, P., & Swinnen, S.P. (2012). Graph analysis of functional brain networks for cognitive control of action in traumatic brain injury. *Brain* 135**,** 1293-1307.

Carlesimo, G.A., Casadio, P., & Caltagirone, C. (2004). Prospective and retrospective components in the memory for actions to be performed in patients with severe closed-head injury. *J Int Neuropsychol Soc* 10**,** 679-688.

Catroppa, C., Anderson, V., Godfrey, C., & Rosenfeld, J.V. (2011). Attentional skills 10 years post-paediatric traumatic brain injury (TBI). *Brain Inj* 25**,** 858-869.

Chan, R.C. (2000). Attentional deficits in patients with closed head injury: a further study to the discriminative validity of the test of everyday attention. *Brain Inj* 14**,** 227-236.

Chan, R.C. (2002). Attentional deficits in patients with persisting postconcussive complaints: a general deficit or specific component deficit? *J Clin Exp Neuropsychol* 24**,** 1081-1093.

Chang, Y.S., Owen, J.P., Pojman, N.J., Thieu, T., Bukshpun, P., Wakahiro, M.L., Berman, J.I., Roberts, T.P., Nagarajan, S.S., Sherr, E.H., & Mukherjee, P. (2015). White matter changes of neurite density and fiber orientation dispersion during human brain maturation. *PLoS One* 10**,** e0123656.

Churchill, N.W., Hutchison, M.G., Richards, D., Leung, G., Graham, S.J., & Schweizer, T.A. (2017). Neuroimaging of sport concussion: persistent alterations in brain structure and function at medical clearance. *Sci Rep* 7**,** 8297.

Cocchi, L., Bramati, I.E., Zalesky, A., Furukawa, E., Fontenelle, L.F., Moll, J., Tripp, G., & Mattos, P. (2012). Altered functional brain connectivity in a non-clinical sample of young adults with attention-deficit/hyperactivity disorder. *J Neurosci* 32**,** 17753-17761.

Cohen, B.A., Inglese, M., Rusinek, H., Babb, J.S., Grossman, R.I., & Gonen, O. (2007). Proton MR spectroscopy and MRI-volumetry in mild traumatic brain injury. *AJNR Am J Neuroradiol* 28**,** 907-913.

Colvin, A.C., Mullen, J., Lovell, M.R., West, R.V., Collins, M.W., & Groh, M. (2009). The role of concussion history and gender in recovery from soccer-related concussion. *Am J Sports Med* 37**,** 1699-1704.

Covassin, T., Elbin, R.J., Bleecker, A., Lipchik, A., & Kontos, A.P. (2013). Are there differences in neurocognitive function and symptoms between male and female soccer players after concussions? *Am J Sports Med* 41**,** 2890-2895.

Covassin, T., Elbin, R.J., Harris, W., Parker, T., & Kontos, A. (2012). The role of age and sex in symptoms, neurocognitive performance, and postural stability in athletes after concussion. *Am J Sports Med* 40**,** 1303-1312.

Covassin, T., Schatz, P., & Swanik, C.B. (2007). Sex differences in neuropsychological function and post-concussion symptoms of concussed collegiate athletes. *Neurosurgery* 61**,** 345-350; discussion 350-341.

Covassin, T., Swanik, C.B., Sachs, M., Kendrick, Z., Schatz, P., Zillmer, E., & Kaminaris, C. (2006). Sex differences in baseline neuropsychological function and concussion symptoms of collegiate athletes. *Br J Sports Med* 40**,** 923-927; discussion 927.

Cremona-Meteyard, S.L., Clark, C.R., Wright, M.J., & Geffen, G.M. (1992). Covert orientation of visual attention after closed head injury. *Neuropsychologia* 30**,** 123-132.

Croall, I.D., Cowie, C.J., He, J., Peel, A., Wood, J., Aribisala, B.S., Mitchell, P., Mendelow, A.D., Smith, F.E., Millar, D., Kelly, T., & Blamire, A.M. (2014). White matter correlates of cognitive dysfunction after mild traumatic brain injury. *Neurology* 83**,** 494-501.

Dale, A.M., Fischl, B., & Sereno, M.I. (1999). Cortical surface-based analysis. I. Segmentation and surface reconstruction. *Neuroimage* 9**,** 179-194.

Dall'acqua, P., Johannes, S., Mica, L., Simmen, H.P., Glaab, R., Fandino, J., Schwendinger, M., Meier, C., Ulbrich, E.J., Muller, A., Jancke, L., & Hanggi, J. (2016). Connectomic and surface-based morphometric correlates of acute mild traumatic brain injury. *Front Hum Neurosci* 10**,** 127.

Dall'acqua, P., Johannes, S., Mica, L., Simmen, H.P., Glaab, R., Fandino, J., Schwendinger, M., Meier, C., Ulbrich, E.J., Muller, A., Jancke, L., & Hanggi, J. (2017). Prefrontal cortical thickening after mild traumatic brain injury: A one-year magnetic resonance imaging study. *J Neurotrauma* 34**,** 3270-3279.

Daneshvar, D.H., Riley, D.O., Nowinski, C.J., Mckee, A.C., Stern, R.A., & Cantu, R.C. (2011). Long-term consequences: effects on normal development profile after concussion. *Phys Med Rehabil Clin N Am* 22**,** 683-700, ix.

De Freitas Cardoso, M.G., Faleiro, R.M., De Paula, J.J., Kummer, A., Caramelli, P., Teixeira, A.L., De Souza, L.C., & Miranda, A.S. (2019). Cognitive impairment following acute mild traumatic brain injury. *Front Neurol* 10**,** 198.

De La Fuente, A., Xia, S., Branch, C., & Li, X. (2013). A review of attention-deficit/hyperactivity disorder from the perspective of brain networks. *Front Hum Neurosci* 7**,** 192.

Dean, P.J., Sato, J.R., Vieira, G., Mcnamara, A., & Sterr, A. (2015). Long-term structural changes after mTBI and their relation to post-concussion symptoms. *Brain Inj***,** 1-8.

Depue, B.E., Orr, J.M., Smolker, H.R., Naaz, F., & Banich, M.T. (2016). The organization of right prefrontal networks reveals common mechanisms of inhibitory regulation across cognitive, emotional, and motor processes. *Cereb Cortex* 26**,** 1634-1646.

Desikan, R.S., Segonne, F., Fischl, B., Quinn, B.T., Dickerson, B.C., Blacker, D., Buckner, R.L., Dale, A.M., Maguire, R.P., Hyman, B.T., Albert, M.S., & Killiany, R.J. (2006). An automated labeling system for subdividing the human cerebral cortex on MRI scans into gyral based regions of interest. *Neuroimage* 31**,** 968-980.

Dewan, M.C., Rattani, A., Gupta, S., Baticulon, R.E., Hung, Y.C., Punchak, M., Agrawal, A., Adeleye, A.O., Shrime, M.G., Rubiano, A.M., Rosenfeld, J.V., & Park, K.B. (2018). Estimating the global incidence of traumatic brain injury. *J Neurosurg***,** 1-18.

Ding, K., Marquez De La Plata, C., Wang, J.Y., Mumphrey, M., Moore, C., Harper, C., Madden, C.J., Mccoll, R., Whittemore, A., Devous, M.D., & Diaz-Arrastia, R. (2008). Cerebral atrophy after traumatic white matter injury: correlation with acute neuroimaging and outcome. *J Neurotrauma* 25**,** 1433-1440.

Dona, O., Noseworthy, M.D., Dematteo, C., & Connolly, J.F. (2017). Fractal analysis of brain blood oxygenation level dependent (BOLD) signals from children with mild traumatic brain injury (mTBI). *PLoS One* 12**,** e0169647.

Donders, J., & Hoffman, N.M. (2002). Gender differences in learning and memory after pediatric traumatic brain injury. *Neuropsychology* 16**,** 491-499.

Donders, J., & Woodward, H.R. (2003). Gender as a moderator of memory after traumatic brain injury in children. *J Head Trauma Rehabil* 18**,** 106-115.

Dymowski, A.R., Owens, J.A., Ponsford, J.L., & Willmott, C. (2015). Speed of processing and strategic control of attention after traumatic brain injury. *J Clin Exp Neuropsychol* 37**,** 1024-1035.

Eaton-Rosen, Z., Melbourne, A., Orasanu, E., Cardoso, M.J., Modat, M., Bainbridge, A., Kendall, G.S., Robertson, N.J., Marlow, N., & Ourselin, S. (2015). Longitudinal measurement of the developing grey matter in preterm subjects using multi-modal MRI. *Neuroimage* 111**,** 580-589.

Echemendia, R.J., Giza, C.C., & Kutcher, J.S. (2015). Developing guidelines for return to play: consensus and evidence-based approaches. *Brain Inj* 29**,** 185-194.

Edlow, B.L., Copen, W.A., Izzy, S., Bakhadirov, K., Van Der Kouwe, A., Glenn, M.B., Greenberg, S.M., Greer, D.M., & Wu, O. (2016). Diffusion tensor imaging in acute-to-subacute traumatic brain injury: a longitudinal analysis. *BMC Neurol* 16**,** 2.

Eker, C., Schalen, W., Asgeirsson, B., Grande, P.O., Ranstam, J., & Nordstrom, C.H. (2000). Reduced mortality after severe head injury will increase the demands for rehabilitation services. *Brain Inj* 14**,** 605-619.

Emanuelson, I., & V Wendt, L. (1997). Epidemiology of traumatic brain injury in children and adolescents in south-western Sweden. *Acta Paediatr* 86**,** 730-735.

Epstein, J.N., Johnson, D., & Conners, C. K. (2006). Conners' adult ADHD diagnostic interview for DSM-IV. North Tonawanda, NY: Multi-Health Systems.

Eva M. Palacios, J.P.O., Esther L. Yuh, Maxwell B. Wang, Mary J. Vassar, Adam R. Ferguson, Ramon Diaz-Arrastia, Joseph T. Giacino, David O. Okonkwo, Claudia S. Robertson, Murray B. Stein, Nancy Temkin, Sonia Jain, Michael Mccrea, Christine L. Mac Donald, Harvey S. Levin, Geoffrey T. Manley, Pratik Mukherjee (2018). The evolution of white matter changes after mild traumatic brain injury: A DTI and NODDI study. *bioRxiv*.

Fakhran, S., Yaeger, K., Collins, M., & Alhilali, L. (2014). Sex differences in white matter abnormalities after mild traumatic brain injury: localization and correlation with outcome. *Radiology* 272**,** 815-823.

Fan, J., Mccandliss, B.D., Fossella, J., Flombaum, J.I., & Posner, M.I. (2005). The activation of attentional networks. *Neuroimage* 26**,** 471-479.

Fan, L., Li, H., Zhuo, J., Zhang, Y., Wang, J., Chen, L., Yang, Z., Chu, C., Xie, S., Laird, A.R., Fox, P.T., Eickhoff, S.B., Yu, C., & Jiang, T. (2016). The human brainnetome atlas: A new brain atlas based on connectional architecture. *Cereb Cortex* 26**,** 3508-3526.

Farahani, F.V., Karwowski, W., & Lighthall, N.R. (2019). Application of graph theory for identifying connectivity patterns in human brain networks: A aystematic review. *Front Neurosci* 13**,** 585.

Farbota, K.D., Bendlin, B.B., Alexander, A.L., Rowley, H.A., Dempsey, R.J., & Johnson, S.C. (2012). Longitudinal diffusion tensor imaging and neuropsychological correlates in traumatic brain injury patients. *Front Hum Neurosci* 6**,** 160.

Felmingham, K.L., Baguley, I.J., & Green, A.M. (2004). Effects of diffuse axonal injury on speed of information processing following severe traumatic brain injury. *Neuropsychology* 18**,** 564-571.

Ferrari, M., & Quaresima, V. (2012). A brief review on the history of human functional near-infrared spectroscopy (fNIRS) development and fields of application. *Neuroimage* 63**,** 921-935.

Ford, J.H., Giovanello, K.S., & Guskiewicz, K.M. (2013). Episodic memory in former professional football players with a history of concussion: an event-related functional neuroimaging study. *J Neurotrauma* 30**,** 1683-1701.

Friston, K.J. (2011). Functional and effective connectivity: a review. *Brain Connect* 1**,** 13-36.

Fujiwara, E., Schwartz, M.L., Gao, F., Black, S.E., & Levine, B. (2008). Ventral frontal cortex functions and quantified MRI in traumatic brain injury. *Neuropsychologia* 46**,** 461-474.

Gagnon, L., Cooper, R.J., Yucel, M.A., Perdue, K.L., Greve, D.N., & Boas, D.A. (2012). Short separation channel location impacts the performance of short channel regression in NIRS. *Neuroimage* 59**,** 2518-2528.

Gale, S.D., Baxter, L., Roundy, N., & Johnson, S.C. (2005). Traumatic brain injury and grey matter concentration: a preliminary voxel based morphometry study. *J Neurol Neurosurg Psychiatry* 76**,** 984-988.

Gale, S.D., Johnson, S.C., Bigler, E.D., & Blatter, D.D. (1995). Nonspecific white matter degeneration following traumatic brain injury. *J Int Neuropsychol Soc* 1**,** 17-28.

Geary, E.K., Kraus, M.F., Pliskin, N.H., & Little, D.M. (2010). Verbal learning differences in chronic mild traumatic brain injury. *J Int Neuropsychol Soc* 16**,** 506-516.

Ginstfeldt, T., & Emanuelson, I. (2010). An overview of attention deficits after paediatric traumatic brain injury. *Brain Inj* 24**,** 1123-1134.

Gosselin, N., Bottari, C., Chen, J.K., Petrides, M., Tinawi, S., De Guise, E., & Ptito, A. (2011). Electrophysiology and functional MRI in post-acute mild traumatic brain injury. *J Neurotrauma* 28**,** 329-341.

Govindarajan, K.A., Narayana, P.A., Hasan, K.M., Wilde, E.A., Levin, H.S., Hunter, J.V., Miller, E.R., Patel, V.K., Robertson, C.S., & Mccarthy, J.J. (2016). Cortical thickness in mild traumatic brain injury. *J Neurotrauma* 33**,** 1809-1817.

Halperin, J.M., O'brien, J.D., Newcorn, J.H., Healey, J.M., Pascualvaca, D.M., Wolf, L.E., & Young, J.G. (1990). Validation of hyperactive, aggressive, and mixed hyperactive/aggressive childhood disorders: a research note. *J Child Psychol Psychiatry* 31**,** 455-459.

Hammeke, T.A., Mccrea, M., Coats, S.M., Verber, M.D., Durgerian, S., Flora, K., Olsen, G.S., Leo, P.D., Gennarelli, T.A., & Rao, S.M. (2013). Acute and subacute changes in neural activation during the recovery from sport-related concussion. *J Int Neuropsychol Soc* 19**,** 863-872.

Hampshire, A., Macdonald, A., & Owen, A.M. (2013). Hypoconnectivity and hyperfrontality in retired American football players. *Sci Rep* 3**,** 2972.

Han, S., Jiang, Y., Gu, H., Rao, H., Mao, L., Cui, Y., & Zhai, R. (2004). The role of human parietal cortex in attention networks. *Brain* 127**,** 650-659.

Hart, J., Jr., Kraut, M.A., Womack, K.B., Strain, J., Didehbani, N., Bartz, E., Conover, H., Mansinghani, S., Lu, H., & Cullum, C.M. (2013). Neuroimaging of cognitive dysfunction and depression in aging retired National Football League players: a cross-sectional study. *JAMA Neurol* 70**,** 326-335.

Henry, J.D., Phillips, L.H., Crawford, J.R., Kliegel, M., Theodorou, G., & Summers, F. (2007). Traumatic brain injury and prospective memory: influence of task complexity. *J Clin Exp Neuropsychol* 29**,** 457-466.

Henry, L.C., Tremblay, J., Tremblay, S., Lee, A., Brun, C., Lepore, N., Theoret, H., Ellemberg, D., & Lassonde, M. (2011). Acute and chronic changes in diffusivity measures after sports concussion. *J Neurotrauma* 28**,** 2049-2059.

Hibino, S., Mase, M., Shirataki, T., Nagano, Y., Fukagawa, K., Abe, A., Nishide, Y., Aizawa, A., Iida, A., Ogawa, T., Abe, J., Hatta, T., Yamada, K., & Kabasawa, H. (2013). Oxyhemoglobin changes during cognitive rehabilitation after traumatic brain injury using near infrared spectroscopy. *Neurol Med Chir (Tokyo)* 53**,** 299-303.

Himanen, L., Portin, R., Isoniemi, H., Helenius, H., Kurki, T., & Tenovuo, O. (2005). Cognitive functions in relation to MRI findings 30 years after traumatic brain injury. *Brain Inj* 19**,** 93-100.

Holdsworth, S.J., & Bammer, R. (2008). Magnetic resonance imaging techniques: fMRI, DWI, and PWI. *Semin Neurol* 28**,** 395-406.

Hsu, H.L., Chen, D.Y., Tseng, Y.C., Kuo, Y.S., Huang, Y.L., Chiu, W.T., Yan, F.X., Wang, W.S., & Chen, C.J. (2015). Sex differences in working memory after mild traumatic brain injury: A functional MR imaging study. *Radiology* 276**,** 828-835.

Hu, P., Fan, J., Xu, P., Zhou, S., Zhang, L., Tian, Y., & Wang, K. (2013). Attention network impairments in patients with focal frontal or parietal lesions. *Neurosci Lett* 534**,** 177-181.

Hutchinson, J.B., Uncapher, M.R., & Wagner, A.D. (2009). Posterior parietal cortex and episodic retrieval: convergent and divergent effects of attention and memory. *Learn Mem* 16**,** 343-356.

Inglese, M., Makani, S., Johnson, G., Cohen, B.A., Silver, J.A., Gonen, O., & Grossman, R.I. (2005). Diffuse axonal injury in mild traumatic brain injury: a diffusion tensor imaging study. *J Neurosurg* 103**,** 298-303.

Irani, F., Platek, S.M., Bunce, S., Ruocco, A.C., & Chute, D. (2007). Functional near infrared spectroscopy (fNIRS): an emerging neuroimaging technology with important applications for the study of brain disorders. *Clin Neuropsychol* 21**,** 9-37.

Jenkinson, M., Bannister, P., Brady, M., & Smith, S. (2002). Improved optimization for the robust and accurate linear registration and motion correction of brain images. *Neuroimage* 17**,** 825-841.

Jenkinson, M., Beckmann, C.F., Behrens, T.E., Woolrich, M.W., & Smith, S.M. (2012). Fsl. *Neuroimage* 62**,** 782-790.

Jenkinson, M., & Smith, S. (2001). A global optimisation method for robust affine registration of brain images. *Med Image Anal* 5**,** 143-156.

Johansson, B., Berglund, P., & Ronnback, L. (2009). Mental fatigue and impaired information processing after mild and moderate traumatic brain injury. *Brain Inj* 23**,** 1027-1040.

Kaufmann, P.M., Fletcher, J.M., Levin, H.S., Miner, M.E., & Ewing-Cobbs, L. (1993). Attentional disturbance after pediatric closed head injury. *J Child Neurol* 8**,** 348-353.

Keightley, M.L., Saluja, R.S., Chen, J.K., Gagnon, I., Leonard, G., Petrides, M., & Ptito, A. (2014). A functional magnetic resonance imaging study of working memory in youth after sports-related concussion: is it still working? *J Neurotrauma* 31**,** 437-451.

Kennedy, E., Cohen, M., & Munafo, M. (2017). Childhood traumatic brain injury and the associations with risk behavior in adolescence and young adulthood: A systematic review. *J Head Trauma Rehabil* 32**,** 425-432.

Kinder, H.A., Baker, E.W., Wang, S., Fleischer, C.C., Howerth, E.W., Duberstein, K.J., Mao, H., Platt, S.R., & West, F.D. (2019). Traumatic brain injury results in dynamic brain structure changes leading to acute and chronic motor function deficits in a pediatric piglet model. *J Neurotrauma* 36**,** 2930-2942.

Kinsella, G., Murtagh, D., Landry, A., Homfray, K., Hammond, M., O'beirne, L., Dwyer, L., Lamont, M., & Ponsford, J. (1996). Everyday memory following traumatic brain injury. *Brain Inj* 10**,** 499-507.

Kliegel, M., Eschen, A., & Thone-Otto, A.I. (2004). Planning and realization of complex intentions in traumatic brain injury and normal aging. *Brain Cogn* 56**,** 43-54.

Knight, R.G., Harnett, M., & Titov, N. (2005). The effects of traumatic brain injury on the predicted and actual performance of a test of prospective remembering. *Brain Inj* 19**,** 19-27.

Knight, R.G., Titov, N., & Crawford, M. (2006). The effects of distraction on prospective remembering following traumatic brain injury assessed in a simulated naturalistic environment. *J Int Neuropsychol Soc* 12**,** 8-16.

Kocsis, L., Herman, P., & Eke, A. (2006). The modified Beer-Lambert law revisited. *Phys Med Biol* 51**,** N91-98.

Kohl, A.D., Wylie, G.R., Genova, H.M., Hillary, F.G., & Deluca, J. (2009). The neural correlates of cognitive fatigue in traumatic brain injury using functional MRI. *Brain Inj* 23**,** 420-432.

Konigs, M., Engenhorst, P.J., & Oosterlaan, J. (2016). Intelligence after traumatic brain injury: meta-analysis of outcomes and prognosis. *Eur J Neurol* 23**,** 21-29.

Kontos, A.P., Huppert, T.J., Beluk, N.H., Elbin, R.J., Henry, L.C., French, J., Dakan, S.M., & Collins, M.W. (2014). Brain activation during neurocognitive testing using functional near-infrared spectroscopy in patients following concussion compared to healthy controls. *Brain Imaging Behav* 8**,** 621-634.

Kramer, M.E., Chiu, C.Y., Walz, N.C., Holland, S.K., Yuan, W., Karunanayaka, P., & Wade, S.L. (2008). Long-term neural processing of attention following early childhood traumatic brain injury: fMRI and neurobehavioral outcomes. *J Int Neuropsychol Soc* 14**,** 424-435.

Kraus, M.F., Susmaras, T., Caughlin, B.P., Walker, C.J., Sweeney, J.A., & Little, D.M. (2007). White matter integrity and cognition in chronic traumatic brain injury: a diffusion tensor imaging study. *Brain* 130**,** 2508-2519.

Krivitzky, L.S., Roebuck-Spencer, T.M., Roth, R.M., Blackstone, K., Johnson, C.P., & Gioia, G. (2011). Functional magnetic resonance imaging of working memory and response inhibition in children with mild traumatic brain injury. *J Int Neuropsychol Soc* 17**,** 1143-1152.

Kunz, N., Zhang, H., Vasung, L., O'brien, K.R., Assaf, Y., Lazeyras, F., Alexander, D.C., & Huppi, P.S. (2014). Assessing white matter microstructure of the newborn with multi-shell diffusion MRI and biophysical compartment models. *Neuroimage* 96**,** 288-299.

Landis, J.R., & Koch, G.G. (1977). The measurement of observer agreement for categorical data. *Biometrics* 33**,** 159-174.

Lange, R.T., Iverson, G.L., Brubacher, J.R., Madler, B., & Heran, M.K. (2012). Diffusion tensor imaging findings are not strongly associated with postconcussional disorder 2 months following mild traumatic brain injury. *J Head Trauma Rehabil* 27**,** 188-198.

Langlois, J.A., Rutland-Brown, W., & Wald, M.M. (2006). The epidemiology and impact of traumatic brain injury: a brief overview. *J Head Trauma Rehabil* 21**,** 375-378.

Latora, V., & Marchiori, M. (2001). Efficient behavior of small-world networks. *Phys Rev Lett* 87**,** 198701.

Leclercq, M., Couillet, J., Azouvi, P., Marlier, N., Martin, Y., Strypstein, E., & Rousseaux, M. (2000). Dual task performance after severe diffuse traumatic brain injury or vascular prefrontal damage. *J Clin Exp Neuropsychol* 22**,** 339-350.

Lemkaddem, A., Daducci, A., Kunz, N., Lazeyras, F., Seeck, M., Thiran, J.P., & Vulliemoz, S. (2014). Connectivity and tissue microstructural alterations in right and left temporal lobe epilepsy revealed by diffusion spectrum imaging. *Neuroimage Clin* 5**,** 349-358.

Lengenfelder, J., Schultheis, M.T., Al-Shihabi, T., Mourant, R., & Deluca, J. (2002). Divided attention and driving: a pilot study using virtual reality technology. *J Head Trauma Rehabil* 17**,** 26-37.

Levin, H.S., Hanten, G., Zhang, L., Swank, P.R., & Hunter, J. (2004). Selective impairment of inhibition after TBI in children. *J Clin Exp Neuropsychol* 26**,** 589-597.

Levine, B., Kovacevic, N., Nica, E.I., Cheung, G., Gao, F., Schwartz, M.L., & Black, S.E. (2008). The Toronto traumatic brain injury study: injury severity and quantified MRI. *Neurology* 70**,** 771-778.

Lewine, J.D., Plis, S., Ulloa, A., Williams, C., Spitz, M., Foley, J., Paulson, K., Davis, J., Bangera, N., Snyder, T., & Weaver, L. (2019). Quantitative EEG Biomarkers for Mild Traumatic Brain Injury. *J Clin Neurophysiol* 36**,** 298-305.

Li, F., Lu, L., Chen, H., Wang, P., Zhang, H., Chen, Y.C., & Yin, X. (2019). Neuroanatomical and functional alterations of insula in mild traumatic brain injury patients at the acute stage. *Brain Imaging Behav*.

Li, T., Gong, H., & Luo, Q. (2011). Visualization of light propagation in visible Chinese human head for functional near-infrared spectroscopy. *J Biomed Opt* 16**,** 045001.

Li, X., Branch, C., De La Fuente, A., & Xia, S. (2013). Role of pulvinar-cortical functional brain pathways in attention-deficit/hyperactivity disorder. *J Am Acad Child Adolesc Psychiatry* 52**,** 756-758.

Li, X., Sroubek, A., Kelly, M.S., Lesser, I., Sussman, E., He, Y., Branch, C., & Foxe, J.J. (2012a). Atypical pulvinar-cortical pathways during sustained attention performance in children with attention-deficit/hyperactivity disorder. *J Am Acad Child Adolesc Psychiatry* 51**,** 1197-1207 e1194.

Li, X., Xia, S., Bertisch, H.C., Branch, C.A., & Delisi, L.E. (2012b). Unique topology of language processing brain network: a systems-level biomarker of schizophrenia. *Schizophr Res* 141**,** 128-136.

Lipton, M.L., Gellella, E., Lo, C., Gold, T., Ardekani, B.A., Shifteh, K., Bello, J.A., & Branch, C.A. (2008). Multifocal white matter ultrastructural abnormalities in mild traumatic brain injury with cognitive disability: a voxel-wise analysis of diffusion tensor imaging. *J Neurotrauma* 25**,** 1335-1342.

Lipton, M.L., Gulko, E., Zimmerman, M.E., Friedman, B.W., Kim, M., Gellella, E., Gold, T., Shifteh, K., Ardekani, B.A., & Branch, C.A. (2009). Diffusion-tensor imaging implicates prefrontal axonal injury in executive function impairment following very mild traumatic brain injury. *Radiology* 252**,** 816-824.

Lipton, M.L., Kim, N., Park, Y.K., Hulkower, M.B., Gardin, T.M., Shifteh, K., Kim, M., Zimmerman, M.E., Lipton, R.B., & Branch, C.A. (2012). Robust detection of traumatic axonal injury in individual mild traumatic brain injury patients: intersubject variation, change over time and bidirectional changes in anisotropy. *Brain Imaging Behav* 6**,** 329-342.

Lo, C., Shifteh, K., Gold, T., Bello, J.A., & Lipton, M.L. (2009). Diffusion tensor imaging abnormalities in patients with mild traumatic brain injury and neurocognitive impairment. *J Comput Assist Tomogr* 33**,** 293-297.

Lu, L., Li, F., Ma, Y., Chen, H., Wang, P., Peng, M., Chen, Y.C., & Yin, X. (2019). Functional connectivity disruption of the substantia nigra associated with cognitive impairment in acute mild traumatic brain injury. *Eur J Radiol* 114**,** 69-75.

Mackenzie, J.D., Siddiqi, F., Babb, J.S., Bagley, L.J., Mannon, L.J., Sinson, G.P., & Grossman, R.I. (2002). Brain atrophy in mild or moderate traumatic brain injury: a longitudinal quantitative analysis. *AJNR Am J Neuroradiol* 23**,** 1509-1515.

Mallat, S. (1998). *A Wavelet Tour of Signal Processing.* Cambridge, Massachusetts: Academic Press.

Mallott, J.M., Palacios, E.M., Maruta, J., Ghajar, J., & Mukherjee, P. (2019). Disrupted white matter microstructure of the cerebellar peduncles in scholastic athletes after concussion. *Front Neurol* 10**,** 518.

Mangels, J.A., Craik, F.I., Levine, B., Schwartz, M.L., & Stuss, D.T. (2002). Effects of divided attention on episodic memory in chronic traumatic brain injury: a function of severity and strategy. *Neuropsychologia* 40**,** 2369-2385.

Mangeot, S., Armstrong, K., Colvin, A.N., Yeates, K.O., & Taylor, H.G. (2002). Long-term executive function deficits in children with traumatic brain injuries: assessment using the behavior rating inventory of executive function (BRIEF). *Child Neuropsychol* 8**,** 271-284.

Maruta, J., Suh, M., Niogi, S.N., Mukherjee, P., & Ghajar, J. (2010). Visual tracking synchronization as a metric for concussion screening. *J Head Trauma Rehabil* 25**,** 293-305.

Mathias, J.L., & Mansfield, K.M. (2005). Prospective and declarative memory problems following moderate and severe traumatic brain injury. *Brain Inj* 19**,** 271-282.

Max, J.E., Schachar, R.J., Levin, H.S., Ewing-Cobbs, L., Chapman, S.B., Dennis, M., Saunders, A., & Landis, J. (2005a). Predictors of attention-deficit/hyperactivity disorder within 6 months after pediatric traumatic brain injury. *J Am Acad Child Adolesc Psychiatry* 44**,** 1032-1040.

Max, J.E., Schachar, R.J., Levin, H.S., Ewing-Cobbs, L., Chapman, S.B., Dennis, M., Saunders, A., & Landis, J. (2005b). Predictors of secondary attention-deficit/hyperactivity disorder in children and adolescents 6 to 24 months after traumatic brain injury. *J Am Acad Child Adolesc Psychiatry* 44**,** 1041-1049.

Mayer, A.R., Ling, J., Mannell, M.V., Gasparovic, C., Phillips, J.P., Doezema, D., Reichard, R., & Yeo, R.A. (2010). A prospective diffusion tensor imaging study in mild traumatic brain injury. *Neurology* 74**,** 643-650.

Mayer, A.R., Mannell, M.V., Ling, J., Elgie, R., Gasparovic, C., Phillips, J.P., Doezema, D., & Yeo, R.A. (2009). Auditory orienting and inhibition of return in mild traumatic brain injury: a FMRI study. *Hum Brain Mapp* 30**,** 4152-4166.

Mcallister, T.W., Saykin, A.J., Flashman, L.A., Sparling, M.B., Johnson, S.C., Guerin, S.J., Mamourian, A.C., Weaver, J.B., & Yanofsky, N. (1999). Brain activation during working memory 1 month after mild traumatic brain injury: a functional MRI study. *Neurology* 53**,** 1300-1308.

Mcallister, T.W., Sparling, M.B., Flashman, L.A., Guerin, S.J., Mamourian, A.C., & Saykin, A.J. (2001). Differential working memory load effects after mild traumatic brain injury. *Neuroimage* 14**,** 1004-1012.

Mcdonald, B.C., Flashman, L.A., & Saykin, A.J. (2002). Executive dysfunction following traumatic brain injury: neural substrates and treatment strategies. *NeuroRehabilitation* 17**,** 333-344.

Mcdonald, B.C., Saykin, A.J., & Mcallister, T.W. (2012). Functional MRI of mild traumatic brain injury (mTBI): progress and perspectives from the first decade of studies. *Brain Imaging Behav* 6**,** 193-207.

Mcglade, E., Rogowska, J., & Yurgelun-Todd, D. (2015). Sex differences in orbitofrontal connectivity in male and female veterans with TBI. *Brain Imaging Behav* 9**,** 535-549.

Mckee, A.C., & Daneshvar, D.H. (2015). The neuropathology of traumatic brain injury. *Handb Clin Neurol* 127**,** 45-66.

Mckinlay, A., Grace, R.C., Horwood, L.J., Fergusson, D.M., Ridder, E.M., & Macfarlane, M.R. (2008). Prevalence of traumatic brain injury among children, adolescents and young adults: prospective evidence from a birth cohort. *Brain Inj* 22**,** 175-181.

Messe, A., Caplain, S., Pelegrini-Issac, M., Blancho, S., Levy, R., Aghakhani, N., Montreuil, M., Benali, H., & Lehericy, S. (2013). Specific and evolving resting-state network alterations in post-concussion syndrome following mild traumatic brain injury. *PLoS One* 8**,** e65470.

Meunier, D., Fonlupt, P., Saive, A.L., Plailly, J., Ravel, N., & Royet, J.P. (2014). Modular structure of functional networks in olfactory memory. *Neuroimage* 95**,** 264-275.

Miotto, E.C., Cinalli, F.Z., Serrao, V.T., Benute, G.G., Lucia, M.C., & Scaff, M. (2010). Cognitive deficits in patients with mild to moderate traumatic brain injury. *Arq Neuropsiquiatr* 68**,** 862-868.

Mirsky, A.F., Anthony, B.J., Duncan, C.C., Ahearn, M.B., & Kellam, S.G. (1991). Analysis of the elements of attention: a neuropsychological approach. *Neuropsychol Rev* 2**,** 109-145.

Mori, S., & Van Zijl, P. (2007). Human white matter atlas. *Am J Psychiatry* 164**,** 1005.

Mori, S., & Zhang, J. (2006). Principles of diffusion tensor imaging and its applications to basic neuroscience research. *Neuron* 51**,** 527-539.

Mukherjee, P., Berman, J.I., Chung, S.W., Hess, C.P., & Henry, R.G. (2008). Diffusion tensor MR imaging and fiber tractography: theoretic underpinnings. *AJNR Am J Neuroradiol* 29**,** 632-641.

Munivenkatappa, A., Devi, B.I., Shukla, D.P., & Rajeswaran, J. (2014). Three time point changes in diffusion tensor values and their association with cognitive sequel among mild injury patients. *J Neurosurg Sci* 63, 525-530.

Nadebaum, C., Anderson, V., & Catroppa, C. (2007). Executive function outcomes following traumatic brain injury in young children: a five year follow-up. *Dev Neuropsychol* 32**,** 703-728.

Nakamura, T., Hillary, F.G., & Biswal, B.B. (2009). Resting network plasticity following brain injury. *PLoS One* 4**,** e8220.

Nazeri, A., Chakravarty, M.M., Rotenberg, D.J., Rajji, T.K., Rathi, Y., Michailovich, O.V., & Voineskos, A.N. (2015). Functional consequences of neurite orientation dispersion and density in humans across the adult lifespan. *J Neurosci* 35**,** 1753-1762.

Niogi, S.N., Mukherjee, P., Ghajar, J., Johnson, C., Kolster, R.A., Sarkar, R., Lee, H., Meeker, M., Zimmerman, R.D., Manley, G.T., & Mccandliss, B.D. (2008a). Extent of microstructural white matter injury in postconcussive syndrome correlates with impaired cognitive reaction time: a 3T diffusion tensor imaging study of mild traumatic brain injury. *AJNR Am J Neuroradiol* 29**,** 967-973.

Niogi, S.N., Mukherjee, P., Ghajar, J., Johnson, C.E., Kolster, R., Lee, H., Suh, M., Zimmerman, R.D., Manley, G.T., & Mccandliss, B.D. (2008b). Structural dissociation of attentional control and memory in adults with and without mild traumatic brain injury. *Brain* 131**,** 3209-3221.

Novack, T.A., Bush, B.A., Meythaler, J.M., & Canupp, K. (2001). Outcome after traumatic brain injury: pathway analysis of contributions from premorbid, injury severity, and recovery variables. *Arch Phys Med Rehabil* 82**,** 300-305.

Oehr, L., & Anderson, J. (2017). Diffusion-tensor imaging findings and cognitive function following hospitalized mixed-mechanism mild traumatic brain injury: A systematic review and meta-analysis. *Arch Phys Med Rehabil* 98**,** 2308-2319.

Ogawa, S., Lee, T.M., Kay, A.R., & Tank, D.W. (1990). Brain magnetic resonance imaging with contrast dependent on blood oxygenation. *Proc Natl Acad Sci U S A* 87**,** 9868-9872.

Ogawa, S., Tank, D.W., Menon, R., Ellermann, J.M., Kim, S.G., Merkle, H., & Ugurbil, K. (1992). Intrinsic signal changes accompanying sensory stimulation: functional brain mapping with magnetic resonance imaging. *Proc Natl Acad Sci U S A* 89**,** 5951-5955.

Okada, E., Firbank, M., Schweiger, M., Arridge, S.R., Cope, M., & Delpy, D.T. (1997). Theoretical and experimental investigation of near-infrared light propagation in a model of the adult head. *Appl Opt* 36**,** 21-31.

Oldfield, R.C. (1971). The assessment and analysis of handedness: the edinburgh inventory. *Neuropsychologia* 9**,** 97-113.

Owen, J.P., Chang, Y.S., Pojman, N.J., Bukshpun, P., Wakahiro, M.L., Marco, E.J., Berman, J.I., Spiro, J.E., Chung, W.K., Buckner, R.L., Roberts, T.P., Nagarajan, S.S., Sherr, E.H., Mukherjee, P., & Simons, V.I.P.C. (2014). Aberrant white matter microstructure in children with 16p11.2 deletions. *J Neurosci* 34**,** 6214-6223.

Pandit, A.S., Expert, P., Lambiotte, R., Bonnelle, V., Leech, R., Turkheimer, F.E., & Sharp, D.J. (2013). Traumatic brain injury impairs small-world topology. *Neurology* 80**,** 1826-1833.

Park, N.W., Moscovitch, M., & Robertson, I.H. (1999). Divided attention impairments after traumatic brain injury. *Neuropsychologia* 37**,** 1119-1133.

Paterno, R., Folweiler, K.A., & Cohen, A.S. (2017). Pathophysiology and treatment of memory dysfunction after traumatic brain injury. *Curr Neurol Neurosci Rep* 17**,** 52.

Petersen, S.E., & Posner, M.I. (2012). The attention system of the human brain: 20 years after. *Annu Rev Neurosci* 35**,** 73-89.

Phillips, M.L., Travis, M.J., Fagiolini, A., & Kupfer, D.J. (2008). Medication effects in neuroimaging studies of bipolar disorder. *Am J Psychiatry* 165**,** 313-320.

Platel, H., Price, C., Baron, J.C., Wise, R., Lambert, J., Frackowiak, R.S., Lechevalier, B., & Eustache, F. (1997). The structural components of music perception. A functional anatomical study. *Brain* 120 (Pt 2)**,** 229-243.

Ponsford, J., & Kinsella, G. (1992). Attentional deficits following closed-head injury. *J Clin Exp Neuropsychol* 14**,** 822-838.

Power, J.D., Barnes, K.A., Snyder, A.Z., Schlaggar, B.L., & Petersen, S.E. (2012). Spurious but systematic correlations in functional connectivity MRI networks arise from subject motion. *Neuroimage* 59**,** 2142-2154.

Power, J.D., Cohen, A.L., Nelson, S.M., Wig, G.S., Barnes, K.A., Church, J.A., Vogel, A.C., Laumann, T.O., Miezin, F.M., Schlaggar, B.L., & Petersen, S.E. (2011). Functional network organization of the human brain. *Neuron* 72**,** 665-678.

Rajashree Doshi, A.P. (2013). Non-Invasive Optical Sensor for Hemoglobin Determination. *IJERA* 3**,** p559-562.

Rios, M., Perianez, J.A., & Munoz-Cespedes, J.M. (2004). Attentional control and slowness of information processing after severe traumatic brain injury. *Brain Inj* 18**,** 257-272.

Rodriguez Merzagora, A.C., Izzetoglu, M., Onaral, B., & Schultheis, M.T. (2014). Verbal working memory impairments following traumatic brain injury: an fNIRS investigation. *Brain Imaging Behav* 8**,** 446-459.

Rubia, K., Halari, R., Cubillo, A., Mohammad, A.M., Brammer, M., & Taylor, E. (2009). Methylphenidate normalises activation and functional connectivity deficits in attention and motivation networks in medication-naive children with ADHD during a rewarded continuous performance task. *Neuropharmacology* 57**,** 640-652.

Saluja, R.S., Chen, J.K., Gagnon, I.J., Keightley, M., & Ptito, A. (2015). Navigational memory functional magnetic resonance imaging: a test for concussion in children. *J Neurotrauma* 32**,** 712-722.

Sanchez-Carrion, R., Gomez, P.V., Junque, C., Fernandez-Espejo, D., Falcon, C., Bargallo, N., Roig-Rovira, T., Ensenat-Cantallops, A., & Bernabeu, M. (2008). Frontal hypoactivation on functional magnetic resonance imaging in working memory after severe diffuse traumatic brain injury. *J Neurotrauma* 25**,** 479-494.

Sandel, N.K., Schatz, P., Goldberg, K.B., & Lazar, M. (2017). Sex-based differences in cognitive deficits and symptom reporting among acutely concussed adolescent lacrosse and soccer players. *Am J Sports Med* 45**,** 937-944.

Scarapicchia, V., Brown, C., Mayo, C., & Gawryluk, J.R. (2017). Functional magnetic resonance imaging and functional near-infrared spectroscopy: Insights from combined recording studies. *Front Hum Neurosci* 11**,** 419.

Scheibel, R.S., Newsome, M.R., Steinberg, J.L., Pearson, D.A., Rauch, R.A., Mao, H., Troyanskaya, M., Sharma, R.G., & Levin, H.S. (2007). Altered brain activation during cognitive control in patients with moderate to severe traumatic brain injury. *Neurorehabil Neural Repair* 21**,** 36-45.

Schmahmann, J.D., Smith, E.E., Eichler, F.S., & Filley, C.M. (2008). Cerebral white matter: neuroanatomy, clinical neurology, and neurobehavioral correlates. *Ann N Y Acad Sci* 1142**,** 266-309.

Schmitter-Edgecombe, M., & Wright, M.J. (2004). Event-based prospective memory following severe closed-head injury. *Neuropsychology* 18**,** 353-361.

Schneider, M.F., Krick, C.M., Retz, W., Hengesch, G., Retz-Junginger, P., Reith, W., & Rosler, M. (2010). Impairment of fronto-striatal and parietal cerebral networks correlates with attention deficit hyperactivity disorder (ADHD) psychopathology in adults - a functional magnetic resonance imaging (fMRI) study. *Psychiatry Res* 183**,** 75-84.

Schonberger, M., Ponsford, J., Reutens, D., Beare, R., & O'sullivan, R. (2009). The Relationship between age, injury severity, and MRI findings after traumatic brain injury. *J Neurotrauma* 26**,** 2157-2167.

Schwartz, E.D., Shumsky, J.S., Wehrli, S., Tessler, A., Murray, M., & Hackney, D.B. (2003). Ex vivo MR determined apparent diffusion coefficients correlate with motor recovery mediated by intraspinal transplants of fibroblasts genetically modified to express BDNF. *Exp Neurol* 182**,** 49-63.

Scott A. Huettel, A.W.S., Gregory Mccarthy *Functional Magnetic Resonance Imaging, Third Edition*, Sunderland, Massachusetts: Sinauer Associates, Inc.

Shah, S.A., Goldin, Y., Conte, M.M., Goldfine, A.M., Mohamadpour, M., Fidali, B.C., Cicerone, K., & Schiff, N.D. (2017). Executive attention deficits after traumatic brain injury reflect impaired recruitment of resources. *Neuroimage Clin* 14**,** 233-241.

Shao, M., Cao, J., Bai, L., Huang, W., Wang, S., Sun, C., Gan, S., Ye, L., Yin, B., Zhang, D., Gu, C., Hu, L., Bai, G., & Yan, Z. (2018). Preliminary evidence of sex differences in cortical thickness following acute mild traumatic brain injury. *Front Neurol* 9**,** 878.

Shin, J., Muller, K.R., & Hwang, H.J. (2016). Near-infrared spectroscopy (NIRS)-based eyes-closed brain-computer interface (BCI) using prefrontal cortex activation due to mental arithmetic. *Sci Rep* 6**,** 36203.

Shrout, P.E., & Fleiss, J.L. (1979). Intraclass correlations: uses in assessing rater reliability. *Psychol Bull* 86**,** 420-428.

Shum, D., Valentine, M., & Cutmore, T. (1999). Performance of individuals with severe long-term traumatic brain injury on time-, event-, and activity-based prospective memory tasks. *J Clin Exp Neuropsychol* 21**,** 49-58.

Siddiqui, M.F., Lloyd-Fox, S., Kaynezhad, P., Tachtsidis, I., Johnson, M.H., & Elwell, C.E. (2017). Non-invasive measurement of a metabolic marker of infant brain function. *Sci Rep* 7**,** 1330.

Sinopoli, K.J., Schachar, R., & Dennis, M. (2011). Traumatic brain injury and secondary attention-deficit/hyperactivity disorder in children and adolescents: the effect of reward on inhibitory control. *J Clin Exp Neuropsychol* 33**,** 805-819.

Smits, M., Houston, G.C., Dippel, D.W., Wielopolski, P.A., Vernooij, M.W., Koudstaal, P.J., Hunink, M.G., & Van Der Lugt, A. (2011). Microstructural brain injury in post-concussion syndrome after minor head injury. *Neuroradiology* 53**,** 553-563.

Soeda, A., Nakashima, T., Okumura, A., Kuwata, K., Shinoda, J., & Iwama, T. (2005). Cognitive impairment after traumatic brain injury: a functional magnetic resonance imaging study using the Stroop task. *Neuroradiology* 47**,** 501-506.

Sollmann, N., Echlin, P.S., Schultz, V., Viher, P.V., Lyall, A.E., Tripodis, Y., Kaufmann, D., Hartl, E., Kinzel, P., Forwell, L.A., Johnson, A.M., Skopelja, E.N., Lepage, C., Bouix, S., Pasternak, O., Lin, A.P., Shenton, M.E., & Koerte, I.K. (2018). Sex differences in white matter alterations following repetitive subconcussive head impacts in collegiate ice hockey players. *Neuroimage Clin* 17**,** 642-649.

Sozda, C.N., Larson, M.J., Kaufman, D.A., Schmalfuss, I.M., & Perlstein, W.M. (2011). Error-related processing following severe traumatic brain injury: an event-related functional magnetic resonance imaging (fMRI) study. *Int J Psychophysiol* 82**,** 97-106.

Spikman, J.M., Van Zomeren, A.H., & Deelman, B.G. (1996). Deficits of attention after closed-head injury: slowness only? *J Clin Exp Neuropsychol* 18**,** 755-767.

Sporns, O., Honey, C.J., & Kotter, R. (2007). Identification and classification of hubs in brain networks. *PLoS One* 2**,** e1049.

Strangman, G.E., Li, Z., & Zhang, Q. (2013). Depth sensitivity and source-detector separations for near infrared spectroscopy based on the Colin27 brain template. *PLoS One* 8**,** e66319.

Strangman, G.E., O'neil-Pirozzi, T.M., Supelana, C., Goldstein, R., Katz, D.I., & Glenn, M.B. (2010). Regional brain morphometry predicts memory rehabilitation outcome after traumatic brain injury. *Front Hum Neurosci* 4**,** 182.

Stulemeijer, M., Vos, P.E., Van Der Werf, S., Van Dijk, G., Rijpkema, M., & Fernandez, G. (2010). How mild traumatic brain injury may affect declarative memory performance in the post-acute stage. *J Neurotrauma* 27**,** 1585-1595.

Stuss, D.T., Stethem, L.L., Hugenholtz, H., Picton, T., Pivik, J., & Richard, M.T. (1989). Reaction time after head injury: fatigue, divided and focused attention, and consistency of performance. *J Neurol Neurosurg Psychiatry* 52**,** 742-748.

Szczepanski, S.M., Konen, C.S., & Kastner, S. (2010). Mechanisms of spatial attention control in frontal and parietal cortex. *J Neurosci* 30**,** 148-160.

Tana, M.M., E. Cerutti, S. Bianchi, Am. (2010). Exploring cortical attentional system by using fMRI during a Continuous Perfomance Test. *Comput Intell Neurosci***,** 329213.

Tang, L., Ge, Y., Sodickson, D.K., Miles, L., Zhou, Y., Reaume, J., & Grossman, R.I. (2011). Thalamic resting-state functional networks: disruption in patients with mild traumatic brain injury. *Radiology* 260**,** 831-840.

Tanveer, S., Zecavati, N., Delasobera, E.B., & Oyegbile, T.O. (2017). Gender differences in concussion and postinjury cognitive findings in an older and younger pediatric population. *Pediatr Neurol* 70**,** 44-49.

Tate, D.F., & Bigler, E.D. (2000). Fornix and hippocampal atrophy in traumatic brain injury. *Learn Mem* 7**,** 442-446.

Tate, D.F., York, G.E., Reid, M.W., Cooper, D.B., Jones, L., Robin, D.A., Kennedy, J.E., & Lewis, J. (2014). Preliminary findings of cortical thickness abnormalities in blast injured service members and their relationship to clinical findings. *Brain Imaging Behav* 8**,** 102-109.

Tay, S.Y., Ang, B.T., Lau, X.Y., Meyyappan, A., & Collinson, S.L. (2010). Chronic impairment of prospective memory after mild traumatic brain injury. *J Neurotrauma* 27**,** 77-83.

Timmers, I., Zhang, H., Bastiani, M., Jansma, B.M., Roebroeck, A., & Rubio-Gozalbo, M.E. (2015). White matter microstructure pathology in classic galactosemia revealed by neurite orientation dispersion and density imaging. *J Inherit Metab Dis* 38**,** 295-304.

Tong, Y., Hocke, L.M., Licata, S.C., & Frederick, B. (2012). Low-frequency oscillations measured in the periphery with near-infrared spectroscopy are strongly correlated with blood oxygen level-dependent functional magnetic resonance imaging signals. *J Biomed Opt* 17**,** 106004.

Tong, Y., Hocke, L.M., Lindsey, K.P., Erdogan, S.B., Vitaliano, G., Caine, C.E., & Frederick, B. (2016). Systemic low-frequency oscillations in BOLD signal vary with tissue type. *Front Neurosci* 10**,** 313.

Tong, Y., Hocke, L.M., Nickerson, L.D., Licata, S.C., Lindsey, K.P., & Frederick, B. (2013). Evaluating the effects of systemic low frequency oscillations measured in the periphery on the independent component analysis results of resting state networks. *Neuroimage* 76**,** 202-215.

Treble-Barna, A., Schultz, H., Minich, N., Taylor, H.G., Yeates, K.O., Stancin, T., & Wade, S.L. (2017). Long-term classroom functioning and its association with neuropsychological and academic performance following traumatic brain injury during early childhood. *Neuropsychology* 31**,** 486-498.

Trivedi, M.A., Ward, M.A., Hess, T.M., Gale, S.D., Dempsey, R.J., Rowley, H.A., & Johnson, S.C. (2007). Longitudinal changes in global brain volume between 79 and 409 days after traumatic brain injury: relationship with duration of coma. *J Neurotrauma* 24**,** 766-771.

Turner, G.R., & Levine, B. (2008). Augmented neural activity during executive control processing following diffuse axonal injury. *Neurology* 71**,** 812-818.

Vakil, E., Blachstein, H., & Hoofien, D. (1991). Automatic temporal order judgment: the effect of intentionality of retrieval on closed-head-injured patients. *J Clin Exp Neuropsychol* 13**,** 291-298.

Vakorin, V.A., Doesburg, S.M., Da Costa, L., Jetly, R., Pang, E.W., & Taylor, M.J. (2016). Detecting mild traumatic brain injury using resting state magnetoencephalographic connectivity. *PLoS Comput Biol* 12**,** e1004914.

Van Dijk, K.R., Sabuncu, M.R., & Buckner, R.L. (2012). The influence of head motion on intrinsic functional connectivity MRI. *Neuroimage* 59**,** 431-438.

Vas, A.K., Chapman, S.B., & Cook, L.G. (2015). Language impairments in traumatic brain injury: a window into complex cognitive performance. *Handb Clin Neurol* 128**,** 497-510.

Villapol, S., Loane, D.J., & Burns, M.P. (2017). Sexual dimorphism in the inflammatory response to traumatic brain injury. *Glia* 65**,** 1423-1438.

Wang, L., Zhu, C., He, Y., Zang, Y., Cao, Q., Zhang, H., Zhong, Q., & Wang, Y. (2009). Altered small-world brain functional networks in children with attention-deficit/hyperactivity disorder. *Hum Brain Mapp* 30**,** 638-649.

Wang, S., Hu, L., Cao, J., Huang, W., Sun, C., Zheng, D., Wang, Z., Gan, S., Niu, X., Gu, C., Bai, G., Ye, L., Zhang, D., Zhang, N., Yin, B., Zhang, M., & Bai, L. (2018). Sex differences in abnormal intrinsic functional connectivity after acute mild traumatic brain injury. *Front Neural Circuits* 12**,** 107.

Wang, X., Ren, Y., & Zhang, W. (2017). Depression disorder classification of fMRI data using sparse low-rank functional brain network and graph-based features. *Comput Math Methods Med* 2017**,** 3609821.

Wang, X., Xie, H., Cotton, A.S., Tamburrino, M.B., Brickman, K.R., Lewis, T.J., Mclean, S.A., & Liberzon, I. (2015). Early cortical thickness change after mild traumatic brain injury following motor vehicle collision. *J Neurotrauma* 32**,** 455-463.

Warner, M.A., Marquez De La Plata, C., Spence, J., Wang, J.Y., Harper, C., Moore, C., Devous, M., & Diaz-Arrastia, R. (2010a). Assessing spatial relationships between axonal integrity, regional brain volumes, and neuropsychological outcomes after traumatic axonal injury. *J Neurotrauma* 27**,** 2121-2130.

Warner, M.A., Youn, T.S., Davis, T., Chandra, A., Marquez De La Plata, C., Moore, C., Harper, C., Madden, C.J., Spence, J., Mccoll, R., Devous, M., King, R.D., & Diaz-Arrastia, R. (2010b). Regionally selective atrophy after traumatic axonal injury. *Arch Neurol* 67**,** 1336-1344.

Watts, D.J., & Strogatz, S.H. (1998). Collective dynamics of 'small-world' networks. *Nature* 393**,** 440-442.

Wig, G.S., Laumann, T.O., Cohen, A.L., Power, J.D., Nelson, S.M., Glasser, M.F., Miezin, F.M., Snyder, A.Z., Schlaggar, B.L., & Petersen, S.E. (2014). Parcellating an individual subject's cortical and subcortical brain structures using snowball sampling of resting-state correlations. *Cereb Cortex* 24**,** 2036-2054.

Winston, G.P., Micallef, C., Symms, M.R., Alexander, D.C., Duncan, J.S., & Zhang, H. (2014). Advanced diffusion imaging sequences could aid assessing patients with focal cortical dysplasia and epilepsy. *Epilepsy Res* 108**,** 336-339.

Witt, S.T., Lovejoy, D.W., Pearlson, G.D., & Stevens, M.C. (2010). Decreased prefrontal cortex activity in mild traumatic brain injury during performance of an auditory oddball task. *Brain Imaging Behav* 4**,** 232-247.

Wood, R.L., & Rutterford, N.A. (2006). Long-term effect of head trauma on intellectual abilities: a 16-year outcome study. *J Neurol Neurosurg Psychiatry* 77**,** 1180-1184.

Wu, Y., Wang, J., Zhang, Y., Zheng, D., Zhang, J., Rong, M., Wu, H., Wang, Y., Zhou, K., & Jiang, T. (2016). The neuroanatomical basis for posterior superior parietal lobule control lateralization of visuospatial attention. *Front Neuroanat* 10**,** 32.

Wu, Y.C., Mustafi, S.M., Harezlak, J., Kodiweera, C., Flashman, L.A., & Mcallister, T.W. (2018a). Hybrid diffusion imaging in mild traumatic brain injury. *J Neurotrauma* 35**,** 2377-2390.

Wu, Z., Mazzola, C.A., Catania, L., Owoeye, O., Yaramothu, C., Alvarez, T., Gao, Y., & Li, X. (2018b). Altered cortical activation and connectivity patterns for visual attention processing in young adults post-traumatic brain injury: A functional near infrared spectroscopy study. *CNS Neurosci Ther* 24, 539-548.

Xia, S., Foxe, J.J., Sroubek, A.E., Branch, C., & Li, X. (2014). Topological organization of the "small-world" visual attention network in children with attention deficit/hyperactivity disorder (ADHD). *Front Hum Neurosci* 8**,** 162.

Xiong, Y., Mahmood, A., & Chopp, M. (2018). Current understanding of neuroinflammation after traumatic brain injury and cell-based therapeutic opportunities. *Chin J Traumatol* 21**,** 137-151.

Yallampalli, R., Wilde, E.A., Bigler, E.D., Mccauley, S.R., Hanten, G., Troyanskaya, M., Hunter, J.V., Chu, Z., Li, X., & Levin, H.S. (2013). Acute white matter differences in the fornix following mild traumatic brain injury using diffusion tensor imaging. *J Neuroimaging* 23**,** 224-227.

Yan, Y., Song, J., Xu, G., Yao, S., Cao, C., Li, C., Peng, G., & Du, H. (2017). Correlation between standardized assessment of concussion scores and small-world brain network in mild traumatic brain injury. *J Clin Neurosci* 44**,** 114-121.

Yasuno, F., Matsuoka, K., Kitamura, S., Kiuchi, K., Kosaka, J., Okada, K., Tanaka, S., Shinkai, T., Taoka, T., & Kishimoto, T. (2014). Decision-making deficit of a patient with axonal damage after traumatic brain injury. *Brain Cogn* 84**,** 63-68.

Yeates, K.O., Armstrong, K., Janusz, J., Taylor, H.G., Wade, S., Stancin, T., & Drotar, D. (2005). Long-term attention problems in children with traumatic brain injury. *J Am Acad Child Adolesc Psychiatry* 44**,** 574-584.

Yin, B., Li, D.D., Huang, H., Gu, C.H., Bai, G.H., Hu, L.X., Zhuang, J.F., & Zhang, M. (2019). Longitudinal changes in diffusion tensor imaging following mild traumatic brain injury and correlation with outcome. *Front Neural Circuits* 13**,** 28.

Yount, R., Raschke, K.A., Biru, M., Tate, D.F., Miller, M.J., Abildskov, T., Gandhi, P., Ryser, D., Hopkins, R.O., & Bigler, E.D. (2002). Traumatic brain injury and atrophy of the cingulate gyrus. *J Neuropsychiatry Clin Neurosci* 14**,** 416-423.

Yuh, E.L., Cooper, S.R., Mukherjee, P., Yue, J.K., Lingsma, H.F., Gordon, W.A., Valadka, A.B., Okonkwo, D.O., Schnyer, D.M., Vassar, M.J., Maas, A.I., Manley, G.T., & Track-Tbi, I. (2014). Diffusion tensor imaging for outcome prediction in mild traumatic brain injury: a TRACK-TBI study. *J Neurotrauma* 31**,** 1457-1477.

Yurgelun-Todd, D.A., Bueler, C.E., Mcglade, E.C., Churchwell, J.C., Brenner, L.A., & Lopez-Larson, M.P. (2011). Neuroimaging correlates of traumatic brain injury and suicidal behavior. *J Head Trauma Rehabil* 26**,** 276-289.

Zhang, H., Schneider, T., Wheeler-Kingshott, C.A., & Alexander, D.C. (2012). NODDI: practical in vivo neurite orientation dispersion and density imaging of the human brain. *Neuroimage* 61**,** 1000-1016.

Zhang, K., Johnson, B., Pennell, D., Ray, W., Sebastianelli, W., & Slobounov, S. (2010). Are functional deficits in concussed individuals consistent with white matter structural alterations: combined FMRI & DTI study. *Exp Brain Res* 204**,** 57-70.

Zhou, Y. (2017). Abnormal structural and functional hypothalamic connectivity in mild traumatic brain injury. *J. MAGN. RESON. IMAGING* 45**,** 1105-1112.

Zuckerman, S.L., Solomon, G.S., Forbes, J.A., Haase, R.F., Sills, A.K., & Lovell, M.R. (2012). Response to acute concussive injury in soccer players: is gender a modifying factor? *J Neurosurg Pediatr* 10**,** 504-510.